
Doctoral Dissertations

Student Theses and Dissertations

Spring 2022

Advances in Control of Uncertain Dynamical Systems with Optimal and Adaptive Approaches

Meryem Deniz

Missouri University of Science and Technology

Follow this and additional works at: https://scholarsmine.mst.edu/doctoral_dissertations



Part of the [Mechanical Engineering Commons](#)

Department: **Mechanical and Aerospace Engineering**

Recommended Citation

Deniz, Meryem, "Advances in Control of Uncertain Dynamical Systems with Optimal and Adaptive Approaches" (2022). *Doctoral Dissertations*. 3196.

https://scholarsmine.mst.edu/doctoral_dissertations/3196

This thesis is brought to you by Scholars' Mine, a service of the Missouri S&T Library and Learning Resources. This work is protected by U. S. Copyright Law. Unauthorized use including reproduction for redistribution requires the permission of the copyright holder. For more information, please contact scholarsmine@mst.edu.

ADVANCES IN CONTROL OF UNCERTAIN DYNAMICAL SYSTEMS WITH
OPTIMAL AND ADAPTIVE APPROACHES

by

MERYEM DENIZ

A DISSERTATION

Presented to the Graduate Faculty of the

MISSOURI UNIVERSITY OF SCIENCE AND TECHNOLOGY

In Partial Fulfillment of the Requirements for the Degree

DOCTOR OF PHILOSOPHY

in

MECHANICAL ENGINEERING

2022

Approved by:

S. N. Balakrishnan, Advisor

Tansel Yucelen, Co-Advisor

K. Krishnamurthy

Douglas A. Bristow

Jagannathan Sarangapani

K. Merve Dogan

Copyright 2022
MERYEM DENIZ
All Rights Reserved

To Dr. S.N. Balakrishnan, who was the principal advisor for my work leading to completion of all necessary requirements for receiving of a Ph.D. in Mechanical and Aerospace Engineering. Dr. Balakrishnan passed away one year before my final defense.

PUBLICATION DISSERTATION OPTION

This dissertation consists of the following six articles, formatted in the style used by the Missouri University of Science and Technology.

Paper I: Pages 10-36 appeared in the AIAA Guidance, Navigation, and Control Conference.

Paper II: Pages 37-58 appeared in the AIAA Guidance, Navigation, and Control Conference

Paper III: Pages 59-76 appeared in the IEEE American Control Conference.

Paper IV: Pages 77-94 appeared in the AIAA Guidance, Navigation, and Control Conference.

Paper V: Pages 95-121 has intended for submission.

Paper VI: Pages 122-140 has been submitted to IEEE American Control Conference.

ABSTRACT

This research starts with designing optimal control for uncertain systems, adding the adaptive control input to suppress the uncertainty. It then follows with designing the optimal control for state constraint, designing the optimal nonlinear reference model, designing adaptive control to handle state constraint and uncertainty. Finally, it designs the finite-time controller for uncertain multiagent systems.

It is well known that the design of the control algorithm for an uncertain dynamical system is not trivial. Motivated by this standpoint, this study focuses on optimal and adaptive control approaches with stability and performance guarantees for uncertain sole and multiagent dynamical systems. From the different perspectives of the controller design, designing the proper control input with the optimal method and suppressing the uncertain part with adaptive control are considered. An adaptive guidance/control method is also presented that has the capability to land the aircraft safely once a fault has occurred. Then, the extension of optimal control with state constraint is considered based inverse optimal control formulation with a set-theoretic barrier Lyapunov function (STBLF). The optimal nonlinear reference model with the Θ -D method is also proposed since linear reference model may not provide desired behavior of these systems. Another challenge in state constraint problems is that the dynamical system also has uncertainty. To solve both state constraint and uncertainty problems together, a new set-theoretic model reference adaptive control is further proposed with an adaptive control approach for uncertain nonlinear systems. Finally, the nonlinear reference model is proposed for multiagent systems with finite-time stability guarantees using a distributed adaptive control approach.

To conclude, the proposed new optimal and adaptive control methods are introduced with stability analysis using the optimal solution and Lyapunov stability. The efficacy of the proposed methods is further demonstrated with illustrative numerical and experimental results.

ACKNOWLEDGMENTS

I would like to express the deepest appreciation to my advisor, Dr. S. N. Balakrishnan. I would also like to thank Dr. Tansel Yucelen for his help, inspiration, guidance, and encouragement throughout a couple of months and for being my co-advisor after Dr. S. N. Balakrishnan passed away. I gratefully acknowledge the other members of my Ph.D. committee, Dr. K. Krishnamurthy, Dr. Douglas A. Bristow, Dr. Jagannathan Sarangapani, Dr. K. Merve Dogan, for their time and helpful comments.

I would like to also thank Dr. Enver Tatlicioglu for his continuous support, motivation, and extensive academic guidance. I would also like to thank Dr. Takeshi Yamasaki and Dr. Ehsan Arabi for the fruitful collaboration opportunities. In addition, I would like to acknowledge the support from the Turkish Ministry of National Education of the Republic of Turkey. I would also like to thank the NASA, for their Grants NNX15AM51A and NNX15AN04A, to partially support this research.

My sincere thanks also goes to my fellow labmates and friends for all the personal and professional discussions. I am thankful to Daniel Peterson, Merve, Devi P.L., Arnold Fernandes, Nathan Lutes, Akhilesh Raj, Chandreyee Bhowmick, Sambad Regmi, Sreevalsan Menon, Michelle Gegel, Joy Lollar, Abdul Ghafoor, Atta Ur Rehman, Alia, Huseyin Sahiner, Ersin Unkaracalar, Efecan Karademir, Murat Tuter, Mete Sarikaya, Onur Akturk, Havva Malone, Sema Erenmemis and Yasemin Koylu.

Last but not least, I would like to thank my parents, Hanife and Hulusi Deniz, for their unconditional love. In addition, my warmest and deepest thank goes to my mother, Hanife Deniz, who has always been a source of motivation and inspiration for me. Without her constant support, encouragement, and prayers, I would not have achieved this work. I would also like to thank my sister and brother, Hazal and Onur Akan Deniz, for their unconditional support and love. I also wish to thank my aunts Derya Ekmekci, Ziyet Coskun, Soner Kaymaz, and my grandmother Saadet Ekmekci for their support and prayer.

TABLE OF CONTENTS

	Page
PUBLICATION DISSERTATION OPTION	iii
ABSTRACT	iv
ACKNOWLEDGMENTS	v
LIST OF ILLUSTRATIONS	xii
 SECTION	
1. INTRODUCTION.....	1
1.1. INTEGRATED GUIDANCE AND CONTROL	1
1.2. STATE CONSTRAINTS	3
1.3. NONLINEAR REFERENCE MODEL.....	4
1.4. OPTIMAL SOLUTIONS WITH NONLINEAR CONTROL PROBLEMS ..	5
1.5. FINITE-TIME FOR MULTIAGENT SYSTEM.....	6
1.6. CONTRIBUTIONS.....	7
1.7. ORGANIZATION	8
 PAPER	
I. INTEGRATED PATH PLANNING AND CONTROL FOR IMPAIRED AIR- CRAFT APPROACH AND LANDING.....	10
ABSTRACT	10
1. INTRODUCTION	11
2. PROCEDURE FOR CONTROL DESIGN	13
2.1. NEURAL NETWORK BASED APPROXIMATION.....	14
2.2. NOMINAL CONTROLLER DESIGN	15
2.3. SOLUTION PROCESS FOR LINEAR QUADRATIC PROBLEMS	17

2.4.	SOLVING STATE DEPENDENT DRE FOR OPTIMAL CONTROL OF NONLINEAR SYSTEMS	18
3.	SIMULATION STUDIES	20
3.1.	KINEMATIC AND DYNAMICS OF AIRCRAFT IN VERTICAL PLANE	20
3.2.	RESULTS AND DISCUSSION	22
3.3.	SIMULATION RESULTS	24
3.3.1.	Simulation Results with One Time Varying Uncertainty ..	24
3.3.2.	Simulation Results with One Constant Uncertainty	26
3.3.3.	Simulation Results with Two Constant Uncertainties	28
3.3.4.	Simulation Results with Two Time Varying Uncertainties	30
4.	CONCLUSIONS	31
	ACKNOWLEDGEMENTS	32
	REFERENCES	33
II.	SLIDING MODE BASED PATH PLANNING AND CONTROL OF IMPAIRED AIRCRAFT	37
	ABSTRACT	37
1.	INTRODUCTION	37
2.	KINEMATIC AND DYNAMICS OF AIRCRAFT IN VERTICAL PLANE .	39
3.	INTEGRATED PATH PLANNING AND CONTROLLER DESIGN	42
3.1.	SLIDING SURFACE DESIGN	43
3.2.	SECOND-ORDER SLIDING MODE FRAMEWORK AND HIGH-ORDER SLIDING MODE DIFFERENTIATOR	45
3.2.1.	Second-Order Sliding Mode Framework	45
3.2.2.	High-Order Sliding Mode Differentiator	45
4.	NUMERICAL STUDIES	46
4.1.	SIMULATION RESULTS	47

4.1.1.	Case1: $\delta_e = 2^\circ$ (stuck) with Different Altitudes and Final Downrange = 50000 ft	47
4.1.2.	Case2: $\delta_e = -2^\circ$ (stuck) with Different Altitudes and Final Downrange = 100000 ft	51
5.	CONCLUSIONS	56
	ACKNOWLEDGEMENTS	56
	REFERENCES	56
III.	INVERSE OPTIMAL CONTROL WITH SET-THEORETIC BARRIER LYAPUNOV FUNCTION FOR HANDLING STATE CONSTRAINTS	59
	ABSTRACT	59
1.	INTRODUCTION	59
2.	INVERSE OPTIMAL CONTROL BASED ON AN STBLF FOR REGULATOR PROBLEMS	61
2.1.	INVERSE OPTIMAL CONTROL DESIGN	61
2.2.	SET-THEORETIC BARRIER LYAPUNOV FUNCTION	62
2.3.	COMBINING INVERSE OPTIMAL CONTROL AND STBLF.....	64
2.4.	STABILITY ANALYSIS	64
3.	INVERSE OPTIMAL CONTROL BASED ON STBLF FOR TRACKING PROBLEMS	66
3.1.	INVERSE OPTIMAL CONTROL DESIGN	66
4.	NUMERICAL RESULTS	68
4.1.	REGULATOR PROBLEM	69
4.1.1.	Case 1	69
4.1.2.	Case 2	71
4.2.	TRACKING PROBLEMS	72
4.2.1.	Case 1	72
4.2.2.	Case 2	73
5.	CONCLUSION	75

ACKNOWLEDGEMENTS	75
REFERENCES	75
IV. ADAPTIVE CONTROL OF UNCERTAIN DYNAMICAL SYSTEMS WITH AN OPTIMAL NONLINEAR REFERENCE MODEL	77
ABSTRACT	77
1. INTRODUCTION	77
2. AN OVERVIEW ON $\Theta - D$ SUBOPTIMAL CONTROL METHOD	79
3. ADAPTIVE CONTROL WITH THE $\Theta - D$ NONLINEAR REFERENCE MODEL	81
4. ILLUSTRATIVE NUMERICAL EXAMPLES	85
4.1. FIRST EXAMPLE	85
4.2. SECOND EXAMPLE	87
5. CONCLUSION	92
REFERENCES	92
V. SET-THEORETIC MODEL REFERENCE ADAPTIVE CONTROL OF UN- CERTAIN DYNAMICAL SYSTEMS WITH STATE CONSTRAINTS	95
ABSTRACT	95
1. INTRODUCTION	96
2. SET-THEORETIC BARRIER LYAPUNOV FUNCTION WITH STATE CONSTRAINTS	98
2.1. CASE 1	100
2.2. CASE 2	100
2.3. CASE 3	100
3. ILLUSTRATIVE NUMERICAL AND EXPERIMENTAL EXAMPLES	110
3.1. ILLUSTRATIVE NUMERICAL RESULTS	113
3.1.1. Case 1	113
3.1.2. Case 2	114

3.1.3.	Case 3	114
3.2.	ILLUSTRATIVE EXPERIMENTAL RESULTS	116
3.2.1.	Case 1	117
3.2.2.	Case 2	118
3.2.3.	Case 3	118
4.	CONCLUSION	119
	ACKNOWLEDGEMENTS	120
	REFERENCES	120
VI. A FINITE-TIME ARCHITECTURE FOR DISTRIBUTED ADAPTIVE CONTROL OF UNCERTAIN MULTIAGENT SYSTEMS		
	ABSTRACT	122
1.	INTRODUCTION	123
2.	MATHEMATICAL PRELIMINARIES	124
3.	PROBLEM FORMULATION	126
4.	SYSTEM-THEORETICAL ANALYSES	127
4.1.	ANALYSIS FOR OBJECTIVE A).....	127
4.2.	ANALYSIS FOR OBJECTIVE B).....	130
5.	ILLUSTRATIVE NUMERICAL EXAMPLE.....	133
6.	CONCLUSION	137
	REFERENCES	138
SECTION		
2.	SUMMARY AND CONCLUSIONS	141
APPENDICES		
A.	PROOF OF THE THEOREM OF THE PAPER I	143

B. PROOF OF THE THEOREM OF THE PAPER III 147

REFERENCES 150

VITA..... 160

LIST OF ILLUSTRATIONS

Figure	Page
PAPER I	
1. Histories of actual and estimated states, downrange and control [one time varying uncertainty]	25
2. History of uncertainty estimation with time [time varying $C_{L\alpha}$ uncertainty].	26
3. Histories of actual and estimated states, downrange and control [one constant uncertainty]	27
4. History of uncertainty estimation with time [constant $C_{L\alpha}$ uncertainty].	28
5. Histories of actual and estimated states, downrange and control [two constant uncertainties]	29
6. History of two uncertainties estimation with time [constant $C_{L\alpha}$ uncertainty]. ...	30
7. History of two uncertainties estimation with time [constant C_{m_q} uncertainty]. ...	30
8. Histories of actual and estimated states, downrange and control [two time varying uncertainties]	32
9. History of two uncertainties estimation with time [variable $C_{L\alpha}$ uncertainty]. ...	33
10. History of two uncertainties estimation with time [variable C_{m_q} uncertainty]. ...	33
PAPER II	
1. Flight dynamics of the fixed wing aircraft	39
2. Histories of actual and desired altitudes with respect to downrange	48
3. Histories of actual and desired altitudes with respect to time	48
4. States histories for various initial altitudes	49
5. Histories of horizontal and vertical velocities for various initial altitudes	49
6. Histories of controller, thrust and sliding surface for various initial altitudes	50
7. Histories of actual and estimated uncertainties for various initial altitudes	50
8. Histories of actual and desired altitudes with respect to downrange.....	52
9. Histories of actual and desired altitudes with respect to time	52

10.	States histories for various initial altitudes	53
11.	Histories of horizontal and vertical velocities for various initial altitudes	53
12.	Histories of controller, thrust and sliding surface for various initial altitudes	54
13.	Histories of actual and estimated uncertainties for various initial altitudes	54

PAPER III

1.	Histories of states and controller for regulator problem case 1	70
2.	Histories of norm of states and bound for regulator problem case 1	70
3.	Histories of states and controller for regulator problem case 2	71
4.	Histories of norm of states and bound for regulator problem case 2	71
5.	Histories of the states and the references states and controller for tracking problem case 1	73
6.	Histories of norm of error and bounds for tracking problem case 1	73
7.	Histories of the states and the references states and controller for tracking problem case 2	74
8.	Histories of norm of error and bounds for tracking problem case 2	74

PAPER IV

1.	Histories of the actual and reference states without adaptive control	86
2.	History of controller without adaptive control	86
3.	Histories of the actual and reference states with adaptive control	87
4.	History of controller with adaptive control	88
5.	Histories of the actual and model reference state one without adaptive control ..	89
6.	Histories of the actual and model reference state two without adaptive control ..	89
7.	Histories of controller without adaptive control	90
8.	Histories of the actual and model reference state one with adaptive control	90
9.	Histories of the actual and model reference state two with adaptive control	91
10.	Histories of controller with adaptive control	91

PAPER V

1.	Quanser 3 DOF Hover	110
2.	Histories of the actual and model reference states	113
3.	Histories of the norm of the states and the bound	114
4.	Histories of the actual and model reference states	115
5.	Histories of the norm of the states and the bound	115
6.	Histories of the actual and model reference states	116
7.	Histories of the norm of the states and the bound	116
8.	Histories of the actual and model reference states	117
9.	Histories of the norm of the states and the bound	117
10.	Histories of the actual and model reference states	118
11.	Histories of the norm of the states and the bound	119
12.	Histories of the actual and model reference states	119
13.	Histories of the norm of the states and the bound	120

PAPER VI

1.	Three agents on the connected and undirected graph \mathcal{G} with the first agent being the leader (i.e., $k_1 = 1$) and the second and the third agents being followers (i.e., $k_2 = 0$ and $k_3 = 0$).	134
2.	Performance of the states and the references states of each agent (the command available to the first agent is shown in all figures).	135
3.	History of the control signals of each agent.	136
4.	Performance of the states and the references states of each agent when “sgn(\cdot)” is replaced with “tanh(1000(\cdot))” by following the discussion in Remark 4.1 (the command available to the first agent is shown in all figures).	136
5.	History of the control signals of each agent when “sgn(\cdot)” is replaced with “tanh(1000(\cdot))” by following the discussion in Remark 4.1.	137

1. INTRODUCTION

In this section, a summary of the literature review of the mostly related control architectures to the contributions of this dissertation is mentioned. Building the control methods for uncertain dynamical systems is not a trivial task. There are some properties which should be considered. For example, improve the performance, guarantee stability, suppress the uncertainties, and not violate the system states of uncertain dynamical systems. The main goal of this dissertation is to develop control architectures with important constraints (state, time, downrange) for uncertain dynamical systems.

1.1. INTEGRATED GUIDANCE AND CONTROL

There has been a lot of interest in control of unmanned aerial vehicles (UAVs). Specifically, they have missions to accomplish; hence, they have a path to follow and need a controller to keep them on a desired path. Most guidance and control systems for path-following UAVs employ a tracking-error-correction approach [1, 2, 3, 4, 5, 6]. However, such designs do not perform well when tracking errors become large. The error-based techniques can cause control saturation or divergence since the control command magnitudes are usually proportional to the tracking errors.

Many researchers focus on the integrated guidance and control (IGC) algorithms for dynamical systems [7, 8, 9, 10, 11, 12, 13, 14, 15, 16, 17, 18, 19]. Integrated guidance and control is the primary approach, but they use different perspectives to solve the problem. The higher-order sliding mode with integrated guidance and control method is shown in [7, 17]. The higher-order sliding mode is used to design a virtual controller that helps to avoid chattering. Some researchers focus on the adaptive control for IGC method. In [9], the authors use adaptive control with sliding mode control and in [18], adaptive control

with output feedback and backstepping techniques is used. In [10, 19, 16, 14], the feedback control, backstepping control, PID control, and disturbance observer are used with IGC, respectively.

On the other hand, the authors of [15] focus on path-based planning and control method. It uses desired and measurable system output. It tells motion or action reference variable, which is called an event. They derive a closed-form of time and energy optimal motion plans with nonlinear feedback control. In [8], the authors design the integrated guidance and control method that combines three discrete algorithms. It has been shown that the performances of IGC and traditional (decoupled) guidance and control algorithms. Also, in [13], the authors focused on the separated and the integrated guidance and control design. Moreover, they analyze two different integrated guidance and control, which are integrated single loop guidance and integrated two-loop guidance methods.

The researchers in [11] use integrated guidance and control method for trajectory tracking controllers for AUVs (Autonomous Underwater Vehicles). In this method, they design two systems together. This method has two advantages compared to traditional methods. One of the advantages is that the steady-state tracking error reaches zero. The second one is that the proposed controller cover stability of combined control and guidance.

In [12], the authors develop a unified receding horizon optimization (RHO) method for integrated path planning and tracking control of an autonomous underwater vehicle (AUV). The state trajectory of a virtual reference system is used as a planned path; the virtual reference system has the same kinematic and dynamic properties as AUVs. Using the virtual reference makes tracking control problems to the regulation problem of the error dynamics.

1.2. STATE CONSTRAINTS

There are some limitations (such as task space of robot arms, angle of airplanes, and speed of motor) on the dynamical systems, which may violate the designing the control laws when constraints of system are not considered. From this standpoint, some researchers focus on the state constraints for systems [20, 21, 22, 23, 24, 25, 26, 27, 28, 29, 30, 31, 32].

The prescribed performance bound is developed in [20, 21, 22, 28]. This method transforms the constrained system into the unconstrained systems for feedback linearizable nonlinear systems. Specifically, in [21], the single-input single-output (SISO) system, in [20], the multi-input multi-output (MIMO) are used. Also, in [22], the authors extend prescribed performance bound to the MIMO affine systems with measurable state and unknown nonlinearities. In [28], prescribed performance bound is used with neural network control method.

On the other hand, some researchers in [30, 32, 31, 23, 33] focus on the set-theoretic barrier Lyapunov function. In [23], Yucelen *et al* work on the set-theoretic function for multiagent systems, then [30], Arabi *et al* use the set-theoretic barrier Lyapunov function method to keep the error (between actual state and reference model) under the user-defined constant. Then, the work is extended to the user-defined time-varying performance bound [31]. Lastly, the performance of the proposed method on the experimental testbed is demonstrated in [32]. Also, in [29], the author developed an adaptive control method that forced the state of the system to stay in a given region. The reason for the chosen region is to show stability analysis for nonlinear systems. The bounding functions are used to limit the states of a system. These bounding functions keep the states under the limit when the growth rate of the bounding functions is sufficiently large.

The Barrier function is used in many studies [24, 34, 25, 26, 27]. They focus on the multiple state constraints with a combination of other methods or different systems. In [24], Ngo *et al* use integrator backstepping for feedback linearizable system. The Barrier function is defined on the cost function of optimal control in [34]. In [25], the authors

consider the symmetric and asymmetric barrier Lyapunov function for SISO feedback linearizable nonlinear systems. Also, full-state feedback and output feedback methods with tracking the reference trajectory within the air gap are considered in [26]. The neural network control is used for unknown functions, and a barrier Lyapunov function is used to keep the unknown functions within the specified compact set in [27].

The input/state hard constraint is focused in [35] with the filtering of the desired reference trajectory using reference governor. In addition, the survey is given with constrained model predictive control in [36].

1.3. NONLINEAR REFERENCE MODEL

Although the linear model reference adaptive control is a well-known research topic, a linearized model does not always have a better performance in nonlinear systems. The nonlinear dynamical system may have dynamic uncertainties or some limitations on the systems. The linear reference model can achieve desired closed loop in a limited region. Therefore, some researchers focus on the nonlinear reference model to overcome the limitations. The researchers given in [37, 38, 39, 40, 41, 42] consider various method to solve the nonlinear dynamical problems. For example, in [37], Scarritt uses a nonlinear reference model to have the closest approximation of true system with variable structure controller to track desired attitude trajectory. Peter *et al* use nonlinear dynamic inversion (NDI) control with nonlinear reference model [38]. Yucelen *et al* consider the nonlinear reference model based on adaptive control method to handle uncertainties and vanish the error between uncertain dynamical system and the nonlinear reference model in steady-state [39, 42]. The \mathcal{L}_1 adaptive control method with time-varying nonlinear reference model is considered by researchers given in [40]. Also, the passivity based adaptive nonlinear controller with nonlinear reference model is developed in [41].

1.4. OPTIMAL SOLUTIONS WITH NONLINEAR CONTROL PROBLEMS

The optimal control of nonlinear dynamical systems has an ever-increasing interest. The optimal solution depends on the solution of the Hamilton Jacobi Bellman (HJB) equation. The HJB solution is a challenging problem. Therefore, various methods propose to solve the HJB equation. Some researchers in [43, 44, 45, 46, 47, 48, 49, 50, 51, 52] use an approximate solution of the HJB equation.

Another method of optimal control solution for uncertain nonlinear systems is the actor-critic-identifier (ACI) method. This method helps to approximate the HJB equation with neural network (NN) control with no requirement of knowledge of system dynamics [53, 54, 55, 56, 57, 58]. The authors of [59, 60, 61, 62] propose a concurrent learning-based approximate optimal control. Also, the authors of [63, 46] develop a concurrent learning method for synchronization of a leader-follower network of agents.

Other method for for nonlinear system by finding the approximate solution to HJB equation is the suboptimal feedback controller [64, 65, 66, 67, 68, 69, 70, 71, 72, 73, 74]. Burghart et al in [75] and Pan et al in [76] propose a suboptimal feedback control with Tylor's series expansion for nonlinear systems. Also, in [77], power series expansion is proposed.

Reinforcement learning is proposed for solving partially unknown finite-horizon optimal control problems [78]. Zhao *et al* use reinforcement learning based on neural network optimal tracking control for uncertain nonlinear systems [79]. Bradtke *et al* focus on direct optimal adaptive control using reinforcement learning based on dynamic programming. Also, the adaptive optimal tracking control is used with reinforcement learning to solve linear quadratic regulator in [80].

The researchers propose a generalized Hamilton-Jacobi Bellman (GHJB) equation using Galerkin approximation in [81, 82]. This method reduces the computational complexity.

In the current literature, a method called the Θ -D method [83, 84, 85, 83] achieves effective suboptimal solutions for nonlinear dynamical systems. The advantage of this method is that it involves reduced nonlinear computations and control signals with initially small magnitudes. Yet, the authors of [83, 84, 85, 83] do not focus on the presence of uncertainties. Motivated by this standpoint, this dissertation uses the Θ -D method to establish an optimal nonlinear reference model based on the known system dynamics. Building on the critical ideas on nonlinear reference model-based adaptive control architectures [42], the adaptive control algorithm is designed to suppress unknown system dynamics, in this dissertation.

1.5. FINITE-TIME FOR MULTIAGENT SYSTEM

Teams of agents (e.g., unmanned aerial, ground, water, and underwater vehicles) operated through a network are called multiagent systems, where they will play a key role in a wide array of civilian and military applications such as surveillance and reconnaissance, ground and air traffic management, payload, and passenger transportation, and emergency response; to name but a few examples. Whether civilian or military, however, there are essential multiagent systems applications that require operations to be completed in a finite-time duration, such as cooperative engagement, sequential execution of time-critical network operations (i.e., multiagent automation), and rendezvous. There is an increasing interest in problems where the final time matters. The authors of [86, 87, 88, 89, 90] focus on the predefined time of dynamical systems. In [86], the higher order integrator is used to have predefined time converge and in [87, 90], the researchers use sliding mode controller for finite time stability. Likewise, the sliding mode controller is used by some researchers in [91, 92, 93]. Other types of controller is considered by many researchers such as adaptive control in [94], Lyapunov stability in [95, 96, 97], state feedback in [98], single integrator in [99], and double integrator in [100, 86].

The authors of [101, 102, 103] develop the method with time transformation. These methods convert the user-defined finite-time into the infinite-time interval. The researchers of [104, 105] introduce the normalized and signed gradient method with a differentiable function. On the other hands, some researchers focus on the estimation like in [106]; that is, the observer is introduced to estimate the state for single-output observable linear systems. Finally, [107] introduces the method with the calculation of the upper estimate of the convergence time.

1.6. CONTRIBUTIONS

Inspired and motivated by the above research papers, the main contributions of this dissertation are stability and performance guarantees for uncertain dynamical systems with optimal and adaptive control approaches.

Although integrated path planning and control methods are proposed in Section 1.1 with different approaches, the adaptive control based IGC method is presented in Paper I to land the impaired aircraft safely when the engine fails. The combination of kinematic and dynamic equations of an aircraft helps us to design the controller. The optimal control method is developed with a state-dependent Ricatti equation to land the aircraft, and the adaptive control based modified state observer is used the estimate uncertainties. The other approach of the IGC method is presented in Paper II. In this case, the frozen elevator deflection is considered for impaired aircraft. Therefore, the thrust is considered a controller to land the impaired aircraft. The second-order and high-order sliding mode methods are used for designing the controller. The SOSM is used to land the impaired aircraft safely, and HOSM is used to estimate the uncertainties. The efficacy of proposed methods are supported with numerical simulation results.

As discussed in Section 1.2, real-life applications have some limitations. To overcome the aforementioned limitations of the dynamical systems, the optimal solution is proposed in Paper III and the model reference adaptive control is proposed in Paper V

with a set-theoretic approach. The contribution of Paper III is that the set-theoretic barrier Lyapunov function is embedded into the Hamilton-Jacobi-Bellman equation. That helps to solve the optimal control problem when the system has state constraints. In addition, the state constraints are considered with uncertainty for a dynamical system. Therefore, in Paper V, the model reference adaptive control is developed for uncertain dynamical systems when the state of the systems has limitations. The contributions of this paper are to keep the state of the systems under the limit and suppress the uncertainties and have a better tracking performance with suitable STBLF. Experimental studies given in Paper V support the performance of the proposed method.

The literature review for the nonlinear reference model is given in Section 1.3. In contrast to the given nonlinear reference model, the importance of designing a nonlinear reference model in Paper IV is being optimal. The optimal solutions for nonlinear control problems are also given in Section 1.4. According to this section, the Θ -D method gives a suboptimal solution for nonlinear systems with reduced nonlinear computations. Therefore, designing a reference model with the Θ -D method for known system dynamics provides an optimal nonlinear reference model. Then, the adaptive control is utilized to address the presence of system uncertainties. Also, the agent-wise nonlinear reference models are used in Paper VI. The main contribution is that agents rely on stable reference model states in finite-time. The finite-time methods given in Section 1.5 are considered when time is significant.

1.7. ORGANIZATION

First two papers, we focused on the uncertain dynamical system for impaired aircraft to land at the proper location. Therefore, fixed downrange is focused. In the third paper, the state constraint is considered with inverse optimal control method. In the fourth paper, the nonlinear reference model is designed with optimal control. The adaptive control method is developed with state constraints to handle both uncertainties and constraints in paper

fifth. We developed finite-time control approaches with a nonlinear reference model for multiagent systems in paper sixth. Finally, overall conclusions from this dissertation are given in Section 2. Then, appendices are provided for proofs of papers.

PAPER**I. INTEGRATED PATH PLANNING AND CONTROL FOR IMPAIRED
AIRCRAFT APPROACH AND LANDING**

Meryem Deniz¹, S. N. Balakrishnan¹, Tansel Yucelen²

¹Department of Mechanical & Aerospace Engineering
Missouri University of Science and Technology
Rolla, Missouri 65409-0050, United States of America

²Department of Mechanical Engineering
University of South Florida
Tampa, Florida 33620, United States of America

ABSTRACT

Unpredictable conditions experienced by an impaired aircraft in its flight path demands that the guidance techniques for succeeding phases be robust. Therefore, we need new control formalisms to improve the safe flight and landing of impaired aircraft. In particular, new aircraft guidance and control technologies should be developed that can accommodate for aero-surface faults, thrust variations, or dispersions from the desired trajectory and also allow for landing at different landing sites. The developed techniques are particularly critical during the approach and landing (A&L) phase of an impaired aircraft. In this work, an adaptive guidance/control method is presented that lands the aircraft safely once a fault has occurred. Typically, an aircraft travel from one place to another place takes place with a pre planned path and the controller enabling the aircraft to fly the pre planned path. However, once a fault has occurred, the impaired aircraft may or may not be able to fly the pre planned path. A new path will have to be constructed online and the aircraft may have to follow the revised trajectory in order to safely land at an alternate location. This paper considers such a scenario and new schemes are devised based on an integrated

path planning and control approach and adaptive control. A state model comprising of both the kinematic states and the dynamic states are considered in this paper to account for path planning and control of the aircraft to fly on the online defined path. Acting on a combination of optimal and adaptive control schemes, both the path planning and control needs to land the aircraft at a feasible landing site are satisfied. Numerical results are shown that consider and thrust being cut off. Representative results are shown with the new integrated path planning and control scheme.

1. INTRODUCTION

Interest in autonomous flights have increased tremendously in the last two decades. There has been a lot of interest in unmanned air vehicle(UAV) flights. Such flights have missions to accomplish; hence, they have a path to follow and need a controller to keep them on the desired path. Most guidance and control systems for path-following flights of UAVs employ a tracking-error-correction approach [1, 2, 3, 4, 5, 6]. However, such designs do not perform well when tracking errors become large; for example, if the trajectory is a steep, curved path or if wind turbulence exists, the error based techniques can cause control saturation or divergence since the control command magnitudes are usually proportional to the tracking-errors. Baba and Takano [7] proposed a fuzzy logic based technique where variable gains are calculated in proportion to tracking-error quantities. Though its performance was shown to be good, this technique requires many design points and several gains iteratively selected as a part of the process before fuzzy logic is used. By introducing a virtual waypoint along a specified trajectory [8, 9], pure pursuit guidance (PPG)[10] methods can be gainfully used for path-following UAV applications. Results [8, 9] demonstrate excellent results in the presence of wind turbulence. Note that PPG requires only one gain to be tuned. It produces guidance commands that are not dependent on tracking errors and of reasonable magnitudes. Consequently, the PPG based control obviates control divergence; Park et. al. [11, 12] use a similar approach where the distance

error is restricted to a pre-specified distance. The desired path is shaped with cubic spline approximation [13] of arc lengths which are computed based on waypoints for the desired trajectory of the UAVs. Stability analysis for such a waypoint guidance scheme is given in [12]. There are other methods such as sliding mode based integrated guidance and control concepts used in missile applications. An SMIGC “sliding mode based integrated guidance and control” scheme was proposed by Harl et. al. in [14] for missile intercept against weaving targets. Their technique showed robust performance against uncertain target maneuvers. Shtessel has published several papers based on sliding mode [15, 16, 17] techniques for different applications. HOSM was applied to UAV formation flying in Galzi and Shtessel[15] for guidance alone. A sliding mode guidance and autopilot methodology was developed based on a zero-effort-miss guidance concept by Shima, et. al.[18] for missile applications. Sliding mode control (SMC) for a non-minimum phase system was proposed in Shkolnikov and Shtessel [16]. HOSM (e.g., [19, 20, 17, 21]) mitigates the chatter problems associated with SMC, i.e., HOSM is applicable for arbitrary relative degree systems with smooth control. Shtessel et. al.[17] also applied an HOSM for missile interception against uncertain target maneuvers. Note that the many missiles are described as “skid-to-turn” which means that they hardly use any roll motion. The aircraft motion however is different. An integrated tracking and control scheme was proposed and tested on numerical simulations by Yamasaki et. al. [22].

In this study, a new integrated path planning and control problem for an impaired aircraft is formulated. Note that an integrated path planning and control scheme averts the need for the iterative loops used in following an independent path planning and a separate controller design scheme. This formulation combines the kinematic and dynamic equations of an aircraft in a vertical plane. Control of this airplane is obtained from an optimal control expression through the state dependent riccati equation technique. Numerical results are shown that show the efficacy of this formulation of the integrated path planning and control approach. As a second step, uncertainties in the dynamic model are considered. A modified

state observer is used to estimate the uncertainties and produce an adaptive extra control to cancel the uncertainties. A representative set of plots are shown with uncertainties in the parameters associated with the angle of attack and pitching moment equation.

2. PROCEDURE FOR CONTROL DESIGN

The general aircraft dynamics are described by

$$\dot{x} = f(x) + B(x)u \quad (1)$$

where $f(x) \in \mathbb{R}^n$ and $B(x) \in \mathbb{R}^{n \times m}$ are the state and control matrices, respectively. $x \in \mathbb{R}^n$ is the state vector and $u \in \mathbb{R}^m$ ($m \leq n$) is the control vector. However, the actual aircraft dynamics have some nonlinearities which is given by

$$\dot{x} = f(x) + B(x)(u + D(x, u)) \quad (2)$$

where, $D(x, u)$ is the uncertainty in the system dynamics. Equation (2) can be rewritten as

$$\dot{x} = f(x) + B(x)u + E(x, u) \quad (3)$$

where $E(x, u) = B(x)D(x, u)$, is simplified and $E(x, u) \in \mathbb{R}^n$. $E(x, u)$ is the unknown function, and it is estimated using neural networks. In order to estimate unknown function, the observer design is needed. An observer for the system given in (3) be written as

$$\dot{\hat{x}} = f(x) + B(x)u + \hat{E}(x, u) + K_2(x - \hat{x}) \quad (4)$$

where $\hat{E}(x, u)$ is the estimated uncertainty and K_2 is a positive definite matrix [23, 24].

2.1. NEURAL NETWORK BASED APPROXIMATION

The output of each estimated network can be defined as

$$\hat{E}(x, u) = \hat{W}^T \phi(x) \quad (5)$$

\hat{W} is the estimated weight matrices and $\phi(x)$ is defined as basis function vector [25]. Estimation error dynamics are used for the weight update rule to show the performance of unknown parameters. Estimation error is expressed as

$$e_a = x - \hat{x} \quad (6)$$

Using the function approximation property of neural networks [26], it can be stated that there exists an ideal neural network with an optimum weight vector W and basis function vector $\phi(x)$ that approximates $f(x, u)$ to an accuracy of ε that is

$$E(x, u) = W^T \phi(x) + \varepsilon \quad (7)$$

then the estimation error dynamics are given by

$$\dot{e}_a = -K_2 e_a + \tilde{W}^T \phi(x) + \varepsilon \quad (8)$$

where, $\tilde{W}^T \triangleq W - \hat{W}$ is the error between the actual weight and the estimated weight of the neural network.

Theorem 2.1. *A weight update rule, is proposed as*

$$\dot{\hat{W}} = \Gamma \phi(x) e_a^T P - \sigma \hat{W} \quad (9)$$

The error signal e_a and the adaptive weights \hat{W} of the online networks are bounded. Γ is the adaptation gain and σ is a sigma modification factor used to enforce bound on network weights and provide robustness. The adaptation law in Equation (9) is designed to ensure the decrease of the Lyapunov function with time with the Lyapunov function given by

$$V = e_a^T P e_a + tr(\tilde{W}^T \Gamma^{-1} \tilde{W}) \quad (10)$$

The proof of the theorem can be found in [23, 24].

Control u consists of a nominal control term to stabilize system without uncertainty and adaptive control term to cancel the effect of uncertainty given by $D(x, u)$. Nominal control is calculated using the State Dependent Riccati Equation (SDRE) method which is briefly described in the following section.

2.2. NOMINAL CONTROLLER DESIGN

In SDRE, the nonlinear state space in (1) is converted to a linear like form

$$\dot{x}(t) = A(x)x(t) + B(x)u(t) \quad (11)$$

where $A(x)x(t) = f(x)$. Assume that, state equations of x is known at each step, one can solve the following algebraic Riccati equation (ARE) with state dependent coefficients for $P(x)$.

$$P(x)A(x) + A^T(x)P(x) - P(x)B(x)R^{-1}B^T(x)P(x) + Q = 0 \quad (12)$$

By calculating the optimal costate vector λ^* , solution of $P(x)$ is needed

$$\lambda^* = P(x)x(t) \quad (13)$$

Once the optimal costate vector is calculated, necessary conditions for optimal control will yield the nominal controller expressions as

$$u^* = -R^{-1}B^T(x)\lambda^*(t) \quad (14)$$

Reference [27] contains details on this derivation; for information about forming the linear like state equation (11) from (1), one may refer to [28].

Note that SDRE is a solution to infinite horizon optimal control, however, the guidance problem or trajectory generation problem considered here is a finite-horizon problem. A major difference in the finite horizon case is that the feedback solution is also time-dependent and the following differential Riccati equation (DRE) needs to be solved [29].

$$P(x, t)A(x) + A^T(x)P(x, t) - P(x, t)B(x)R^{-1}B^T(x)P(x, t) + Q = -\dot{P}(x, t) \quad (15)$$

with the final condition given by

$$P(x, t_f) = S \quad (16)$$

Note that the Riccati solution here does not have a steady state solution; furthermore, the Riccati matrix is a function of states that vary with time. An approximation is made here that wherein the values of the states are frozen to remain constant from the current instant to the final time. Due to (16) to be satisfied at the boundary, the traditional SDRE is not applicable here. Note that a closed form solution can be obtained by using a transformation with the solution to the ARE that converts the original nonlinear Riccati equation into a linear Lyapunov equation [30] [31], [32]. More details about the approximate solutions are given in the next section.

2.3. SOLUTION PROCESS FOR LINEAR QUADRATIC PROBLEMS

Constant-coefficient differential Riccati equation (DRE) is expressed as

$$P(t)A + A^T P(t) - P(t)BR^{-1}B^T P(t) + Q = -\dot{P}(x, t) \quad (17)$$

where final condition of (DRE) is given by

$$P(t_f) = S \quad (18)$$

where $\dot{P}(x, t)$ is time derivative of the Riccati equation solution of $P(t)$. Quadratic cost function in finite-time is defined as follows:

$$J = \frac{1}{2}x^T(t_f)Sx(t_f) + \frac{1}{2} \int_{t_0}^{t_f} (x^T Qx + u^T Ru)dt \quad (19)$$

In order to solve the nonlinear problem, first, a steady state Algebraic Riccati Equation (ARE) is needed to be solved and that is given by

$$P_{ss}A + A^T P_{ss} - P_{ss}BR^{-1}B^T P_{ss} + Q = 0 \quad (20)$$

subtracting (20) from (17) leads to [32]

$$(P(t) - P_{ss})A + A^T (P(t) - P_{ss}) - P(t)BR^{-1}B^T P(t) + P_{ss}BR^{-1}B^T P_{ss} = -\dot{P}(x, t) \quad (21)$$

In order to simplify the equation, we define $K(t) \equiv (P(t) - P_{ss})^{-1}$, and obtain (21)

$$\dot{K}(t) = A_{cl}K(t) + K(t)A_{cl}^T - BR^{-1}B^T \quad (22)$$

where $A_{cl} \equiv A - BR^{-1}B^T P_{ss}$. The boundary condition of equation (22) is then

$$K(t_f) = (S - P_{ss})^{-1} \quad (23)$$

By substitution of (22) with a final condition of (23) as shown in [33]

$$K(t) = e^{A_{cl}(t-t_f)}(K(t_f) - E)e^{A_{cl}^T(t-t_f)} + E \quad (24)$$

$$A_{cl}E + EA_{cl}^T = BR^{-1}B^T \quad (25)$$

where E is the solution of the algebraic Lyapunov equation (ALE).

One can use (20), (25) and (24), instead of solving (21) equation, to get the Riccati matrix solution as

$$P(t) = K^{-1}(t) + P_{ss} \quad (26)$$

It should be noted that the authors of [34] recommend the use of the negative definite solution of ARE (20) instead of the positive definite one for P_{ss} in order to avoid possible singularity of $P(t) - P_{ss}$ in case of time-dependent solution of DRE converging to the steady state solution for $t \ll t_f$. If one were to use that idea, replace A in (20) with -A, solve the equation and flip the sign of the solution

2.4. SOLVING STATE DEPENDENT DRE FOR OPTIMAL CONTROL OF NON-LINEAR SYSTEMS

Summary of the solution process and the controller expression are presented in this section. This process needs backward integration and states at the final time are not available. Therefore, there needs to be some approximations made though. That is, at each time, we assume that the states are constant all the way until the final time. First, solve the

following SDRE and ALE at each time step

$$P_{ss}(x)A(x) + A^T(x)P_{ss}(x) - P_{ss}(x)B(x)R^{-1}B^T(x)P_{ss}(x) + Q = 0 \quad (27)$$

$$A_{cl}(x)E(x) + E(x)A_{cl}^T(x) = B(x)R^{-1}B^T(x) \quad (28)$$

where $A_{cl} = A(x) - B(x)R^{-1}B^T(x)P_{ss}(x)$, is closed form solution of A.

Solving the following steps

$$K(x, t) = e^{A_{cl}(t-t_f)}(K(x, t_f) - E(x))e^{A_{cl}^T(x)(t-t_f)} + E(x) \quad (29)$$

$$K(x, t_f) = (S - P_{ss}(x))^{-1} \quad (30)$$

Substituting of (27) and (30) to calculate of P(x,t) is given

$$P(x, t) = K^{-1}(x, t) + P_{ss}(x) \quad (31)$$

In order to solve feedback control, P(x,t) is calculated in (31)

$$u^*(x, t) = -R^{-1}B^T(x)P(x, t)x(t) \quad (32)$$

Note that the computational effort to be carried out in real-time at each time step solving an SDRE and performing two matrix inversions. The assumption that the state values are assumed constant over the entire time at each control calculation can be mitigated by making the control computation frequency fast enough.

3. SIMULATION STUDIES

3.1. KINEMATIC AND DYNAMICS OF AIRCRAFT IN VERTICAL PLANE

In this section the dynamic model of the landing of an impaired aircraft is presented. Assuming zero cross range to the runway, longitudinal dynamics of the aircraft in a vertical plane during the approach and landing phase of an impaired vehicle can be modeled as follows:

$$m(\dot{U} + qW - RV) = X - mg\sin(\theta) \quad (33)$$

$$m(\dot{W} + PV - qU) = Z + mg\cos(\theta)\cos(\phi) \quad (34)$$

$$I_{yy}\dot{q} - RP(I_{xx} - I_{zz}) + (P^2 - R^2)I_{xz} = M \quad (35)$$

where q is a kinematics equation is defined as

$$q = \dot{\theta}\cos(\phi) + \dot{\phi}\cos(\theta)\sin(\phi) \quad (36)$$

where assume $R = V = P = \phi = 0$

$$\dot{U} = -qW + \frac{X}{m} - g\sin(\theta) \quad (37)$$

$$\dot{W} = qU + \frac{Z}{m} + g\cos(\theta) \quad (38)$$

Replacing the vertical velocity W by the angle of attack α leads to

$$\dot{\alpha} = q + \frac{Z}{mU} + \frac{g\cos(\theta)}{U} \quad (39)$$

$$\dot{q} = \frac{M}{I_{yy}} \quad (40)$$

$$\dot{\theta} = q \quad (41)$$

$$\dot{h} = U(\theta - \alpha) \quad (42)$$

The forces in the horizontal and vertical directions are respectively defined as X and Z

$$X = T - D\cos(\alpha) + L\sin(\alpha) \quad (43)$$

$$Z = -L\cos(\alpha) - D\sin(\alpha) \quad (44)$$

The pitching moment equation is expressed as

$$M = M_A + Th_T \quad (45)$$

$$L = \bar{q}S_aC_L \quad (46)$$

$$D = \bar{q}S_aC_D \quad (47)$$

$$M_A = \bar{q}S_aC_{MA\bar{c}} \quad (48)$$

$$\bar{q} = \frac{1}{2}\rho U^2 \quad (49)$$

Assuming an exponential air density profile results in

$$\rho = \rho_0 \exp(-h/H) \quad (50)$$

The lift and drag coefficients are modeled as

$$C_L = C_{L_0} + C_{L_\alpha}\alpha + C_{L_{\delta_e}}\delta_e \quad (51)$$

$$C_D = C_{D_0} + C_{D_\alpha}\alpha \quad (52)$$

$$C_{MA} = C_{M_0} + C_{M_\alpha}\alpha + C_{M_{\delta_e}}\delta_e + C_{M_q}\hat{q} \quad (53)$$

where

$$\hat{q} = \frac{q\bar{c}}{U} \quad (54)$$

Symbols used in expression from (33) to (54) are described below: α is angle of attack, q is pitch rate, θ is pitch angle, h is altitude, U is velocity magnitude, δ_e is elevator deflection, C_D is drag coefficient, C_{D_0} is zero-lift drag coefficient, C_L is lift coefficient, C_{L_0} is zero-angle-of-attack lift coefficient, D is drag force, g is earth's gravitational acceleration, H is scale height, L is lift force, m is aircraft mass, S is aerodynamic reference area, T is thrust, ρ is air density, ρ_0 is sea-level air density, q is dynamic pressure.

The state vector can then be formed as

$$x = [U, \alpha, q, h, \theta]^T \quad (55)$$

where superscript T denotes transpose operation. The cost function to be minimized is assumed quadratic as

$$J = \frac{1}{2}x^T(t_f)Sx(t_f) + \frac{1}{2} \int_{t_0}^{t_f} (x^T Qx + u^T Ru)dt \quad (56)$$

3.2. RESULTS AND DISCUSSION

In this section, sample numerical results are presented with stability derivatives values for Cessna 182. The scenario considered is that of the aircraft experiencing engine failure ($T=0$) and having to land. The integrated path planning and control equations are used in conjunction with the SDRE method to produce the elevator deflection histories to land the aircraft successfully with acceptable level of angle attack histories, elevator angle histories, and velocity histories. In order to investigate the aircraft performance with aerodynamic uncertainties, we introduce lift coefficient and moment coefficient uncertainties in C_{L_α} and C_{m_q} .

For simulating the proposed controller on the aircraft landing path planning problem, the following values have been selected from Cessna 182 airplane values $C_{L_0} = 4.41$, $C_{D_0} = 0.0270$, $K_I = 0.0475$, $S/m = 2.1126 ft^2/slug$ [35], [36]. The uncertainty part is given for this numerical simulation as

$$\begin{aligned} \dot{\alpha} = & \frac{\rho_0 \exp(-h/H) U S ((-C_{L_0} - 0.2 C_{L_\alpha} \alpha - C_{L_{\delta_e}} \delta_e) \cos(\alpha) + (-C_{D_0} - C_{D_\alpha} \alpha) \sin(\alpha))}{2m} \\ & + q + \frac{g \cos(\theta)}{U} + d_1 \end{aligned} \quad (57)$$

where d_1 represents the uncertainty of C_{L_α} in equation (57).

$$d_1 = W^T \phi_1(x) \quad (58)$$

$$\dot{q} = \frac{\rho_0 \exp(-h/H) U^2 S \bar{c} (C_{m_0} + C_{M_\alpha} \alpha + C_{M_{\delta_e}} \delta_e + \frac{0.2 C_{mq} q \bar{c}}{U} + \frac{h_t C_T}{\bar{c}})}{2 I_{yy}} + d_2 \quad (59)$$

where d_2 represents the uncertainty of C_{M_q} in equation (59).

$$d_2 = W^T \phi_2(x) \quad (60)$$

The weight matrices were selected as

$$R = 10^8 \quad (61)$$

$$Q = \text{diag}(10^{-7} \ 10^{-7} \ 10^{-5} \ 10^{-7} \ 10^{-5}) \quad (62)$$

$$S = \text{diag}(0 \ 10^7 \ 0 \ 0 \ 10^7) \quad (63)$$

The system dynamics was simulated for 400 seconds with a time step of 0.1. The initial conditions for the simulation are selected with an initial altitude of 5,000 ft, initial velocity of 220.1 ft/sec, while initial q , α and θ were set at zero.

3.3. SIMULATION RESULTS

In this section, four different simulation results are shown. Note that we use an estimator (modified state observer) in this study though all states are assumed to be measured. This is because the uncertainties in the plant need to be estimated and compensated for. Unlike the typical model reference adaptive control schemes, a state observer is used in conjunction in this study. The advantage of this process is that it allows for learning the uncertainties in a fast manner and yet providing smooth control histories. Typical control oscillations observed with traditional model reference adaptive controllers are completely absent in modified state observer based adaptive control results.

From Figures 1, 3, 5, 8, are worth noting that the maximum angle of attack is only 1.5 degrees. The only variable of concern is the vertical velocity, however, in an impaired condition, one cannot expect a smooth ride. Also, these results are preliminary and with more tuning of weights, it is expected that the maximum magnitude could be kept under control. Note that the estimated states and the actual states are on top of each other.

Note that from Figures 2a, 4a, 6a, 7a, 9a, 10a, that the uncertainties are captured quite well and from Figures 2b, 4b, 6b, 7b, 9b, 10b, that the estimated weights converge to the true weights. This shows the effectiveness of the observer based controller.

When an aircraft is impaired, there may arise a lot of uncertainties in its model. In next four subsequent subsections, we investigate the online computation of uncertainties involving C_{L_α} and C_{m_q}

3.3.1. Simulation Results with One Time Varying Uncertainty. In the first case, we assume that, there is a time varying uncertainty associated with C_{L_α} . Relevant uncertainty term in C_{L_α} is given by

$$d_1 = \frac{0.8\rho_0 \exp(-h/H) U S C_{L_\alpha}(\alpha) \cos(\alpha)}{2m} \quad (64)$$

Corresponding basis function in equation (58) is assumed as

$$\phi_1(x) = U \quad (65)$$

The adaptation gain and a σ modification factor were chosen as 0.1 and 0.01, respectively.

An estimation error feedback gain matrix $K_2 = \text{diag}(10^{-3} \ 10^{-5} \ 10^{-3} \ 10^{-3} \ 10^{-3})$ was used.

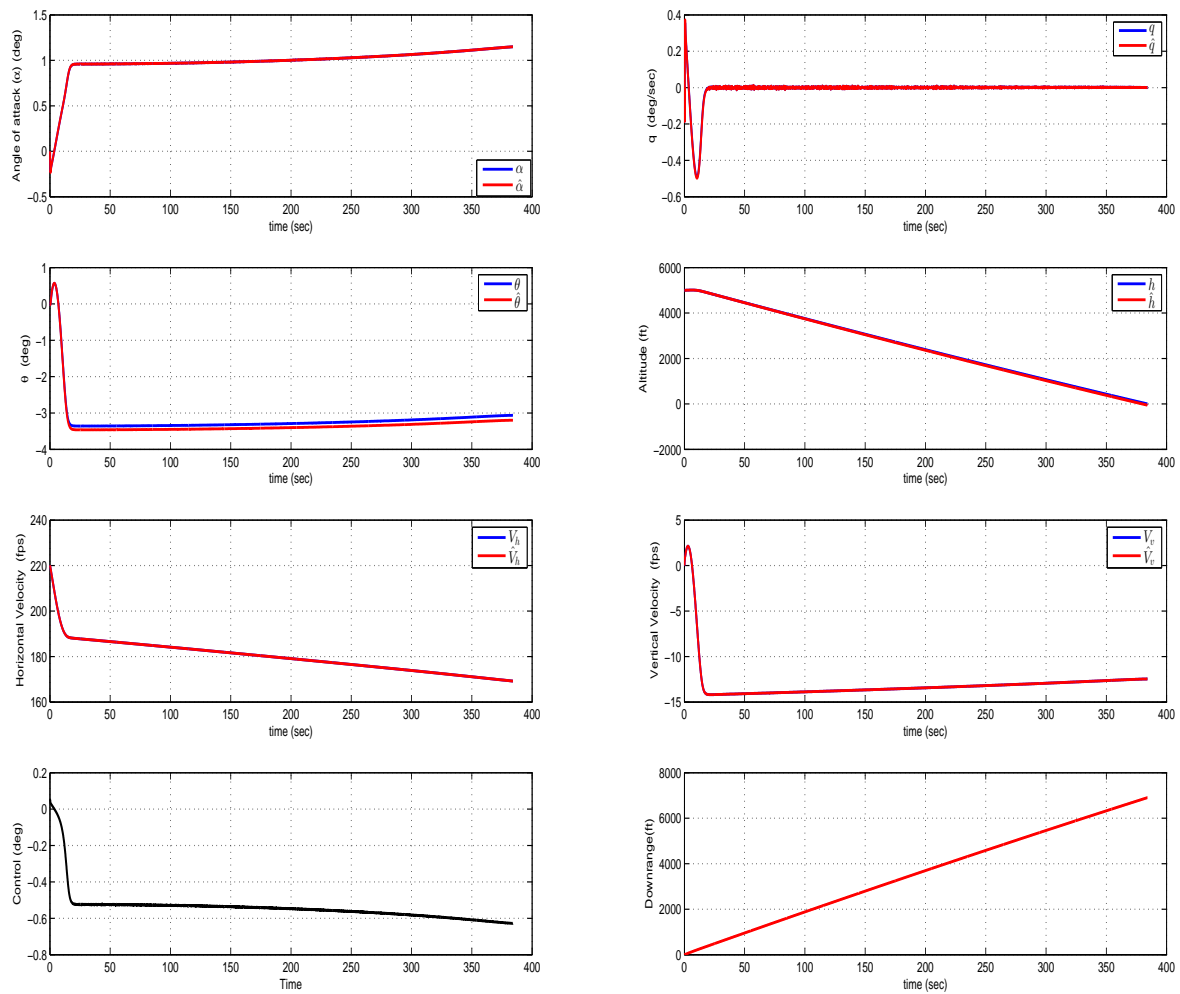


Figure 1. Histories of actual and estimated states, downrange and control [one time varying uncertainty]

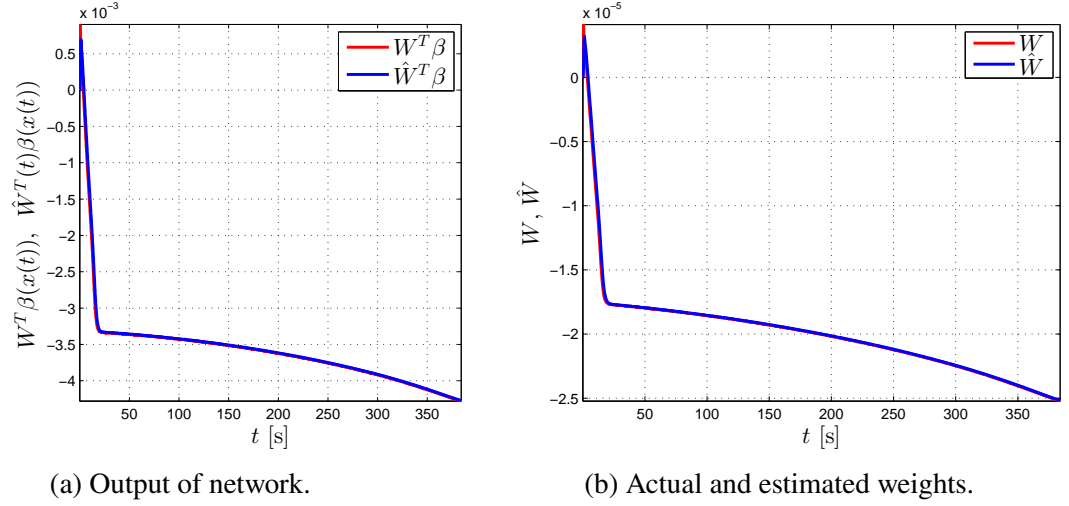


Figure 2. History of uncertainty estimation with time [time varying C_{L_α} uncertainty].

3.3.2. Simulation Results with One Constant Uncertainty. In the second case, we assume that, there is a constant uncertainty associated with C_{L_α} . Relevant uncertainty term in C_{L_α} is given by

$$d_1 = \frac{0.8\rho_0 \exp(-h/H) US C_{L_\alpha}(\alpha) \cos(\alpha)}{2m} \quad (66)$$

Corresponding basis function in equation (58) is assumed as

$$\phi_1(x) = \frac{\rho_0 \exp(-h/H) US(\alpha) \cos(\alpha)}{2m} \quad (67)$$

The adaptation gain and a σ modification factor were chosen as 10 and 0.00001, respectively. An estimation error feedback gain matrix $K_2 = \text{diag}(10^{-4} \ 10^{-11} \ 10^{-5} \ 10^{-4} \ 10^1)$ was used.

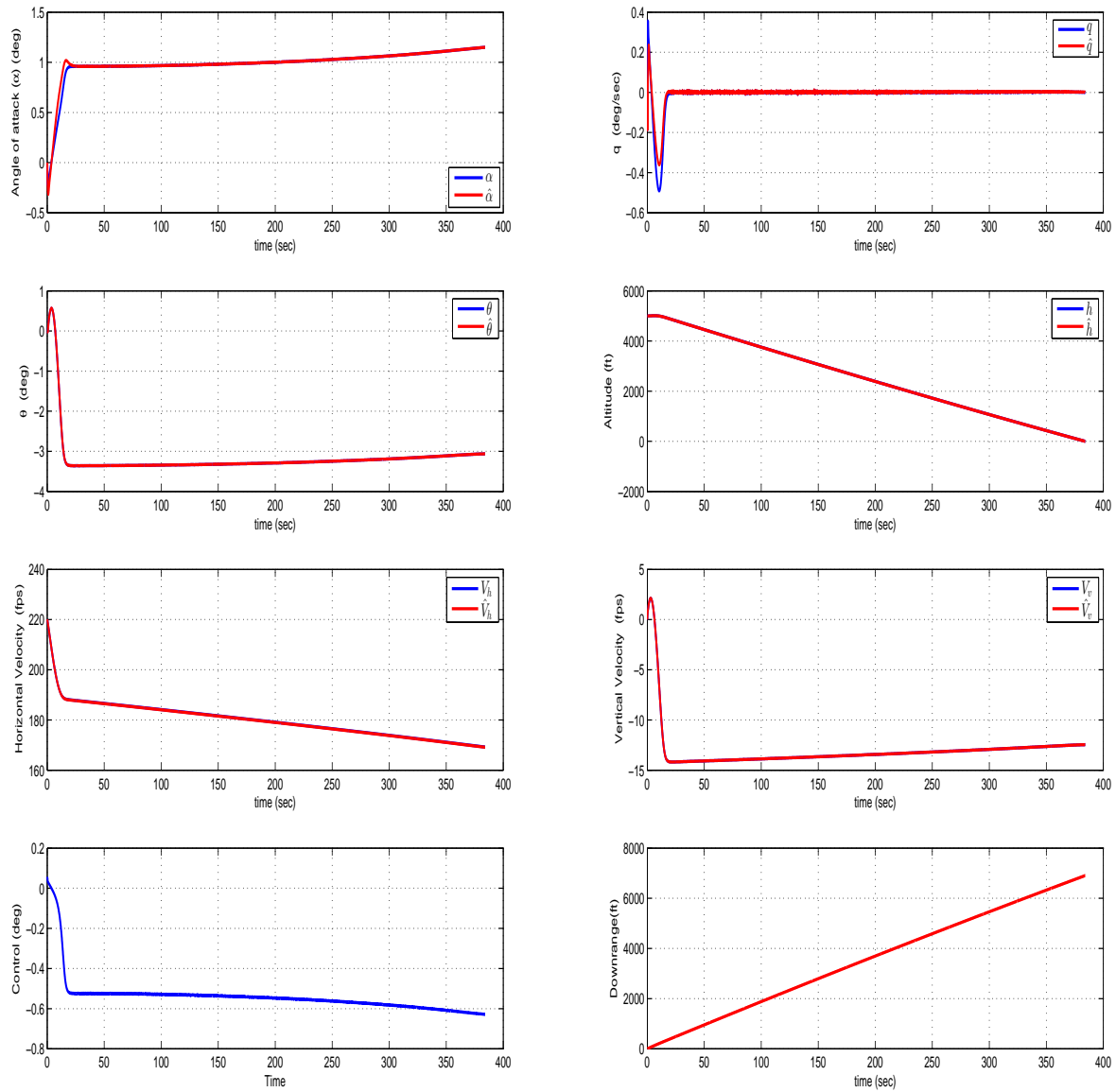
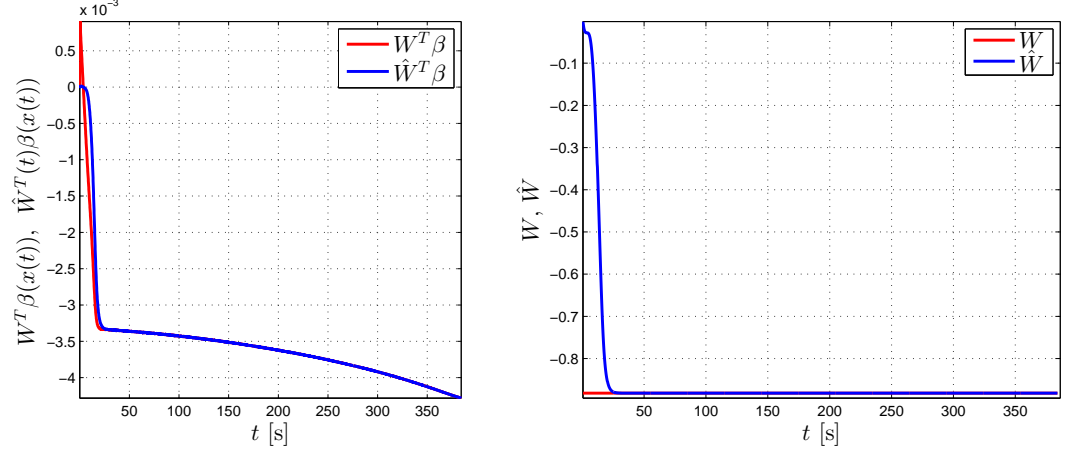


Figure 3. Histories of actual and estimated states, downrange and control [one constant uncertainty]



(a) Output of network.

(b) Actual and estimated weights.

Figure 4. History of uncertainty estimation with time [constant C_{L_α} uncertainty].

3.3.3. Simulation Results with Two Constant Uncertainties. In the third case, we assume that, there are constant uncertainties associated with C_{L_α} and C_{m_q} . Relevant uncertainty term in C_{L_α} is given by

$$d_1 = \frac{0.8\rho_0 \exp(-h/H)USC_{L_\alpha}(\alpha)\cos(\alpha)}{2m} \quad (68)$$

Corresponding basis function in equation (58) is assumed as

$$\phi_1(x) = \frac{\rho_0 \exp(-h/H)US(\alpha)\cos(\alpha)}{2m} \quad (69)$$

Relevant uncertainty term in C_{m_q} is given by

$$d_2 = \frac{0.8\rho_0 \exp(-h/H)US\bar{c}^2 qUC_{m_q}}{I_{yy}} \quad (70)$$

Corresponding basis function in equation (60) is assumed as

$$\phi_2(x) = \frac{\rho_0 \exp(-h/H)US\bar{c}^2 qU}{I_{yy}} \quad (71)$$

The adaptation gains were chosen as 0.1 and 0.01. The two σ modification factors were chosen as 0.001 and 0.0001. An estimation error feedback gain matrix $K_2 = \text{diag}(10^{-3} \ 10^{-14} \ 10^{-12} \ 10^{-1} \ 10^1)$ was used.

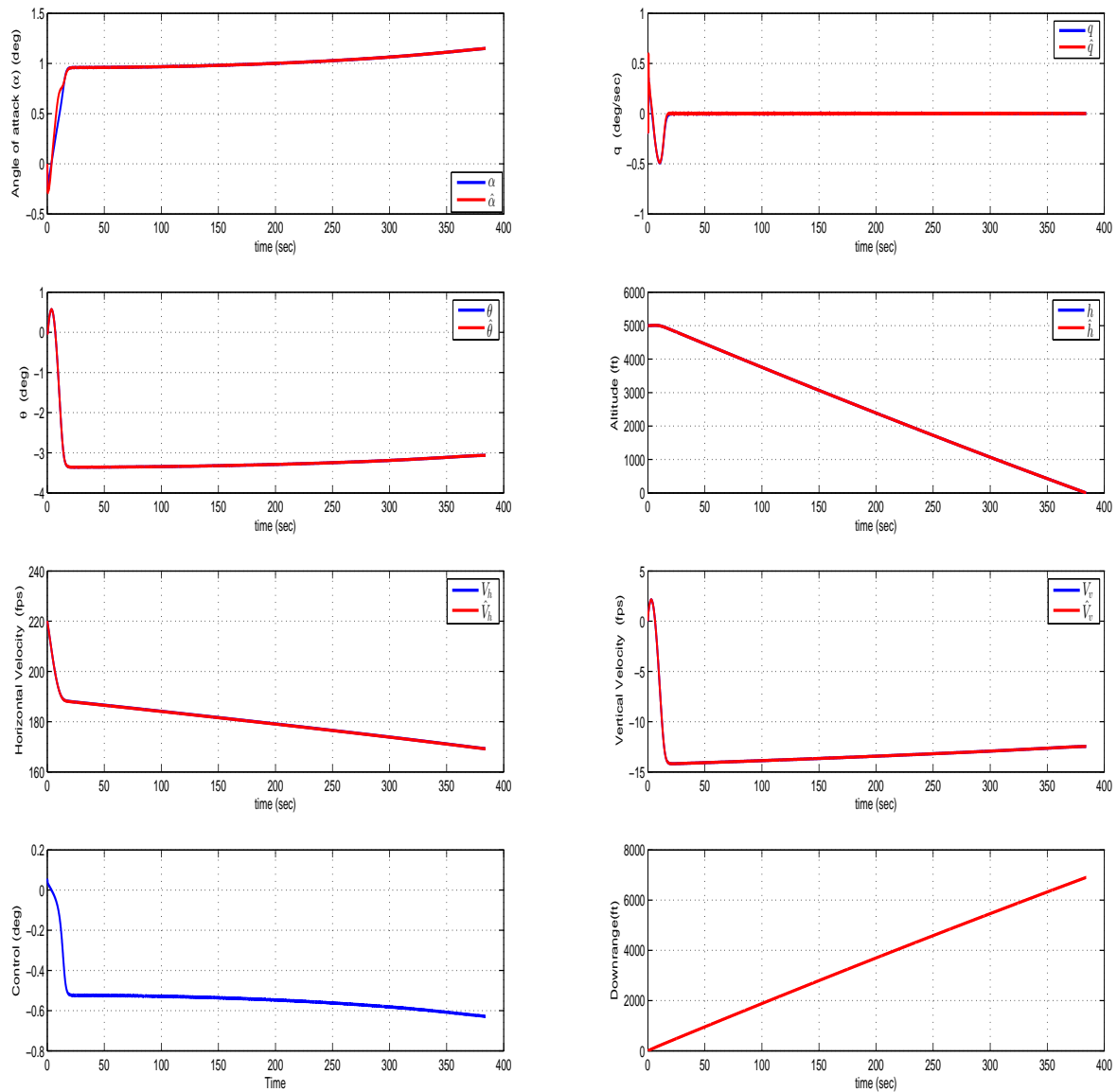
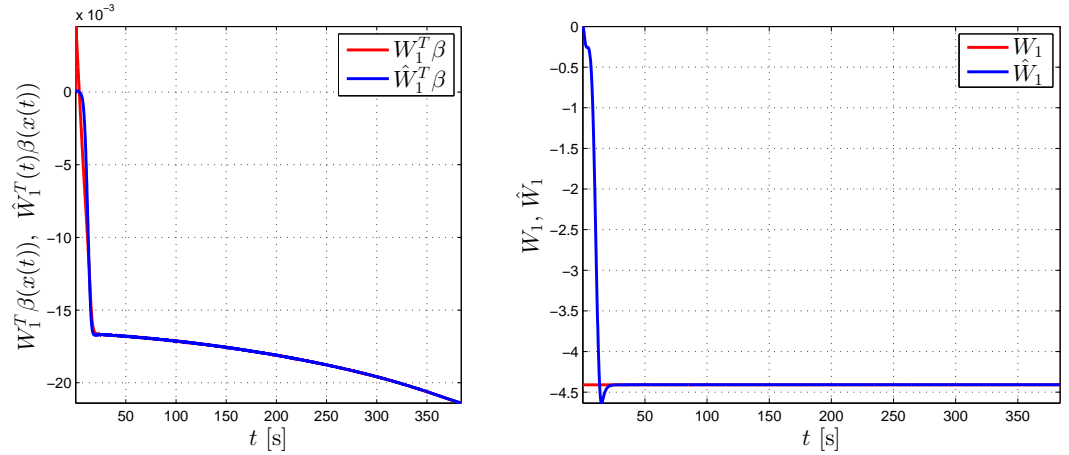
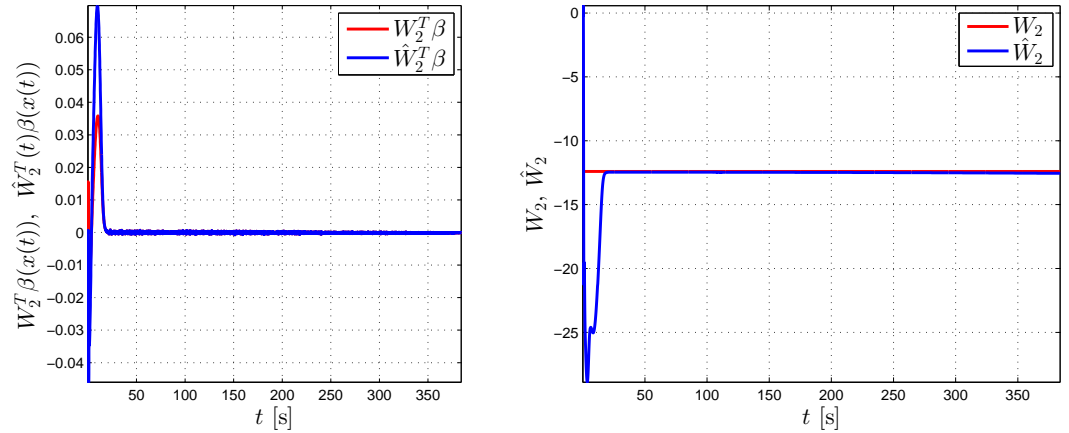


Figure 5. Histories of actual and estimated states, downrange and control [two constant uncertainties]



(a) Output of network.

(b) Actual and estimated weights.

Figure 6. History of two uncertainties estimation with time [constant $C_{L\alpha}$ uncertainty].

(a) Output of network.

(b) Actual and estimated weights.

Figure 7. History of two uncertainties estimation with time [constant C_{m_q} uncertainty].

3.3.4. Simulation Results with Two Time Varying Uncertainties. In the last case, we assume that, there are time varying uncertainties associated with $C_{L\alpha}$ and C_{m_q} . Relevant uncertainty term in $C_{L\alpha}$ is given by

$$d_1 = \frac{0.8\rho_0 \exp(-h/H) U S C_{L\alpha}(\alpha) \cos(\alpha)}{2m} \quad (72)$$

Corresponding basis function in equation (58) is assumed as

$$\phi_1(x) = U \quad (73)$$

Relevant uncertainty term in C_{m_q} is given by

$$d_2 = \frac{0.8\rho_0 \exp(-h/H)US\bar{c}^2 qUC_{m_q}}{I_{yy}} \quad (74)$$

Corresponding basis function in equation (60) is assumed as

$$\phi_2(x) = U \quad (75)$$

The adaptation gains were chosen as 100 and 0.1. The two σ modification factors were chosen 0.0001 and 0.0001. An estimation error feedback gain matrix

$K_2 = \text{diag}(10^{-3} \ 10^{-2} \ 10^{-1} \ 10^{-2} \ 10^{-3})$ was used.

4. CONCLUSIONS

An integrated path planning-controller approach was presented in this study. Equations with kinematics and dynamics were used in the process. An optimal control based controller was used to shape the impaired aircraft's path to safe landing. Furthermore, an adaptive control algorithm based on a modified state observer was used to further account for aerodynamic uncertainties. Sample results show that the integrated path planning and control has good potential to be used for safe flight and landing of impaired aircraft.

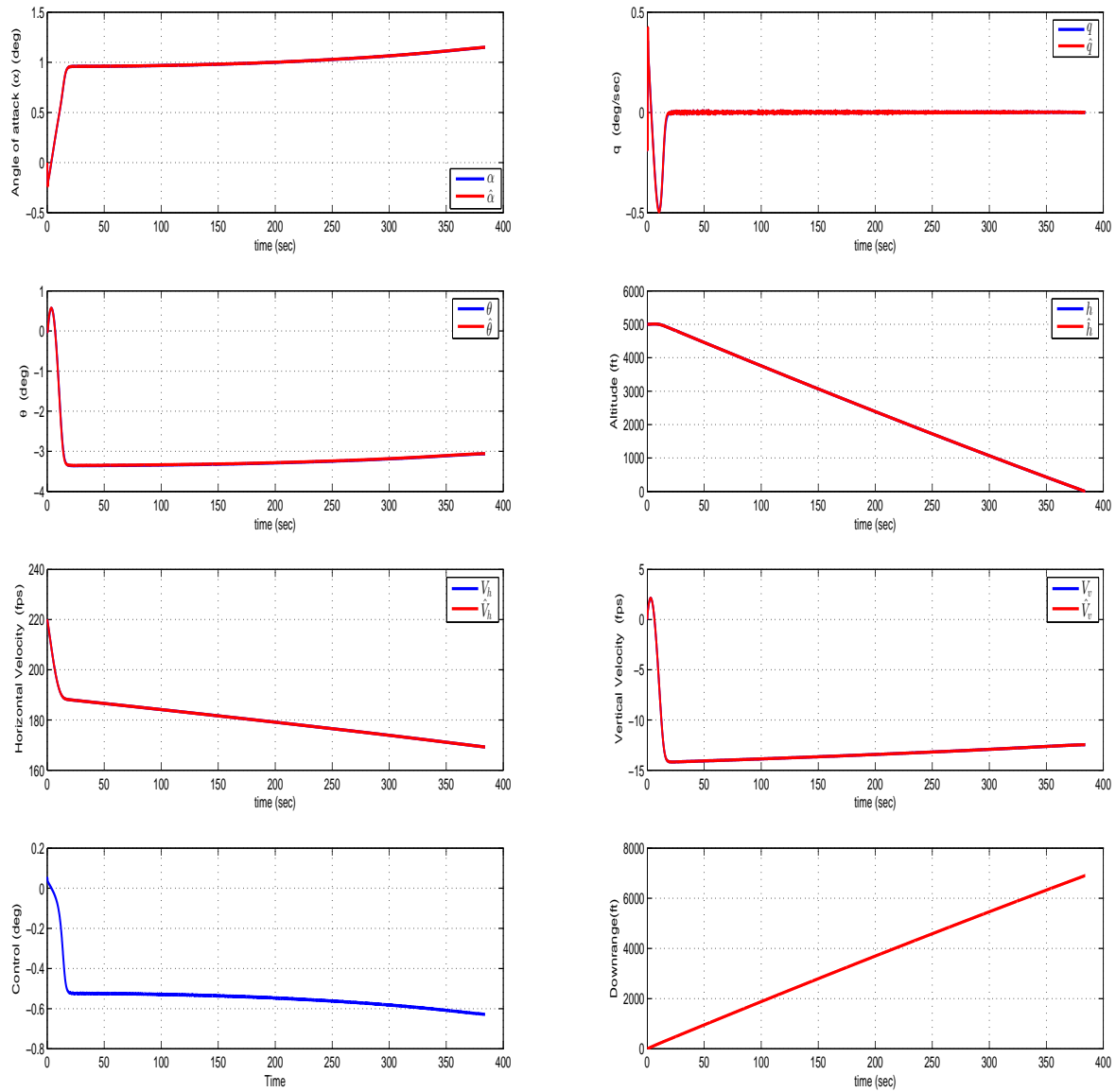
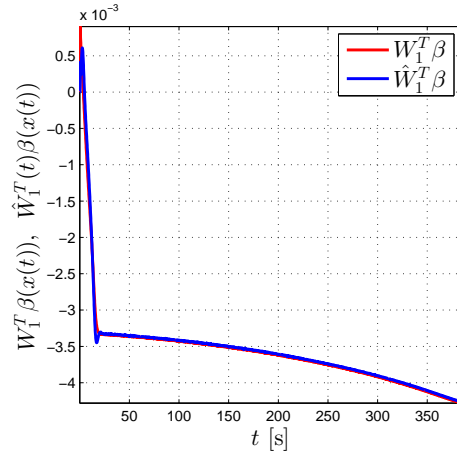


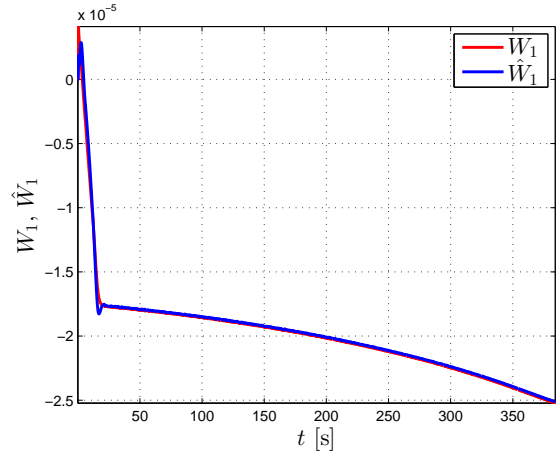
Figure 8. Histories of actual and estimated states, downrange and control [two time varying uncertainties]

ACKNOWLEDGEMENTS

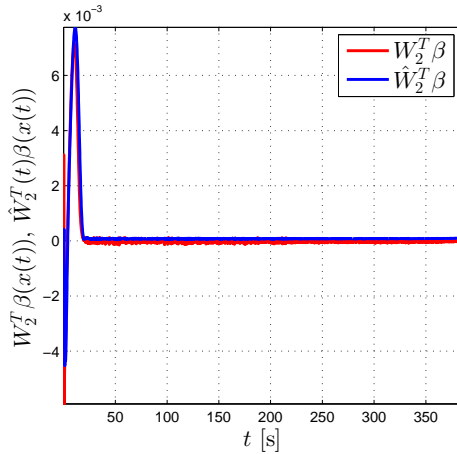
This study was supported in part by the NASA grant NNX15AM51A.



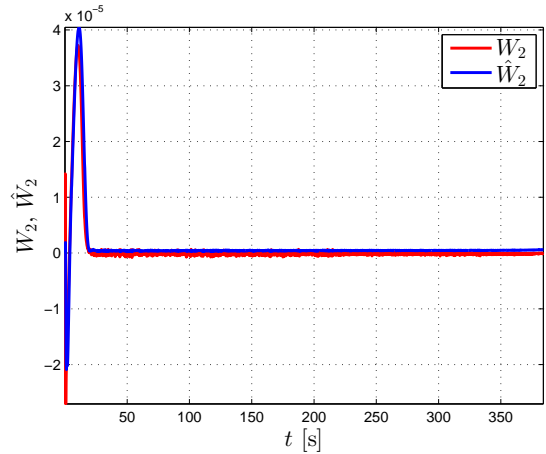
(a) Output of network.



(b) Actual and estimated weights.

Figure 9. History of two uncertainties estimation with time [variable C_{L_α} uncertainty].

(a) Output of network.



(b) Actual and estimated weights.

Figure 10. History of two uncertainties estimation with time [variable C_{m_q} uncertainty].

REFERENCES

- [1] Baba, Y., Takano, H., and Sano, M., ‘Desired trajectory and guidance force generators for an aircraft,’ in ‘Guidance, Navigation, and Control Conference,’ 1996 p. 3873.
- [2] Menon, P., Badgett, M., Walker, R., and Duke, E., ‘Nonlinear flight test trajectory controllers for aircraft,’ *Journal of Guidance, Control, and Dynamics*, 1987, **10**(1), pp. 67–72.
- [3] Kaminer, I., Pascoal, A., Hallberg, E., and Silvestre, C., ‘Trajectory tracking for autonomous vehicles: An integrated approach to guidance and control,’ *Journal of Guidance, Control, and Dynamics*, 1998, **21**(1), pp. 29–38.
- [4] Boyle, D. P. and Chamitoff, G. E., ‘Autonomous maneuver tracking for self-piloted vehicles,’ *Journal of Guidance, Control, and Dynamics*, 1999, **22**(1), pp. 58–67.

- [5] Ochi, S., Takano, H., and Baba, Y., 'Flight trajectory tracking system applied to inverse control for aerobatic maneuvers,' in 'Inverse Problems in Engineering Mechanics III,' pp. 337–344, Elsevier, 2002.
- [6] Rysdyk, R., 'Unmanned aerial vehicle path following for target observation in wind,' *Journal of guidance, control, and dynamics*, 2006, **29**(5), pp. 1092–1100.
- [7] Baba, Y. and Takano, H., 'Robust flight trajectory tracking control using fuzzy logic,' *Proc. the 8th ISDG&A*, 1998, pp. 68–75.
- [8] Sato, Y., Yamasaki, T., Takano, H., and Baba, Y., 'Trajectory guidance and control for a small uav,' *International Journal of Aeronautical and Space Sciences*, 2006, **7**(2), pp. 137–144.
- [9] Yamasaki, T., Sakaida, H., Enomoto, K., Takano, H., and Baba, Y., 'Robust trajectory-tracking method for uav guidance using proportional navigation,' in 'Control, Automation and Systems, 2007. ICCAS'07. International Conference on,' IEEE, 2007 pp. 1404–1409.
- [10] Machol, R. E., 'System engineering handbook,' New York: McGraw-Hill, 1965, edited by Machol, RE, 1965.
- [11] Park, S., Deyst, J., and How, J., 'A new nonlinear guidance logic for trajectory tracking,' in 'AIAA guidance, navigation, and control conference and exhibit,' 2004 p. 4900.
- [12] Park, S., Deyst, J., and How, J. P., 'Performance and lyapunov stability of a nonlinear path following guidance method,' *Journal of Guidance, Control, and Dynamics*, 2007, **30**(6), pp. 1718–1728.
- [13] Blajer, W., 'Aircraft program motion along a predetermined trajectory part ii. numerical simulation with application of spline functions to trajectory definitions,' *The Aeronautical Journal*, 1990, **94**(932), pp. 53–58.
- [14] Harl, N., Balakrishnan, S., and Phillips, C., 'Sliding mode integrated missile guidance and control,' in 'AIAA Guidance, Navigation, and Control Conference,' 2010 p. 7741.
- [15] Galzi, D. and Shtessel, Y., 'Uav formations control using high order sliding modes,' in 'American Control Conference, 2006,' IEEE, 2006 pp. 6–pp.
- [16] Shkolnikov, I. A. and Shtessel, Y. B., 'Aircraft nonminimum phase control in dynamic sliding manifolds,' *Journal of Guidance, Control, and Dynamics*, 2001, **24**(3), pp. 566–572.
- [17] Shtessel, Y. B., Shkolnikov, I. A., and Levant, A., 'Guidance and control of missile interceptor using second-order sliding modes,' *IEEE Transactions on Aerospace and Electronic Systems*, 2009, **45**(1), pp. 110–124.
- [18] Shima, T., Idan, M., and Golan, O. M., 'Sliding-mode control for integrated missile autopilot guidance,' *Journal of guidance, control, and dynamics*, 2006, **29**(2), pp. 250–260.

- [19] Levant, A., ‘Quasi-continuous high-order sliding mode controllers,’ *IEEE TRANSACTIONS ON AUTOMATIC CONTROL*, 2005, **50**(11), pp. 1812–1816.
- [20] Levant, A., ‘Homogeneity approach to high-order sliding mode design,’ *Automatica*, 2005, **41**(5), pp. 823–830.
- [21] Harl, N. and Balakrishnan, S., ‘Reentry terminal guidance through sliding mode control,’ *Journal of guidance, control, and dynamics*, 2010, **33**(1), pp. 186–199.
- [22] Yamasaki, T., Balakrishnan, S., and Takano, H., ‘Separate-channel integrated guidance and autopilot for a path-following uav via high-order sliding modes,’ in ‘AIAA Guidance, Navigation, and Control Conference,’ 2012 p. 4457.
- [23] Rajagopal, K., Balakrishnan, S., Nguyen, N., and Krishnakumar, K., ‘Robust adaptive control of a structurally damaged aircraft,’ in ‘AIAA Guidance, Navigation, and Control Conference,’ 2010 p. 8012.
- [24] Rajagopal, K., Balakrishnan, S., Nguyen, N., Krishnakumar, K., and Mannava, A., ‘Neuroadaptive model following controller design for non-affine and non-square aircraft systems,’ in ‘AIAA Guidance, Navigation, and Control Conference,’ 2009 p. 5737.
- [25] Huang, Z. and Balakrishnan, S., ‘Robust adaptive critic based neurocontrollers for helicopter with unmodeled uncertainties,’ in ‘AIAA Atmospheric Flight Mechanics Conference and Exhibit,’ 2001 p. 4258.
- [26] Ham, F. M. and Kostanic, I., *Principles of neurocomputing for science and engineering*, McGraw-Hill Higher Education, 2000.
- [27] Cloutier, J. R., ‘State-dependent riccati equation techniques: an overview,’ in ‘American Control Conference, 1997. Proceedings of the 1997,’ volume 2, IEEE, 1997 pp. 932–936.
- [28] Cloutier, J. R. and Stansbery, D. T., ‘The capabilities and art of state-dependent riccati equation-based design,’ in ‘American Control Conference, 2002. Proceedings of the 2002,’ volume 1, IEEE, 2002 pp. 86–91.
- [29] Heydari, A. and Balakrishnan, S., ‘Path planning using a novel finite horizon suboptimal controller,’ *Journal of guidance, control, and dynamics*, 2013.
- [30] Heydari, A. and Balakrishnan, S., ‘Optimal online path planning for approach and landing guidance,’ in ‘Proc. AIAA Atmospheric Flight Mechanics Conference, Portland, OR,’ 2011 .
- [31] Anderson, B. D. and Moore, J. B., *Linear optimal control*, volume 197, Prentice-Hall Englewood Cliffs, 1971.
- [32] Nazarzadeh, J., Razzaghi, M., and Nikravesh, K., ‘Solution of the matrix riccati equation for the linear quadratic control problems,’ *Mathematical and Computer Modelling*, 1998, **27**(7), pp. 51–55.

- [33] Barraud, A., 'A new numerical solution of $\dot{X} = a_1 x + a_2 x^2 + d, x(0) = c$,' Automatic Control, IEEE Transactions on, 1977, **22**(6), pp. 976–977.
- [34] Nguyen, T. and Gajic, Z., 'Solving the matrix differential riccati equation: a lyapunov equation approach,' Automatic Control, IEEE Transactions on, 2010, **55**(1), pp. 191–194.
- [35] McRuer, D., Ashkenas, I., and Graham, D., 'Aircraft dynamics and automatic control,' Technical report, DTIC Document, 1968.
- [36] Roskam, J., *Airplane flight dynamics and automatic flight controls*, number pt. 1 in Airplane Flight Dynamics and Automatic Flight Controls, DARcorporation, 1995, ISBN 9781884885174.

II. SLIDING MODE BASED PATH PLANNING AND CONTROL OF IMPAIRED AIRCRAFT

Meryem Deniz¹, Takeshi Yamasaki², S. N. Balakrishnan¹, Tansel Yucelen³

¹Department of Mechanical & Aerospace Engineering
Missouri University of Science and Technology
Rolla, Missouri 65409–0050, United States of America

²Department of Aerospace Engineering
National Defense Academy

Hashirimizu, Yokosuka 1-10-20, Japan

³Department of Mechanical Engineering
University of South Florida

Tampa, Florida 33620, United States of America

ABSTRACT

In this study, the problem of integrated path planning and control of an impaired aircraft is formulated and solved by using a second order sliding mode control (SOSM) and a high order sliding mode (HOSM) differentiator. As an example problem, the case of an impaired aircraft with a frozen elevator is considered. The thrust alone is used as the controller to land the aircraft safely. Representative simulations are presented to demonstrate the performance of proposed controller.

1. INTRODUCTION

There has been a lot of interest in unmanned air vehicle (UAV) flights in the last two decades. Such flights have a path to follow and need a controller to keep them on the desired path. A tracking-error-correction approach has been used for guidance and control systems for path-following flights [1, 2, 3, 4, 5, 6]. However, such designs have drawbacks when tracking errors become large; for example, if the trajectory is a steep, curved path or if wind turbulence exists, the error based techniques can cause control saturation or

divergence since the control command magnitudes are usually proportional to the tracking-errors. Pure pursuit guidance (PPG) is a robust method for path following UAV [7]. Note that the PPG requires only one gain to be tuned. It produces guidance commands that are not dependent on tracking errors and are of reasonable magnitudes. Consequently, the PPG based control helps eliminate control divergence; Park et. al. [8, 9] use a similar approach where the distance error is restricted to a pre-specified value. Performance and stability analysis are presented for nonlinear pure pursuit based path following guidance method [9]. This method shows the asymptotic Lyapunov stability of the nonlinear guidance method when the UAV follows reference circular paths. The method of dynamic inversion is used to control the vehicle and the proportional navigation method is used to guide the trajectory [10, 11]. There are other methods such as sliding mode based integrated guidance and control (SMIGC) concepts used in missile applications. An SMIGC scheme was proposed by Harl et. al. in [12] for missile intercept against weaving targets. Their technique showed robust performance against uncertain target maneuvers. Shtessel has published several papers based on sliding mode [13, 14, 15] techniques for different applications. HOSM was applied to UAV formation flying in Galzi and Shtessel [13] for guidance alone. A sliding mode guidance and autopilot methodology was developed based on a zero-effort-miss guidance concept by Shima, et. al. [16] for missile applications. Sliding mode control (SMC) for a non-minimum phase system was proposed in Shkolnikov and Shtessel [14]. HOSM (e.g., [17, 18, 15, 19]) mitigates the chatter problems associated with SMC, i.e., HOSM is applicable for arbitrary relative degree systems with smooth control. Shtessel et. al. [15] also applied an HOSM for missile interception against uncertain target maneuvers. Note that the many missiles are described as “skid-to-turn” which means that they hardly use any roll motion. The aircraft motion however is different. An integrated tracking and control scheme was proposed and tested on numerical simulations by Yamasaki et. al. [20]. In this study, an integrated path planning and controller problem for an aircraft is proposed. The kinematics and dynamics equations of an aircraft in vertical plane are used. An SOSM

formulation is used to design the control that will land the aircraft safely. Furthermore, a higher order sliding mode differentiator is used to estimate the uncertainties in the dynamic model. The rest of the paper is organized as follows: Kinematic and dynamics equations of aircraft in a vertical plane are given in Section 2. Section 3, the procedure of integrated path planning and controller design is described. In Section 4, A representative set of plots are presented from numerical simulations. Conclusions from this study are given in Section 5.

2. KINEMATIC AND DYNAMICS OF AIRCRAFT IN VERTICAL PLANE

In this section the mathematical model of a fixed wing aircraft is presented [21]. Figure 1 shows the flight dynamics of the fixed wing aircraft. The kinematic and dynamics model of aircraft are given as

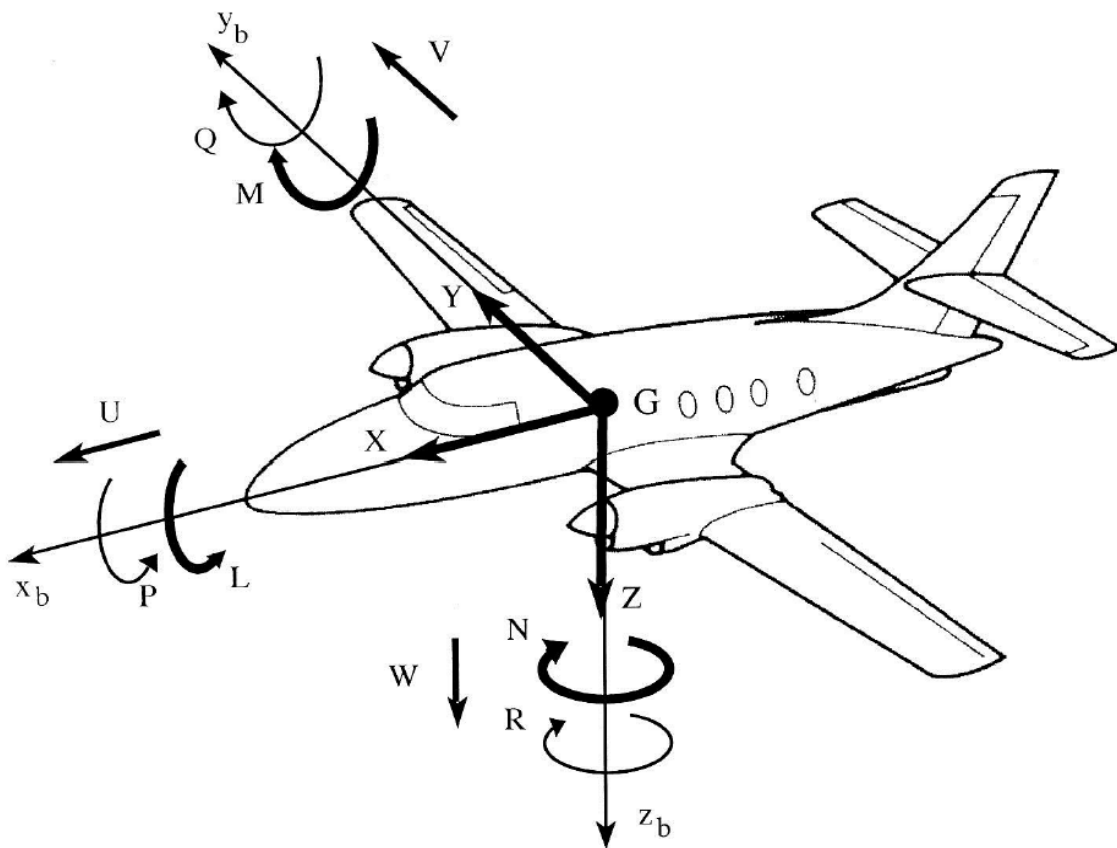


Figure 1. Flight dynamics of the fixed wing aircraft

$$\dot{U} = -QW + \frac{X}{m} - g \sin(\theta) \quad (1)$$

$$\dot{W} = QU + \frac{Z}{m} + g \cos(\theta) \quad (2)$$

$$\dot{Q} = \frac{M}{I_{yy}} \quad (3)$$

$$\dot{\theta} = Q \quad (4)$$

$$\dot{X}_E = U \cos(\theta) + W \sin(\theta) \quad (5)$$

$$\dot{Z}_E = -U \sin(\theta) + W \cos(\theta) \quad (6)$$

The forces in the x_b and z_b directions are denoted respectively as X and Z

$$X = T - D \cos(\alpha) + L \sin(\alpha) \quad (7)$$

$$Z = -L \cos(\alpha) - D \sin(\alpha) \quad (8)$$

The pitching moment equation is expressed as

$$M = M_A + Th_T \quad (9)$$

$$L = \bar{q} S_a C_L \quad (10)$$

$$D = \bar{q} S_a C_D \quad (11)$$

$$M_A = \bar{q} S_a C_{MA} \bar{c} \quad (12)$$

$$\bar{q} = \frac{1}{2} \rho (U^2 + W^2) \quad (13)$$

Assuming an exponential air density profile results in

$$\rho = \rho_0 \exp(-h/H) \quad (14)$$

The lift and drag coefficients are modeled as

$$C_L = C_{L_0} + C_{L_\alpha} \alpha + C_{L_{\delta_e}} \delta_e \quad (15)$$

$$C_D = C_{D_0} + C_{D_\alpha} \alpha \quad (16)$$

$$C_{MA} = C_{M_0} + C_{M_\alpha} \alpha + C_{M_{\delta_e}} \delta_e + C_{M_q} \hat{q} \quad (17)$$

where

$$\hat{q} = \frac{Q\bar{c}}{\sqrt{U^2 + W^2}} \quad (18)$$

Symbols used in expression from (1) to (18) are described below: α is the angle of attack, Q is the pitch rate, θ is the pitch angle, h is the altitude, U and W are the velocity components in x_b and z_b directions, respectively. X_E and Z_E are the position components in earth fixed coordinates. δ_e is the elevator deflection, C_D is the drag coefficient, C_{D_0} is the zero-lift drag coefficient, C_L is the lift coefficient, C_{L_0} is the zero-angle-of-attack lift coefficient, D represents the drag force, g is the earth's gravitational acceleration, H is the scale height, L is the lift force, m is the aircraft mass, S is the aerodynamic reference area, T is the thrust force, ρ is the air density, ρ_0 is the sea-level air density, \bar{q} is the dynamic pressure, h_T is the distance of the thrustline above the x_b axis. The state vector can then be formed as

$$x = [U, W, Q, \theta, X_E, Z_E]^T \quad (19)$$

where superscript ($'$) denotes transposition. These equations are rearranged for later use as

$$\dot{U} = a + \frac{\rho_0 \exp(-h/H)(U^2 + W^2)S(C_T)}{2m} \quad (20)$$

where

$$a = -QW - g \sin(\theta) + \frac{\rho_0 \exp(-h/H)(U^2 + W^2)S(-(C_{D_0} + C_{D_\alpha} \alpha) \cos(\alpha)) + (C_{L_0} + C_{L_\alpha} \alpha + C_{L_{\delta_e}} \delta_e) \sin(\alpha)}{2m} \quad (21)$$

$$\dot{W} = QU + b \quad (22)$$

where

$$b = \frac{\rho_0 \exp(-h/H)(U^2 + W^2)S(-(C_{D_0} + C_{D_\alpha} \alpha) \sin(\alpha)) - (C_{L_0} + C_{L_\alpha} \alpha + C_{L_{\delta_e}} \delta_e) \cos(\alpha)}{2m} + g \cos(\theta) \quad (23)$$

$$\dot{Q} = d + \frac{\rho_0 \exp(-h/H)(U^2 + W^2)S\bar{c} \frac{h_T C_T}{\bar{c}}}{2I_{yy}} \quad (24)$$

where

$$d = \frac{\rho_0 \exp(-h/H)(U^2 + W^2)S\bar{c}(C_{M_0} + C_{M_\alpha} \alpha + C_{M_{\delta_e}} \delta_e + \frac{C_{M_q} Q \bar{c}}{\sqrt{U^2 + W^2}})}{2I_{yy}} \quad (25)$$

$$\dot{\theta} = Q \quad (26)$$

3. INTEGRATED PATH PLANNING AND CONTROLLER DESIGN

The dynamics and kinematics equations required for integrated path planning and controller design are presented in this section. The controller objective is to land the impaired aircraft safely, that is make the final altitude zero. Note that $h = -Z_E$. In this study, the control input is chosen as thrust term (C_T). The position coordinate does not have the thrust term explicitly. Therefore, the relation between position coordinate and control input should be designed. We should take the time derivative of position earth fixed coordinate with z pointing down until the control input appears. In our case, the control input appears in the second derivative.

3.1. SLIDING SURFACE DESIGN

The error between actual and desired altitude is defined as

$$s = h - h_c \quad (27)$$

where h_c is the desired altitude which is designed by using straight line. However, for further extension we will use a waypoint-based path generation with cubic spline functions [20],[22]. The h and the h_c are replaced as $(-Z_E)$ and $(-Z_c)$, respectively.

$$s = (-Z_E + Z_c) \quad (28)$$

Taking the first and second time derivatives of equation (28) as given

$$\dot{s} = (-\dot{Z}_E + \dot{Z}_c) \quad (29)$$

$$\ddot{s} = (-\ddot{Z}_E + \ddot{Z}_c) \quad (30)$$

where \dot{Z}_E has already defined in equation (6). After taking the time derivative of equation (6), the \ddot{Z}_E can be calculated as

$$\ddot{Z}_E = -\dot{U} \sin(\theta) + \dot{W} \cos(\theta) - U \cos(\theta)\dot{\theta} - W \sin(\theta)\dot{\theta} \quad (31)$$

By substituting equations (20), (22) and (4) into (31), \ddot{Z}_E becomes

$$\begin{aligned} \ddot{Z}_E = & - \left[a + \frac{\rho_0 \exp(-h/H)(U^2 + W^2)S(C_T)}{2m} \right] \sin(\theta) \\ & - U \cos(\theta)Q - W \sin(\theta)Q + [QU + b] \cos(\theta) \end{aligned} \quad (32)$$

$$\ddot{Z}_E = \eta - \frac{\rho_0 \exp(-h/H)(U^2 + W^2)S(C_T) \sin(\theta)}{2m} \quad (33)$$

where η is defined as an uncertainty for later use and is given by

$$\eta = -a \sin(\theta) + QU \cos(\theta) + b \cos(\theta) - U \cos(\theta)Q - W \sin(\theta)Q \quad (34)$$

The sliding surface can be constructed as

$$\sigma = \dot{s} + K_1 s \quad (35)$$

where $K_1 > 0$ is a design parameter. In order to show dynamics of sliding surface, the time derivative of (35) is calculated as

$$\dot{\sigma} = \ddot{s} + K_1 \dot{s} \quad (36)$$

By substituting equations (6) and (33) into (36)

$$\dot{\sigma} = \eta + \frac{\rho_0 \exp(-h/H)(U^2 + W^2)S(C_T) \sin(\theta)}{2m} + \ddot{Z}_c + K_1 (-\dot{Z}_E + \dot{Z}_c) \quad (37)$$

$$\dot{\sigma} = \frac{\rho_0 \exp(-h/H)(U^2 + W^2)S(C_T) \sin(\theta)}{2m} + \varphi \quad (38)$$

where

$$\varphi = \eta + \ddot{Z}_c + K_1 (-\dot{Z}_E + \dot{Z}_c) \quad (39)$$

where φ is defined as unknown vector. A high order sliding mode is used to estimate φ .

$$\dot{\sigma} = \varphi + \tilde{u} \quad (40)$$

where

$$\tilde{u} = \frac{\rho_0 \exp(-h/H)(U^2 + W^2)S(C_T) \sin(\theta)}{2m} \quad (41)$$

$$C_T = \frac{2m\tilde{u}}{\rho_0 \exp(-h/H)(U^2 + W^2)S(\sin(\theta))} \quad (42)$$

3.2. SECOND-ORDER SLIDING MODE FRAMEWORK AND HIGH-ORDER SLIDING MODE DIFFERENTIATOR

An SOSM is used in this study for designing the controller an HOSM differentiator is designed to estimate the unknown parameters/expressions in the proposed method. In this section, the SOSM and HOSM equations are derived. The objective here is to design a sliding surface to drive to altitude zero.

3.2.1. Second-Order Sliding Mode Framework. The general form of derivative of σ dynamics is given in following statements

$$\dot{\sigma} = \varphi + \tilde{u} \quad (43)$$

where φ is unknown terms and \tilde{u} is control input. The compensated σ dynamics is chosen similar to [15], [20]

$$\dot{\sigma} = -\alpha_1 |\sigma|^{\nu_1} \text{sign}(\sigma) + \omega \quad (44)$$

$$\dot{\omega} = -\alpha_2 |\sigma|^{\nu_2} \text{sign}(\sigma) \quad (45)$$

where ω represents an integral term related to σ , and $\alpha_1, \alpha_2 > 0$ and $1 > \nu_1 > \nu_2 > 0$.

To calculate the control input, the following expression is used

$$\tilde{u} = -\varphi - \alpha_1 |\sigma|^{\nu_1} \text{sign}(\sigma) + \omega \quad (46)$$

$$\dot{\omega} = -\alpha_2 |\sigma|^{\nu_2} \text{sign}(\sigma) \quad (47)$$

3.2.2. High-Order Sliding Mode Differentiator. In this study, the HOSM is used for estimating the unknown model dynamics [23],[24]. The unknown terms are grouped and defined as φ . It is assumed differentiable and bounded with a Lipschitz constant $C > 0$. The general form of the sliding mode differentiator is described by the following set of equations:

$$\dot{z}_0 = \tilde{u} + \nu_0 \quad (48)$$

$$v_0 = -\lambda_{h,r_h} L_h^{1/r_h} |z_0 - \sigma|^{(r_h-1)/r_h} \text{sign}(z_0 - \sigma) + z_1 \quad (49)$$

$$\dot{z}_k = v_k \quad (50)$$

$$v_k = -\lambda_{h,r_h-k} L_h^{1/r_h} |z_k - v_{k-1}|^{(r_h-k-1)/(r_h-k)} \text{sign}(z_k - v_{k-1}) + z_{k+1} \quad (k = 1, \dots, r_h-2) \quad (51)$$

$$\dot{z}_{r_h-1} = -\lambda_{h,1} L_h \text{sign}(z_{r_h-1} - v_{r_h-2}) \quad (52)$$

where L_h and $\lambda_{h,i}$ ($i = 1, 2, \dots, r_h$) are parameters of differentiator as given in [23],[24]. In this case, the value of r_h is 7 which gives good estimation results. In this case, our system is impaired with a stuck elevator so thrust is the only form of control. Consequently, the coefficient of thrust C_T term is used as control. The output of z_1 is the estimate of φ . To calculate \tilde{u} , z_1 is used instead of φ as shown in the following equation

$$\tilde{u} = -z_1 - \kappa_1 |\sigma|^{\nu_1} \text{sign}(\sigma) + \omega \quad (53)$$

$$\dot{\omega} = -\kappa_2 |\sigma|^{\nu_2} \text{sign}(\sigma) \quad (54)$$

When equations (53) and (54) are compared with equations (46) and (47) and if z_1 converges to φ , the σ dynamics meet the end conditions.

4. NUMERICAL STUDIES

In order to analyze performance of proposed controller the parameters of Cessna-182 airplane are used. The aircraft motion is limited to vertical plane only. The scenario considered is that the aircraft is impaired with elevator deflection stuck at some angle. The integrated path planning and control equations are used to produce the thrust histories to land the aircraft with a low sink rate at landing. For simulating the proposed controller on the aircraft landing path planning problem, the following values have been selected from Cessna 182 airplane values $C_{L_\alpha} = 4.41$, $C_{L_0} = 0.307$, $C_{L_\delta} = 0.43$, $C_{D_0} = 0.0270$, $C_{D_\alpha} = 0.121$, $S/m = 2.1126 \text{ ft}^2/\text{slug}$, $C_{m_0} = 0.04$. [25], [26].

4.1. SIMULATION RESULTS

In this section, several simulation results were shown. We focus on various cases with different initial conditions of altitude and the elevator deflection stuck at some angle.

The initial conditions for the simulation are selected with initial velocities of U and W at 220.1 ft/sec and 0 ft/sec , in the directions of x_b and z_b . While initial Q , θ and X_E were set at zero. The design parameter K_1 is selected as 0.001.

4.1.1. Case1: $\delta_e = 2^\circ$ (stuck) with Different Altitudes and Final Downrange = 50000 ft. The control term limit is $C_T \in [0, 0.04]$ degree and $\delta_e = 2 \text{ deg}$. The upper limit on C_T is so selected to ensure that the actual thrust values do not exceed the airplane capability. The initial altitudes ($-Z_E$) for the simulation are selected as 4000 ft, 4500 ft, 5000 ft.

Figure 2 contains the histories of altitude with the downrange and Figure 3 contains the altitude variation with time for different initial altitudes. In each of these figures, the designed variations and the actual variations are presented. It can be seen from these figures that when the initial altitude is low, equal to 4000 ft., it is easier to meet the desired final downrange but with only thrust as the control variable, it is difficult to bring down the aircraft to the desired final range when the initial altitudes are higher, that is 4500 ft. and 5000 ft. From Figures 4 and 5, it can be observed that all state variable histories are in the acceptable range but the sink rate is higher than desired at about 18 ft/sec. Figure 6 shows the thrust histories and the sliding surface values with time. Not much control effort is used since all cases are descending flight. Though the sliding variable does not reach zero, it is a small value considering that the pitch angle is not zero at landing and the component of the horizontal velocity of about 190 ft/sec impacts the final value of the sliding variable. It can also be noted that the uncertainty estimation in all cases are good as seen from Figure 7.

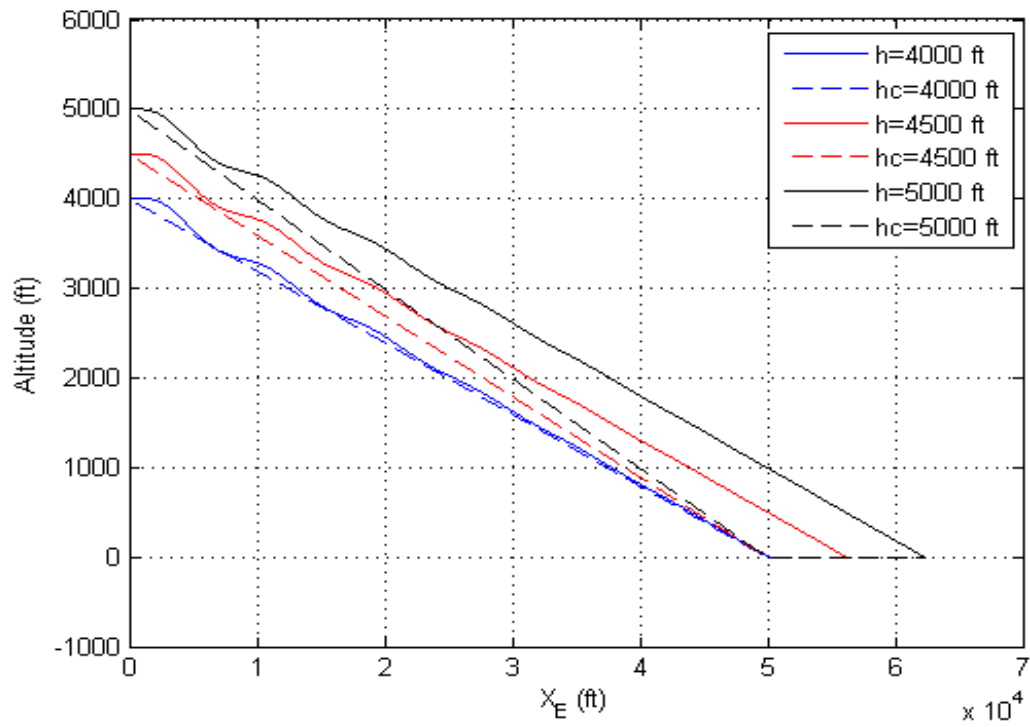


Figure 2. Histories of actual and desired altitudes with respect to downrange

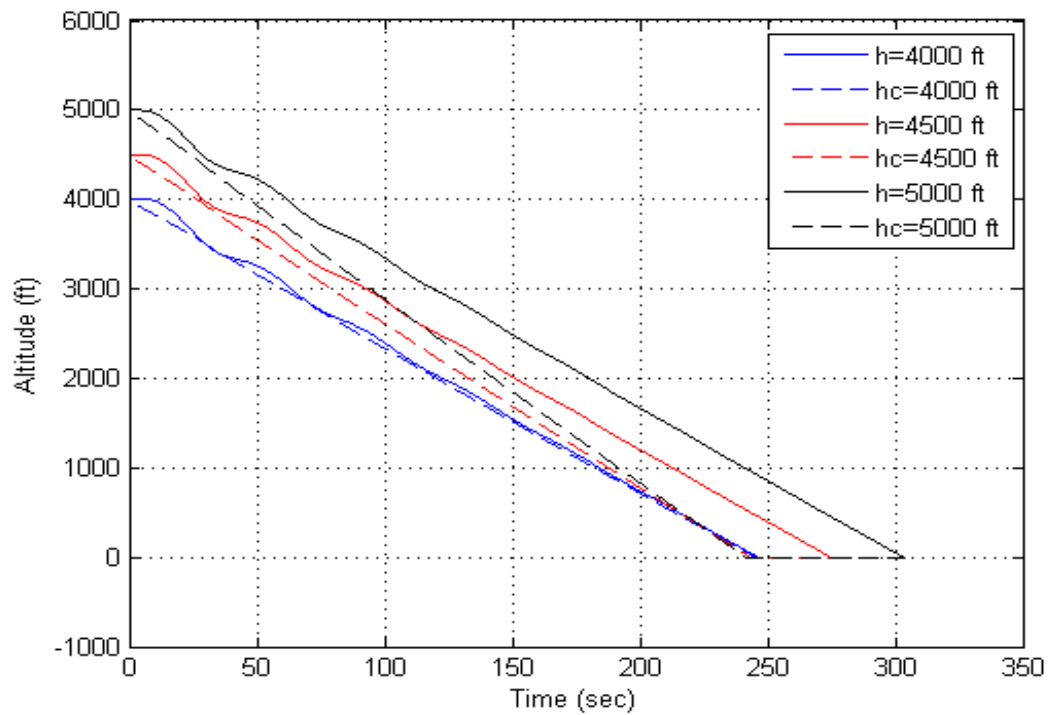


Figure 3. Histories of actual and desired altitudes with respect to time

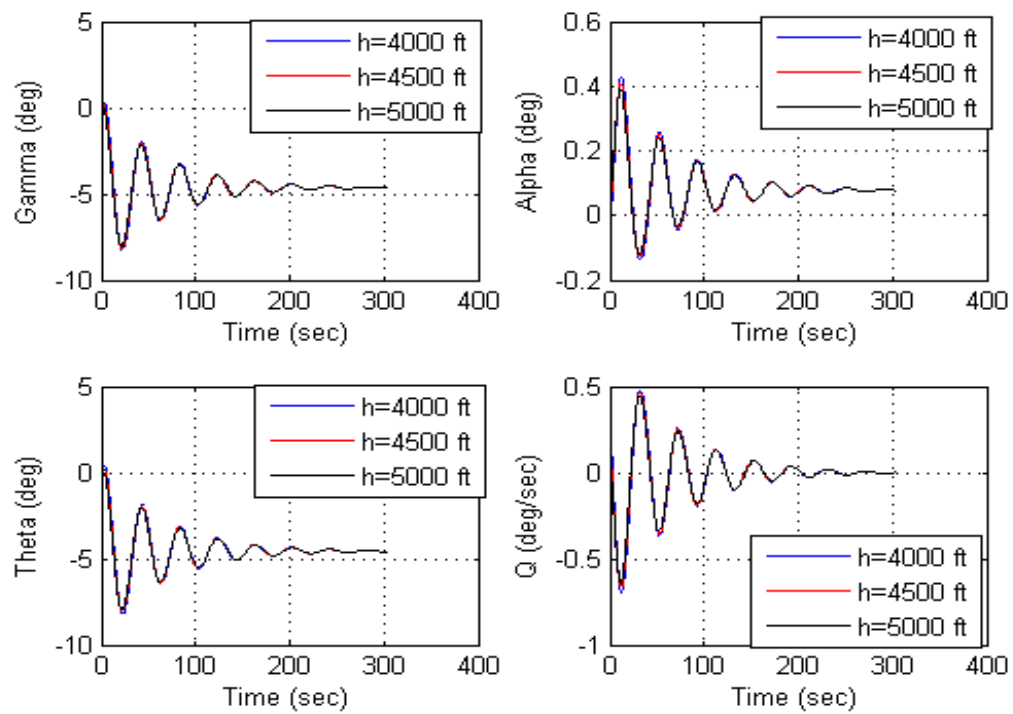


Figure 4. States histories for various initial altitudes

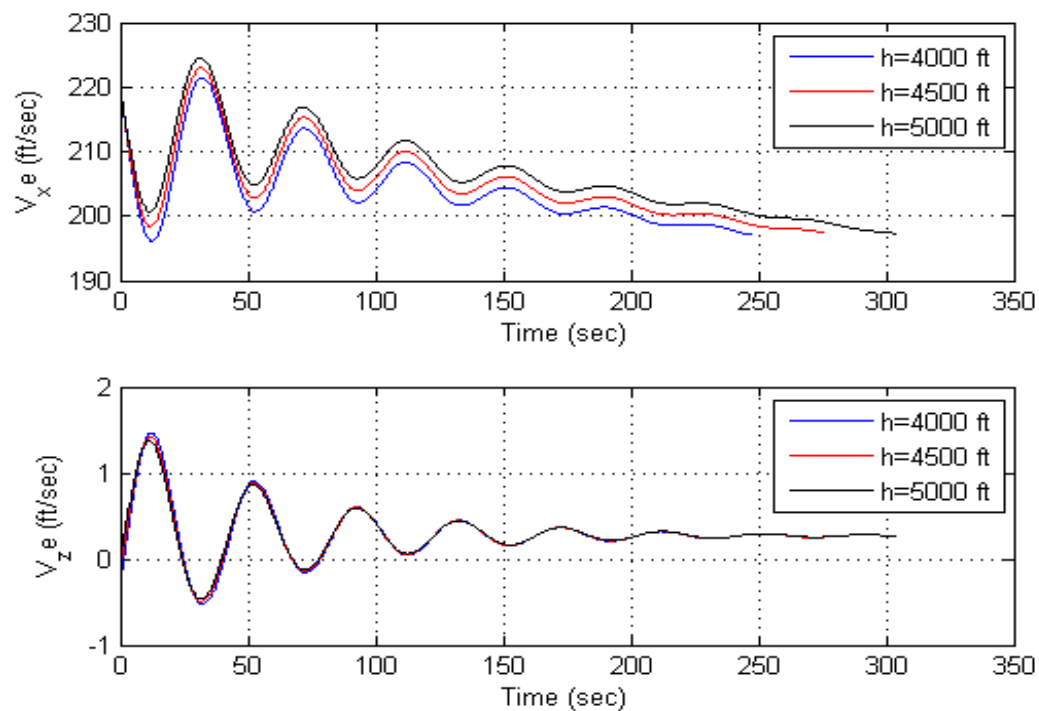


Figure 5. Histories of horizontal and vertical velocities for various initial altitudes

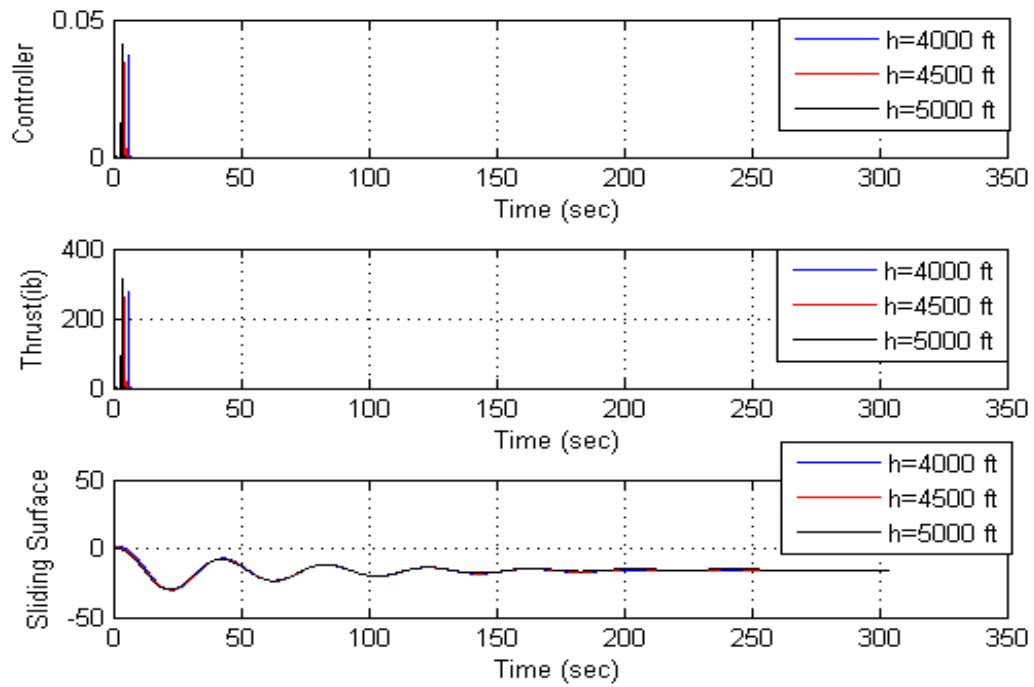


Figure 6. Histories of controller, thrust and sliding surface for various initial altitudes

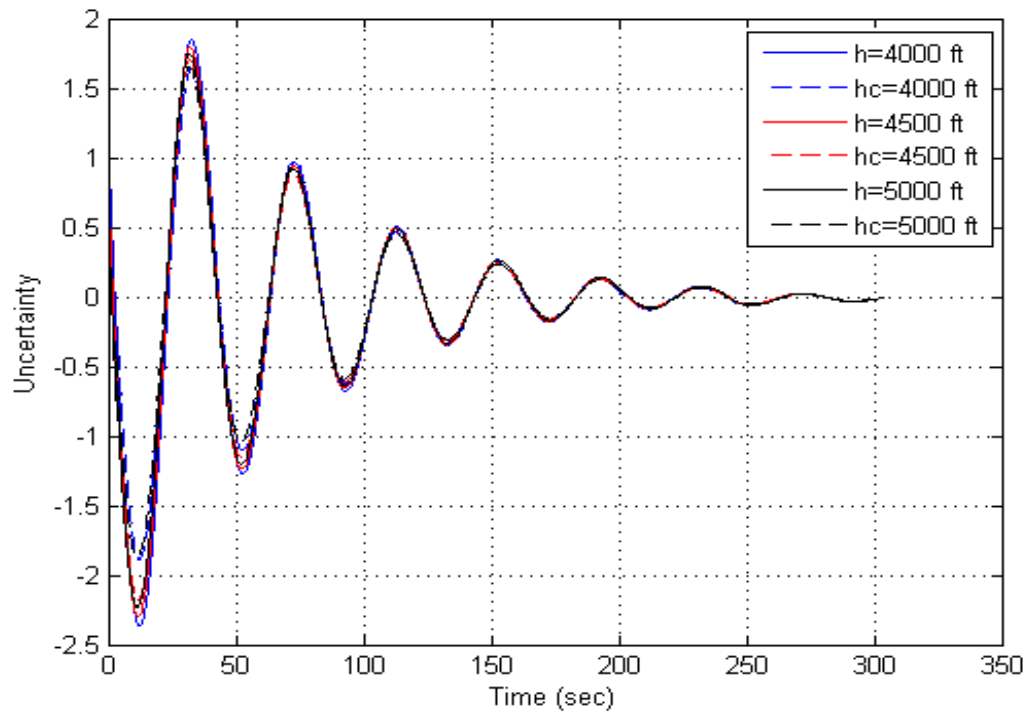


Figure 7. Histories of actual and estimated uncertainties for various initial altitudes

4.1.2. Case2: $\delta_e = -2^\circ$ (stuck) with Different Altitudes and Final Downrange = 100000 ft. The control term limit assumed here is $C_T \in [0, 0.005]$ degree and $\delta_e = -2deg$. The upper limit on C_T is kept at this number to prevent high frequency oscillations in the state variable. Note that only a small amount of thrust is needed since the desired final downrange is relatively large, that is, $100000ft$. As in Case 1, the initial altitudes (Z_E) for the simulation are selected as 4000 ft, 4500 ft, 5000 ft here too.

Figure 8 contains the histories of altitude with the downrange and Figure 9 contains the altitude variation with time for different initial altitudes. In each of these figures, the designed variations and the actual variations are presented. It can be seen from these figures that when the initial altitude is low, equal to $4000ft$, it is easier to meet the desired final downrange but with only thrust as the control variable, it is difficult to bring down the aircraft to the desired final range when the initial altitudes are higher, that is $4500ft$ and $5000ft$. It can also be observed that there are oscillations initially in the altitude history, much more than in Case 1. This is due to the fact that the elevator is stuck at a negative angle here, producing a positive moment. From Figures 10, it can further be observed that the (θ) histories show a higher magnitude of oscillations due to the fact that the negatively frozen elevator leads to a destabilizing moment. From 11, it can be seen that the velocity is much lower as compared to Case 1 because the aircraft dissipates more energy in going through a larger range. Therefore, the sink rate is lower at landing, at about $6.8ft/sec$. Figure 12 shows the thrust histories and the sliding surface values with time. Relative to Case 1, much less control is used since it is a long and downward flight. For the same reason, the terminal sliding variable value is close to zero. It can also be noted that similar to Case 1, the uncertainty estimation in all cases are good as seen from 13.

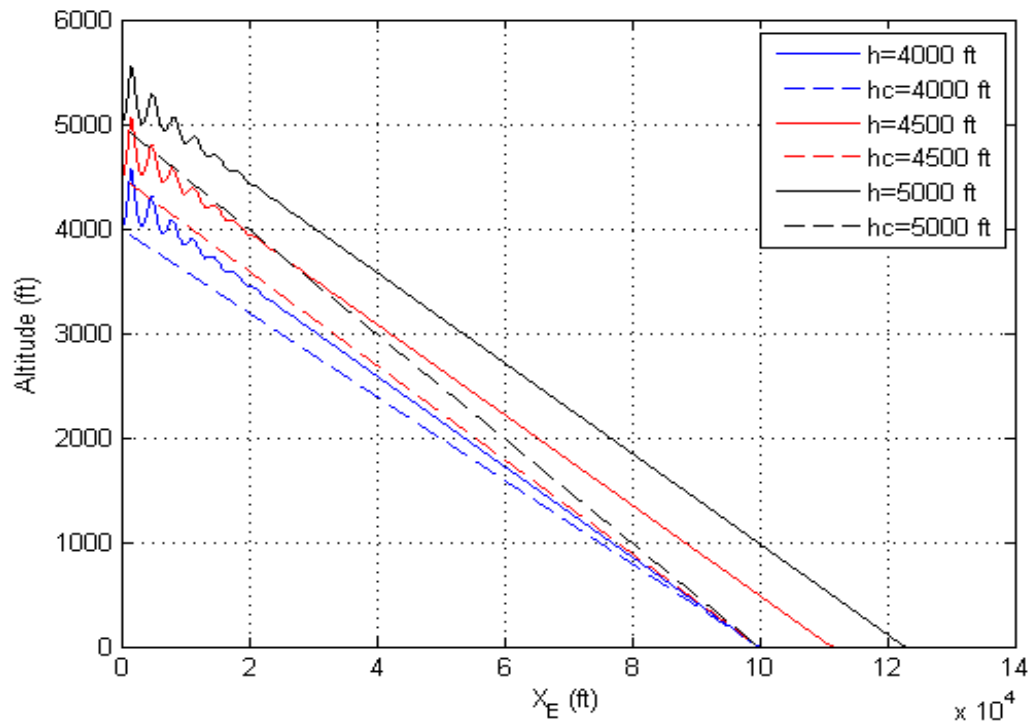


Figure 8. Histories of actual and desired altitudes with respect to downrange

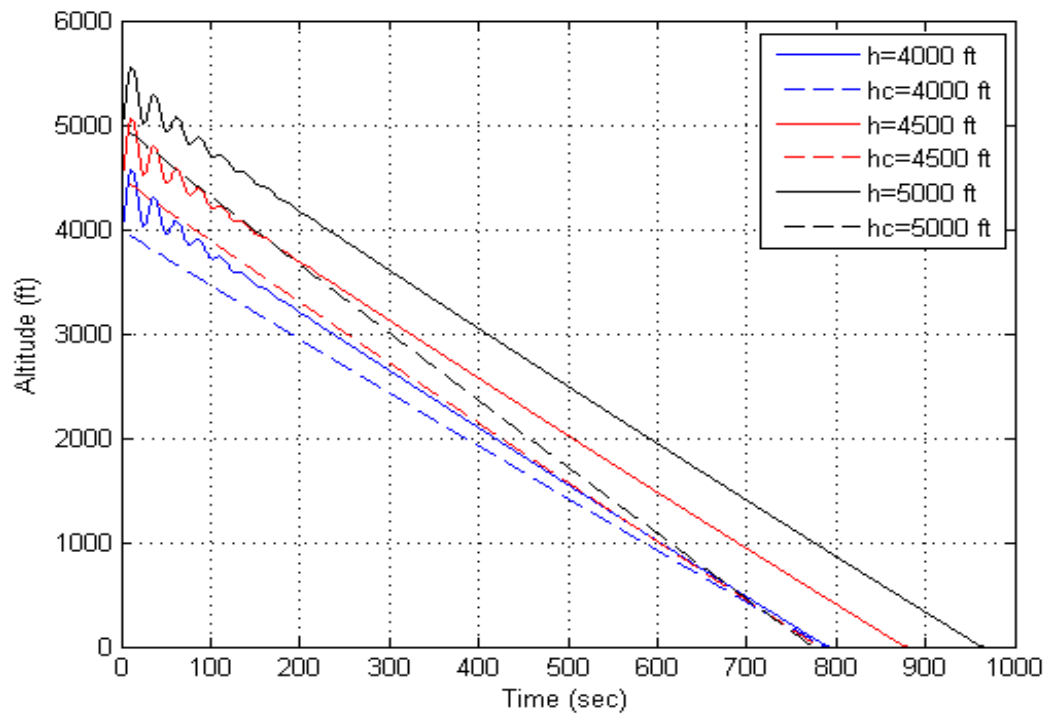


Figure 9. Histories of actual and desired altitudes with respect to time

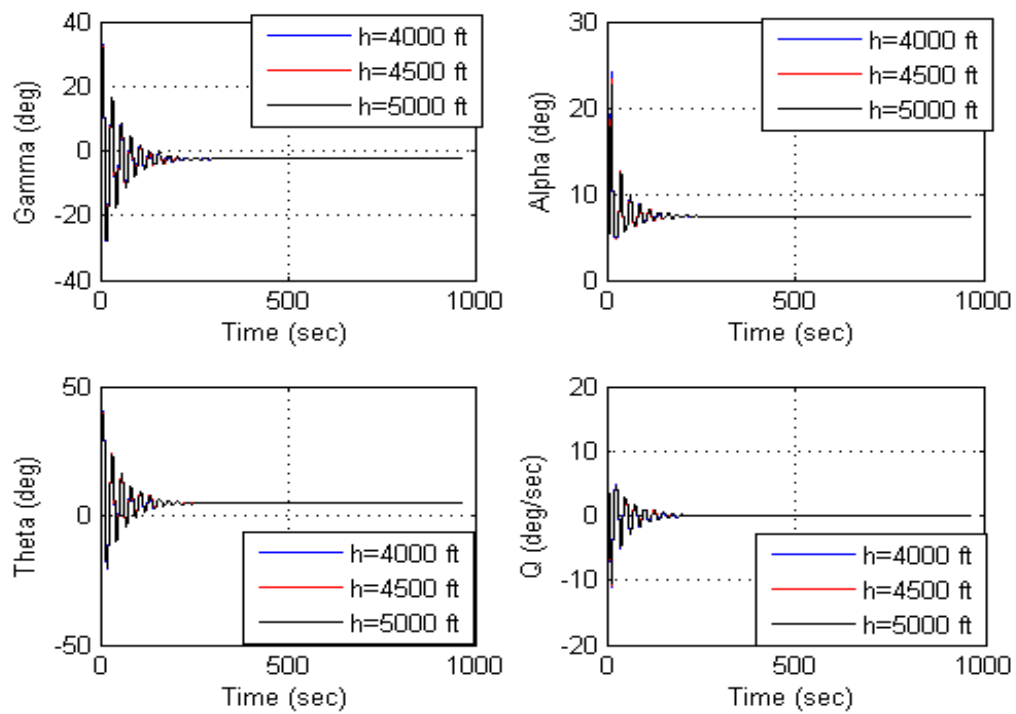


Figure 10. States histories for various initial altitudes

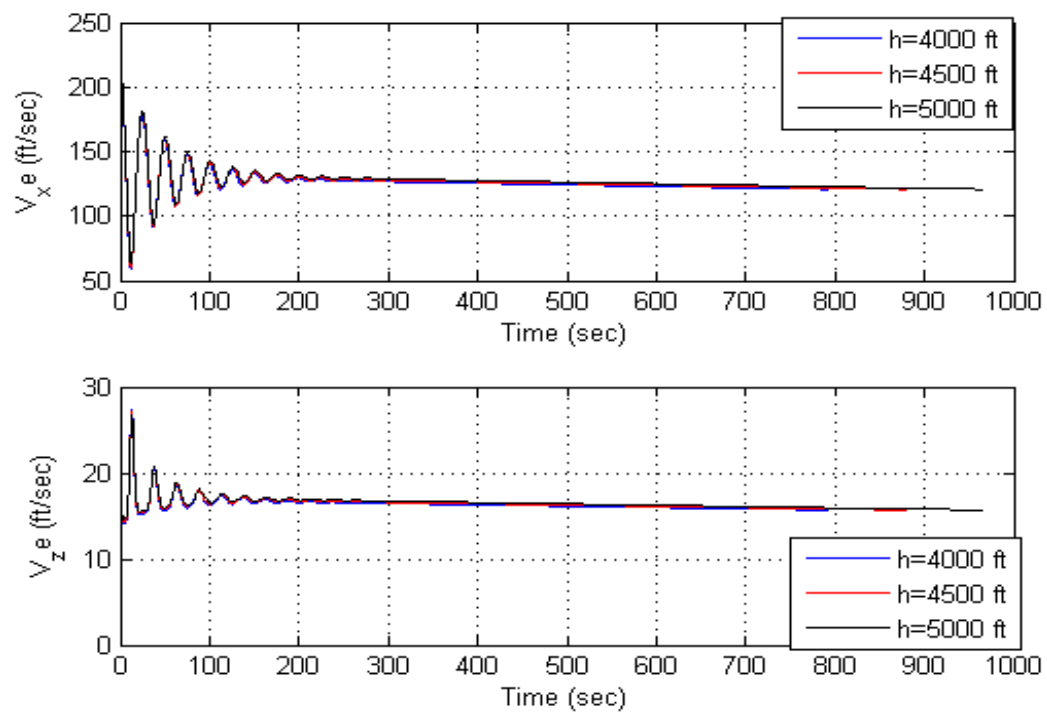


Figure 11. Histories of horizontal and vertical velocities for various initial altitudes

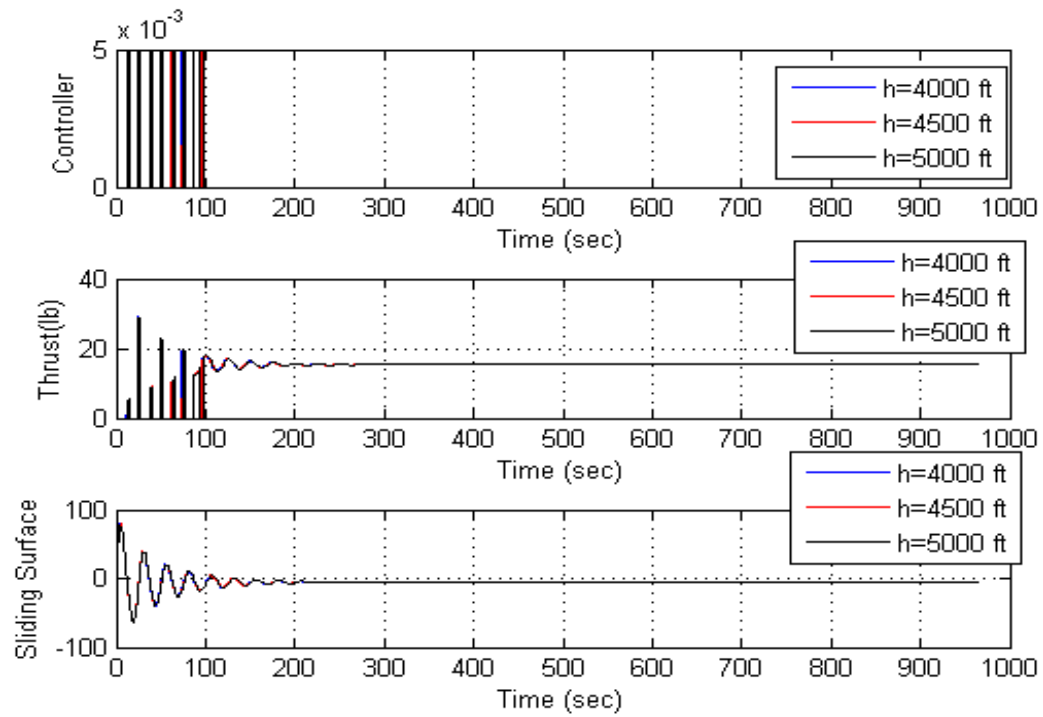


Figure 12. Histories of controller, thrust and sliding surface for various initial altitudes

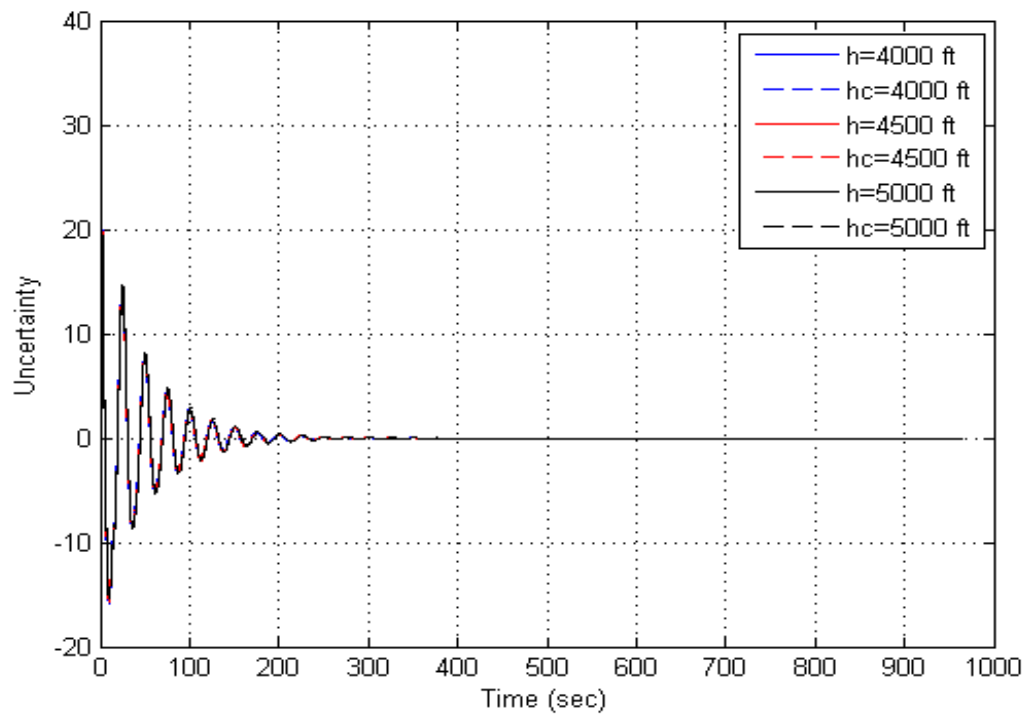


Figure 13. Histories of actual and estimated uncertainties for various initial altitudes

5. CONCLUSIONS

An integrated path planning and control method was presented in this work. A second order sliding mode control was used to design the controller that would land an impaired aircraft safely back to the ground from given initial altitudes. Furthermore, a high order sliding mode differentiator was used to estimate the unknown terms that arise in the formulation. Sample results were from numerical simulations of an aircraft using the numerical values of Cessna 182. Though more impairments and scenarios should be considered, preliminary results from this study indicate that the developed technique has good potential to be used in this class of problems.

ACKNOWLEDGEMENTS

This study was supported in part by the NASA grants NNX15AM51A and NNX15AN04A.

REFERENCES

- [1] Baba, Y., Takano, H., and Sano, M., 'Desired trajectory and guidance force generators for an aircraft,' in 'Guidance, Navigation, and Control Conference,' 1996 p. 3873.
- [2] Menon, P., Badgett, M., Walker, R., and Duke, E., 'Nonlinear flight test trajectory controllers for aircraft,' *Journal of Guidance, Control, and Dynamics*, 1987, **10**(1), pp. 67–72.
- [3] Kaminer, I., Pascoal, A., Hallberg, E., and Silvestre, C., 'Trajectory tracking for autonomous vehicles: An integrated approach to guidance and control,' *Journal of Guidance, Control, and Dynamics*, 1998, **21**(1), pp. 29–38.
- [4] Boyle, D. P. and Chamitoff, G. E., 'Autonomous maneuver tracking for self-piloted vehicles,' *Journal of Guidance, Control, and Dynamics*, 1999, **22**(1), pp. 58–67.
- [5] Ochi, S., Takano, H., and Baba, Y., 'Flight trajectory tracking system applied to inverse control for aerobatic maneuvers,' in 'Inverse Problems in Engineering Mechanics III,' pp. 337–344, Elsevier, 2002.
- [6] Rysdyk, R., 'Unmanned aerial vehicle path following for target observation in wind,' *Journal of guidance, control, and dynamics*, 2006, **29**(5), pp. 1092–1100.

- [7] Machol, R. E., 'System engineering handbook,' New York: McGraw-Hill, 1965, edited by Machol, RE, 1965.
- [8] Park, S., Deyst, J., and How, J., 'A new nonlinear guidance logic for trajectory tracking,' in 'AIAA guidance, navigation, and control conference and exhibit,' 2004 p. 4900.
- [9] Park, S., Deyst, J., and How, J. P., 'Performance and lyapunov stability of a nonlinear path following guidance method,' *Journal of Guidance, Control, and Dynamics*, 2007, **30**(6), pp. 1718–1728.
- [10] Sato, Y., Yamasaki, T., Takano, H., and Baba, Y., 'Trajectory guidance and control for a small uav,' *International Journal of Aeronautical and Space Sciences*, 2006, **7**(2), pp. 137–144.
- [11] Yamasaki, T., Sakaida, H., Enomoto, K., Takano, H., and Baba, Y., 'Robust trajectory-tracking method for uav guidance using proportional navigation,' in 'Control, Automation and Systems, 2007. ICCAS'07. International Conference on,' IEEE, 2007 pp. 1404–1409.
- [12] Harl, N., Balakrishnan, S., and Phillips, C., 'Sliding mode integrated missile guidance and control,' in 'AIAA Guidance, Navigation, and Control Conference,' 2010 p. 7741.
- [13] Galzi, D. and Shtessel, Y., 'Uav formations control using high order sliding modes,' in 'American Control Conference, 2006,' IEEE, 2006 pp. 6–pp.
- [14] Shkolnikov, I. A. and Shtessel, Y. B., 'Aircraft nonminimum phase control in dynamic sliding manifolds,' *Journal of Guidance, Control, and Dynamics*, 2001, **24**(3), pp. 566–572.
- [15] Shtessel, Y. B., Shkolnikov, I. A., and Levant, A., 'Guidance and control of missile interceptor using second-order sliding modes,' *IEEE Transactions on Aerospace and Electronic Systems*, 2009, **45**(1), pp. 110–124.
- [16] Shima, T., Idan, M., and Golan, O. M., 'Sliding-mode control for integrated missile autopilot guidance,' *Journal of guidance, control, and dynamics*, 2006, **29**(2), pp. 250–260.
- [17] Levant, A., 'Quasi-continuous high-order sliding mode controllers,' *IEEE TRANSACTIONS ON AUTOMATIC CONTROL*, 2005, **50**(11), pp. 1812–1816.
- [18] Levant, A., 'Homogeneity approach to high-order sliding mode design,' *Automatica*, 2005, **41**(5), pp. 823–830.
- [19] Harl, N. and Balakrishnan, S., 'Reentry terminal guidance through sliding mode control,' *Journal of guidance, control, and dynamics*, 2010, **33**(1), pp. 186–199.
- [20] Yamasaki, T., Balakrishnan, S., and Takano, H., 'Separate-channel integrated guidance and autopilot for a path-following uav via high-order sliding modes,' in 'AIAA Guidance, Navigation, and Control Conference,' 2012 p. 4457.

- [21] Gilbert, W. P., Nguyen, L. T., and Vangunst, R. W., 'Simulator study of the effectiveness of an automatic control system designed to improve the high-angle-of-attack characteristics of a fighter airplane,' 1976.
- [22] Blajer, W., 'Aircraft program motion along a predetermined trajectory part ii. numerical simulation with application of spline functions to trajectory definitions,' *The Aeronautical Journal*, 1990, **94**(932), pp. 53–58.
- [23] Levant, A., 'Robust exact differentiation via sliding mode technique,' *automatica*, 1998, **34**(3), pp. 379–384.
- [24] Levant, A., 'Higher-order sliding modes, differentiation and output-feedback control,' *International journal of Control*, 2003, **76**(9-10), pp. 924–941.
- [25] McRuer, D., Ashkenas, I., and Graham, D., 'Aircraft dynamics and automatic control,' Technical report, DTIC Document, 1968.
- [26] Roskam, J., *Airplane flight dynamics and automatic flight controls*, number pt. 1 in *Airplane Flight Dynamics and Automatic Flight Controls*, DARcorporation, 1995, ISBN 9781884885174.

III. INVERSE OPTIMAL CONTROL WITH SET-THEORETIC BARRIER LYAPUNOV FUNCTION FOR HANDLING STATE CONSTRAINTS

Meryem Deniz, Devi P.L, S. N. Balakrishnan
Department of Mechanical & Aerospace Engineering
Missouri University of Science and Technology
Rolla, Missouri 65409–0050, United States of America

ABSTRACT

Although rigorous framework exists for handling state variable inequality constraints under optimal control formulations, it is quite involved and difficult to incorporate for online use. In this study, an alternative approach is proposed by combining a state-dependent Riccati equation (SDRE) based inverse optimal control formulation with a set-theoretic barrier Lyapunov function (STBLF). Necessary derivations are presented. Both regulator and tracking type problems are considered. The performance of the proposed method is evaluated using numerical examples.

1. INTRODUCTION

In an optimal control method, the objective is to minimize the cost function. In the case of inverse optimal control, rather than computing an optimal solution for a given cost function, the parameters of the cost function that substantiate the demonstrated optimal behavior is computed. The controller is designed using the Lyapunov stability theory yet at the same time the associated equations satisfy the Hamilton Jacobi Bellman (HJB) equation arising in optimal control formulations.

Interest in the problem of inverse optimal control has increased with applications to several areas in the last few decades. In an earlier paper, Moylan and Anderson some theoretical work on inverse optimal nonlinear regulator. [1]. The stability analysis and

optimal control of nonlinear systems were studied by Bernstein [2]. Krstic worked on inverse optimal stabilization of a rigid spacecraft by using an integrator backstepping controller [3]. In the work by Luo et. al., an inverse optimal adaptive control was applied to attitude tracking of spacecraft [4].

The SDRE technique is a well-known method in the controls area. Cloutier studied the problem of infinite horizon optimal control for nonlinear systems by using the SDRE method [5]. Heydari and Balakrishnan developed a new method for finite horizon suboptimal control of nonlinear systems by using the SDRE approach [6].

As for handling the state variable constraints, adaptive control offers a good technique with STBLF. The STBLF has been used successfully by Ehsan et. al. where they have presented a new model reference adaptive controller [7]. Tee, Ge, and Tay studied barrier Lyapunov functions for the control of output constrained nonlinear systems [8]. Muse developed an adaptive control method that imposes the system state to stay in a chosen region[9].

Optimal controller formulation with state variable inequality constraints is a very difficult and involved problem to solve [10], [11], [12], [13]. Han and Balakrishnan [14] have developed an adaptive critic based neural networks controller scheme for linear and nonlinear systems and presented their results with an agile missile application where the missile flight mach number was constrained to be above certain prescribed value.

This paper proposes quite a different approach to the state constrained optimal control problems. This study uses an inverse optimal control method coupled with an STBLF.

The rest of the paper is organized as follows: Inverse optimal control development with an STBLF for the regulator problem is given in Section 2. In Section 3, inverse optimal control with an STBLF for a tracking problem is described. Simulation results are presented in Section 4. Conclusions are given in Section 5.

2. INVERSE OPTIMAL CONTROL BASED ON AN STBLF FOR REGULATOR PROBLEMS

In the following subsection, the inverse optimal control is designed with an STBLF; related stability analysis is also given.

2.1. INVERSE OPTIMAL CONTROL DESIGN

The system dynamics is given by

$$\dot{x}(t) = Ax(t) + Bu(t) \quad (1)$$

where $x(t) \in \mathbb{R}^n$, $t \geq 0$, is the state vector, $u(t) \in \mathbb{R}^m$, $t \geq 0$, denotes the control input, $A \in \mathbb{R}^{n \times n}$ and $B \in \mathbb{R}^{n \times m}$ denote a known system matrix and a known input matrix, respectively.

The performance variable $L(x, u)$ to be minimized is assumed to be of the form [15]

$$L(x, u) = L_1(x) + L_2(x)u + u^T R_2(x)u \quad (2)$$

where $L_1: \mathbb{R}^n \rightarrow \mathbb{R}$ and $L_2: \mathbb{R}^n \rightarrow \mathbb{R}^{1 \times m}$ and $R_2 \in \mathbb{R}_+^{m \times m}$.

Then a cost function can be defined using (2) as

$$J(x, u) = \int_0^\infty (L_1(x) + L_2(x)u + u^T R_2(x)u) dt. \quad (3)$$

The Hamiltonian function can then be written as

$$H = L_1(x) + L_2(x)u + u^T R_2(x)u + \frac{\partial V^T}{\partial x} (Ax + Bu) \quad (4)$$

where V is assumed to be the solution to the optimal return function in the Hamilton-Jacobi-Bellman (HJB) equation. Taking the partial derivative of the Hamiltonian, H with respect to controller and equating it to zero, we can get an expression for control as

$$u = -\frac{1}{2}R_2^{-1}[L_2^T + B^T \frac{\partial V}{\partial x}]. \quad (5)$$

By using (5) in (4), the following expression for H can be obtained

$$\begin{aligned} H = L_1(x) + \frac{\partial V^T}{\partial x} Ax - \frac{1}{4}L_2R_2^{-1}L_2^T - \frac{1}{4}L_2R_2^{-1}B^T \frac{\partial V}{\partial x} \\ - \frac{1}{4} \frac{\partial V^T}{\partial x} BR_2^{-1}L_2^T - \frac{1}{4} \frac{\partial V^T}{\partial x} BR_2^{-1}B^T \frac{\partial V}{\partial x} = 0 \end{aligned} \quad (6)$$

where equation (6) implies

$$\begin{aligned} -L_1(x) = \frac{\partial V^T}{\partial x} Ax - \frac{1}{4}L_2R_2^{-1}L_2^T - \frac{1}{4}L_2R_2^{-1}B^T \frac{\partial V}{\partial x} \\ - \frac{1}{4} \frac{\partial V^T}{\partial x} BR_2^{-1}L_2^T - \frac{1}{4} \frac{\partial V^T}{\partial x} BR_2^{-1}B^T \frac{\partial V}{\partial x}. \end{aligned} \quad (7)$$

In the next section, an STBLF is defined. The controller will be designed by using the STBLF and $L_1(x)$ that appears in the Hamiltonian.

2.2. SET-THEORETIC BARRIER LYAPUNOV FUNCTION

Definition 2.1. *The weighted Euclidean norm is expressed as $\|m\|_P = \sqrt{\frac{1}{4}m^T P m}$ where $m \in \mathbb{R}^P$ is a column vector and $P \in \mathbb{R}_+^{P \times P}$. A restricted potential function $\phi(\|m\|_P)$, $\phi : \mathbb{R} \rightarrow \mathbb{R}$ can be defined on the set given by*

$$\mathcal{D}_\epsilon \triangleq \{m : \|m\|_P \in [0, \epsilon)\} \quad (8)$$

where $\epsilon \in \mathbb{R}_+$ is a user-defined constant, when following conditions are satisfied [7]:

- i) If $\|m\|_P = 0$, then $\phi(\|m\|_P) = 0$.

ii) If $m \in \mathcal{D}_\epsilon$ and $\|m\|_P \neq 0$, then $\phi(\|m\|_P) > 0$.

iii) If $\|m\|_P \rightarrow \epsilon$, then $\phi(\|m\|_P) \rightarrow \infty$.

iv) $\phi(\|m\|_P)$ is continuously differentiable on \mathcal{D}_ϵ .

v) If $m \in \mathcal{D}_\epsilon$, then $D_\phi(\|m\|_P) > 0$, where $D_\phi(\|m\|_P) \triangleq \frac{d\phi(\|m\|_P)}{d\|m\|_P^2}$.

vi) If $m \in \mathcal{D}_\epsilon$, then $2D_\phi(\|m\|_P)\|m\|_P^2 - \phi(\|m\|_P) > 0$.

$$\phi(\|m\|_P) = \frac{\|m\|_P^2}{\epsilon - \|m\|_P}, \quad \|m\|_P \in \mathcal{D}_\epsilon \quad (9)$$

with the partial derivative

$$D_\phi(\|m\|_P) = \frac{\epsilon - \frac{1}{2}\|m\|_P}{(\epsilon - \|m\|_P)^2} > 0, \quad \|m\|_P \in \mathcal{D}_\epsilon \quad (10)$$

with respect to $\|m\|_P^2$ and

$$2D_\phi(\|m\|_P)\|m\|_P^2 - \phi(\|m\|_P) = \frac{\epsilon\|m\|_P^2}{(\epsilon - \|m\|_P)^2} > 0 \quad \|m\|_P \in \mathcal{D}_\epsilon. \quad (11)$$

Next let the STBLF be,

$$V(x) = \phi(\|x\|_P). \quad (12)$$

The time derivative of (12) is given by

$$\dot{V}(x) = \frac{1}{2}D_\phi(\|x(t)\|_P)x^T(t)Px(t). \quad (13)$$

The above equation can be expanded as

$$\dot{V}(x) = \underbrace{\frac{d\phi(\|x(t)\|_P)}{d\|x(t)\|_P^2}}_{D_\phi} \underbrace{\frac{d\|x(t)\|_P^2}{dx}}_{D_x} \frac{dx}{dt}. \quad (14)$$

$\underbrace{\hspace{10em}}_{D_V^T}$

By using the state dynamics in (1), (14) becomes

$$\dot{V}(x) = D_V^T \dot{x} = D_V^T (Ax + Bu) = \frac{\partial V^T}{\partial x} (Ax + Bu), \quad (15)$$

where D_V is written as $\frac{\partial V}{\partial x}$. By using (5) in (15), we get,

$$\dot{V}(x) = \frac{\partial V^T}{\partial x} Ax - \frac{1}{2} \frac{\partial V^T}{\partial x} BR_2^{-1} L_2^T - \frac{1}{2} \frac{\partial V^T}{\partial x} BR_2^{-1} B^T \frac{\partial V}{\partial x}. \quad (16)$$

2.3. COMBINING INVERSE OPTIMAL CONTROL AND STBLF

Comparing (7) with (16), we get,

$$\begin{aligned} \dot{V}(x) &= -L_1(x) \\ &= \frac{\partial V^T}{\partial x} Ax - \frac{1}{2} \frac{\partial V^T}{\partial x} BR_2^{-1} L_2^T - \frac{1}{2} \frac{\partial V^T}{\partial x} BR_2^{-1} B^T \frac{\partial V}{\partial x} \\ &= \frac{\partial V^T}{\partial x} Ax - \frac{1}{4} L_2 R_2^{-1} L_2^T - \frac{1}{4} L_2 R_2^{-1} B^T \frac{\partial V}{\partial x} \\ &\quad - \frac{1}{4} \frac{\partial V^T}{\partial x} BR_2^{-1} L_2^T - \frac{1}{4} \frac{\partial V^T}{\partial x} BR_2^{-1} B^T \frac{\partial V}{\partial x}. \end{aligned} \quad (17)$$

In (17), if L_2^T is chosen as $B^T \frac{\partial V}{\partial x}$, (17) can be simplified as $\dot{V}(x) = -L_1(x)$. Then the controller (5) becomes

$$u = -R_2^{-1} B^T \frac{\partial V}{\partial x}. \quad (18)$$

2.4. STABILITY ANALYSIS

By using $L_2^T = B^T \frac{\partial V}{\partial x}$ in (16), we get

$$\dot{V}(x) = \frac{\partial V^T}{\partial x} Ax - \frac{\partial V^T}{\partial x} BR_2^{-1} B^T \frac{\partial V}{\partial x}. \quad (19)$$

By using $\frac{\partial V}{\partial x} = D_\phi D_x$ in (19), we get,

$$\dot{V}(x) = D_x^T D_\phi A x - D_x^T D_\phi B R_2^{-1} B^T D_\phi D_x. \quad (20)$$

From $D_x = \frac{d\|x(t)\|_P^2}{dx}$ expression, D_x is calculated as $D_x = \frac{1}{2}P x$ can be substituted in (20) to get the following expression,

$$\dot{V}(x) = \frac{1}{4}x^T [PD_\phi A + A^T PD_\phi - PD_\phi B R_2^{-1} B^T D_\phi P]x \quad (21)$$

where $\dot{V} = -L_1$ and if we choose $L_1 = \frac{1}{4}x^T Q x$, $Q \in \mathbb{R}_+^{n \times n}$, then equating the right hand side (RHS) we get $PD_\phi A + A^T PD_\phi - PD_\phi B R_2^{-1} B^T D_\phi P = -Q$. This expression can be simplified by defining $\bar{A} = D_\phi A$ and $\bar{B} = D_\phi B$ to get, $P\bar{A} + \bar{A}^T P - P\bar{B}R_2^{-1}\bar{B}^T P = -Q$. This state dependent Riccati equation can then be solved to get P [16],[17].

Theorem 2.1. *Consider the system dynamics in (1) with the optimal control effort defined in (18). If the initial weighted Euclidean norm is less than user-defined constant, then the closed-loop systems are bounded, where the system weighted Euclidean norm strictly satisfies user-defined constant given by*

$$\|m\|_P < \epsilon, \quad t \geq 0. \quad (22)$$

Proof. Boundedness of the closed loop system is proven using the Lyapunov function. The STBLF is used in this paper that is given in (12). The time derivative of (12) is given in (13). By using (1) in (13), we get

$$\dot{V}(x) = \frac{1}{2}D_\phi(\|x(t)\|_P)x^T(t)P(Ax(t) + Bu(t)). \quad (23)$$

By using (18) in (23), we get

$$\dot{V}(x) = \frac{1}{2}D_\phi(\|x(t)\|_P)x^T(t)P[A - \frac{1}{2}BR_2^{-1}B^TD_\phi P]x(t) \quad (24)$$

with letting $A_H \triangleq A - \frac{1}{2}BR_2^{-1}B^TD_\phi P$ and P is chosen such that A_H is point-wise Hurwitz.

Then

$$\dot{V}(x) = \frac{1}{4}x^T(t)D_\phi[PA_H + A_H^T P]x(t) \quad (25)$$

where $PA_H + A_H^T P = -Q$ and

$$\dot{V}(x) \leq -\frac{1}{4}D_\phi\lambda_{\min}(Q)x^T x. \quad (26)$$

By adding and subtracting $\frac{1}{8}\lambda_{\min}(Q)\phi(\|x\|_P)$,

$$\begin{aligned} \dot{V}(x) \leq & -\frac{1}{8}\lambda_{\min}(Q)\phi(\|x\|_P) - \lambda_{\min}(Q)\left[\frac{1}{4}D_\phi x^T x \right. \\ & \left. - \frac{1}{8}\phi(\|x\|_P)\right]. \end{aligned} \quad (27)$$

By using the property given in (11), $[\frac{1}{4}D_\phi x^T x - \frac{1}{8}\phi(\|x\|_P)] > 0$. Therefore, it is proved that

$$\dot{V}(x) \leq -\frac{1}{8}\lambda_{\min}(Q)\phi(\|x\|_P). \quad (28)$$

□

3. INVERSE OPTIMAL CONTROL BASED ON STBLF FOR TRACKING PROBLEMS

3.1. INVERSE OPTIMAL CONTROL DESIGN

For a system dynamics defined in Section 2.1.

The reference model can be defined as

$$\dot{x}_m(t) = A_m x_m(t) + B_m r(t) \quad (29)$$

where $x_m(t) \in \mathbb{R}^n$, $t \geq 0$ is the reference state vector. $A_m \triangleq A - BR_2^{-1}B^T D_\phi P$, $A_m \in \mathbb{R}^{n \times n}$ denotes a pointwise Hurwitz matrix, $B_m \triangleq BR_2^{-1}B^T D_\phi PC^T$, $B_m \in \mathbb{R}^{n \times n_r}$ denotes a reference input matrix and $C \in \mathbb{R}^{n_r \times n}$ denotes an output matrix. $r(t) \in \mathbb{R}^{n_r}$ is a given bounded piecewise continuous command. The system error is defined as $e(t) \triangleq x_m(t) - x(t)$, $t \geq 0$. By using (1) and (29), the error dynamics is given by

$$\dot{e}(t) = Ae - Bu - BR_2^{-1}B^T D_\phi P(x_m - C^T r). \quad (30)$$

The controller equation becomes,

$$u = R_2^{-1}B^T \frac{\partial V}{\partial e}. \quad (31)$$

Theorem 3.1. *Consider the system dynamics in (30) with the optimal control effort defined in (31). If the initial weighted Euclidean norm is less than user-defined constant, then the closed-loop systems are bounded, where the system weighted Euclidean norm strictly satisfies user-defined constant given by*

$$\|m\|_P < \epsilon, \quad t \geq 0. \quad (32)$$

Proof. Boundedness of the closed loop system is proven using the Lyapunov function given by

$$V(e) = \phi(\|e\|_P) \quad (33)$$

Taking the time derivative of equation (33) we get,

$$\begin{aligned}\dot{V}(e) &= \frac{d\phi(\|e(t)\|_P)}{dt} = \frac{d\phi(\|e(t)\|_P)}{d\|e(t)\|_P^2} \frac{d\|e(t)\|_P^2}{dt} = \frac{d\phi(\|e(t)\|_P)}{d\|e(t)\|_P^2} \frac{d\|e(t)\|_P^2}{de} \frac{de}{dt} \\ &= \frac{1}{2} D_\phi(\|e(t)\|_P) e^T(t) P \dot{e}(t).\end{aligned}\quad (34)$$

By steps similar to the ones used in Section 2, it can be proven that

$$\dot{V}(e) \leq -\frac{1}{8} \lambda_{\min}(Q) \phi(\|e\|_P). \quad (35)$$

□

4. NUMERICAL RESULTS

In this section, two different problems (regulator and tracking) are considered. The simulation results for two different examples are shown for each problem. The objective is to keep the weighted Euclidean norm under a priori defined bound. The proposed SDRE based inverse optimal control with STBLF is used for this purpose.

For all the examples given below, initial P value is strategically selected such that the weighted Euclidean norm is close to the designed bound in order to test the effectiveness of the proposed method. If P value is selected which is far from the bound, the required control effort is found to be less. To calculate D_ϕ , the initial P needs to be selected. Initial P has to be symmetric and positive definite. Therefore, P is selected for each case as

$$P = \begin{bmatrix} 2 & 1 \\ 1 & 2 \end{bmatrix}.$$

In the two subsequent subsections, the efficacy of the proposed method will be shown for both the regulator and the tracking problems.

In the following problems the state vector is of the form

$$x = [x_1 \ x_2]^T, \quad (36)$$

where x_1 represents the position and x_2 represents the velocity of system.

4.1. REGULATOR PROBLEM

In this problem, two different examples are shown. One is for constant dynamics and the other is for time varying dynamics. For the below regulator problems, the weight matrices that are used in cost function are selected as

$$Q = \alpha \begin{bmatrix} 1 & 0 \\ 0 & 1 \end{bmatrix}, \quad R = 1,$$

where $\alpha = 1$. One can modulate the transient response of the system by picking different values of α . The effect of α on the system response was tested with different values of α . When α is in the range (0,1), the system transient response took longer to settle. Larger values of the parameter α resulted in larger values of control which then lead to shorter transient responses.

4.1.1. Case 1. The system dynamics is as follows

$$A = \begin{bmatrix} 0 & 1 \\ 0 & 0 \end{bmatrix}, \quad B = \begin{bmatrix} 0 \\ 1 \end{bmatrix}.$$

In this example the threshold ϵ is set to be 14. Initial condition of states are chosen as 11 *deg* and 11 *deg/s*, respectively.

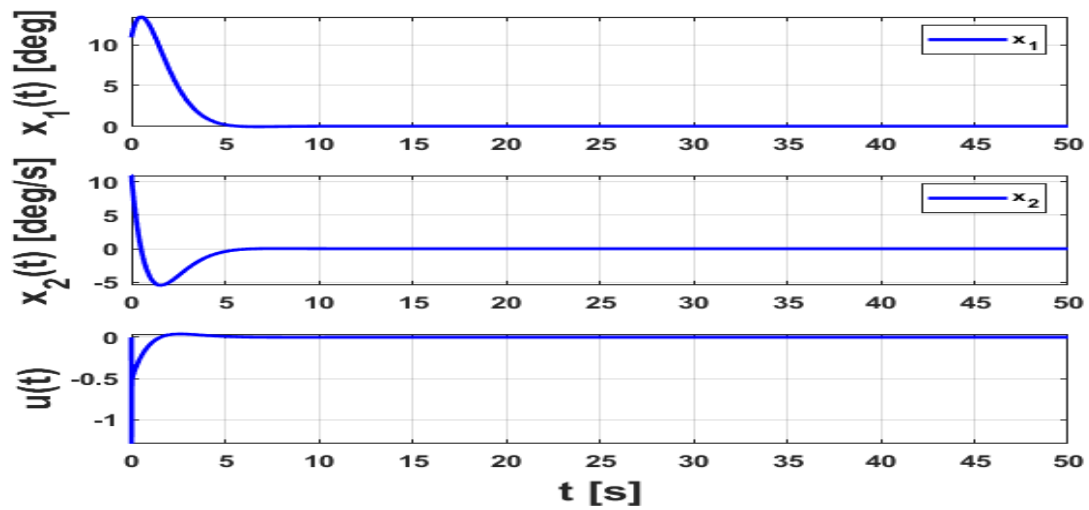


Figure 1. Histories of states and controller for regulator problem case 1

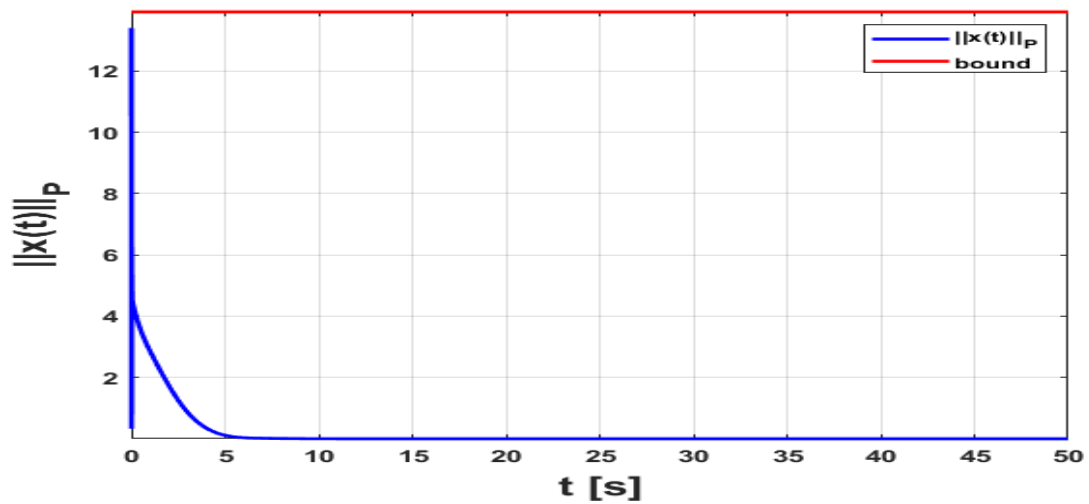


Figure 2. Histories of norm of states and bound for regulator problem case 1

Figure 1 shows the histories of states and controller. It is clearly seen that, the states settling time is around $5s$. In this case, the system has a quick transient response and the controller effort is high, thereby reducing the settling time to $5s$. As we can see from Figure 2, even if the initial states are set close to the threshold, the weighted Euclidean norm remains within the bound.

4.1.2. Case 2. Dynamics of the damped Mathieu equation is given by [18]

$$A = \begin{bmatrix} 0 & 1 \\ -(2 + \sin(t)) & -1 \end{bmatrix}, \quad B = \begin{bmatrix} 0 \\ 1 \end{bmatrix}$$

In this example, the threshold ϵ is set to be 3. The initial condition of states are $x_1 = 4 \text{ deg}$, $x_2 = -4 \text{ deg/s}$.

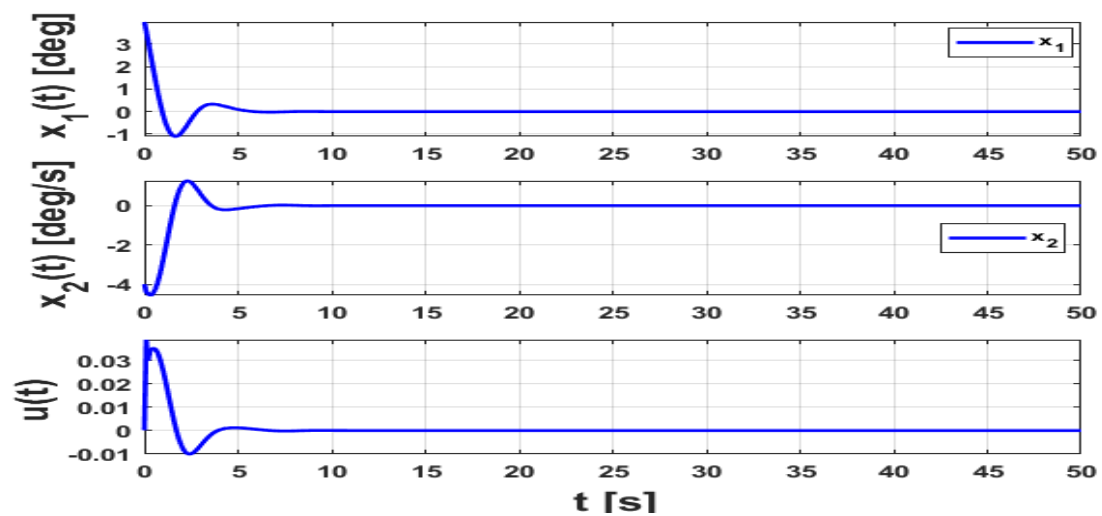


Figure 3. Histories of states and controller for regulator problem case 2

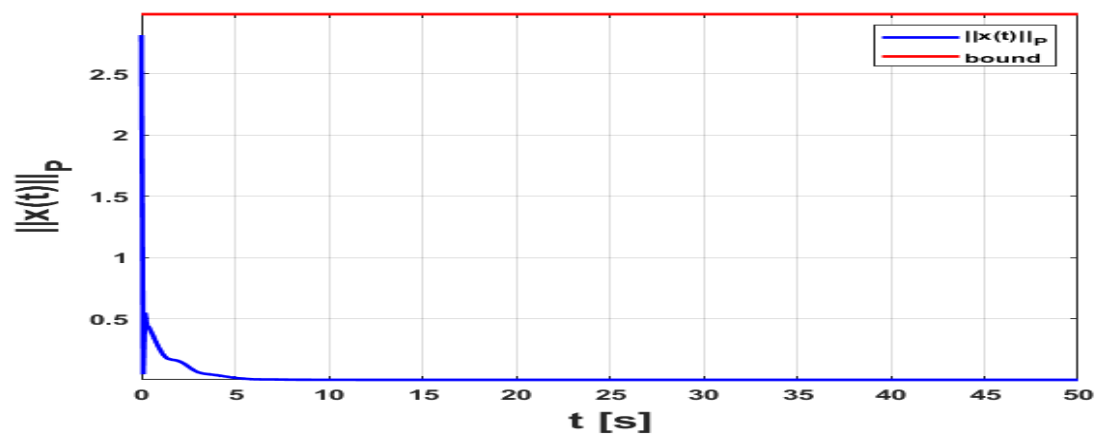


Figure 4. Histories of norm of states and bound for regulator problem case 2

Figure 3 shows the histories of states and controller for time varying dynamics. Even if dynamics are time varying, the states settling time is still around 5s. Also, we can see from Figure 4, the weighted Euclidean norm remains within the bound, even when the initial states are set close to the threshold.

4.2. TRACKING PROBLEMS

The A and B matrices of the system for the following problems are given below:

$$A = \begin{bmatrix} 0 & 1 \\ 0 & 0 \end{bmatrix}, \quad B = \begin{bmatrix} 0 \\ 1 \end{bmatrix}.$$

In the following examples, the weight matrices are selected as

$$Q = \begin{bmatrix} 10 & 0 \\ 0 & 10 \end{bmatrix}, \quad R = 0.01.$$

The initial condition for states are 0 *deg* and 0 *deg/s*, respectively. In this problem, two different trajectories are used.

4.2.1. Case 1. In this case, the threshold ϵ is set to 5×10^{-3} . The system is expected to track a square wave.

Figure 5 presents the histories of the system states and the square wave to be tracked and also the variation of control with time. It can be seen that the control makes the system track the reference square wave quite well. The result shown in Figure 6 confirms that the proposed controller keeps the error under the bound.

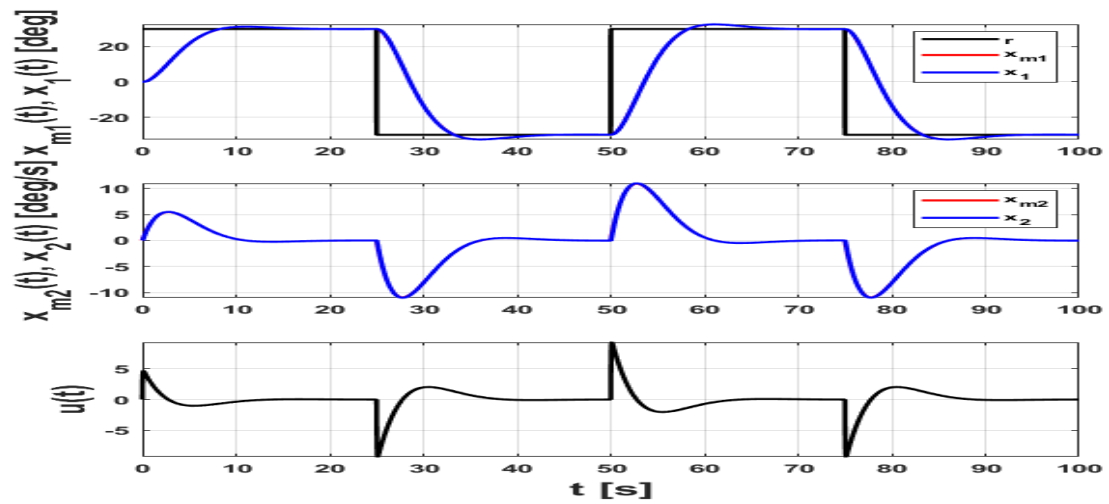


Figure 5. Histories of the states and the references states and controller for tracking problem case 1

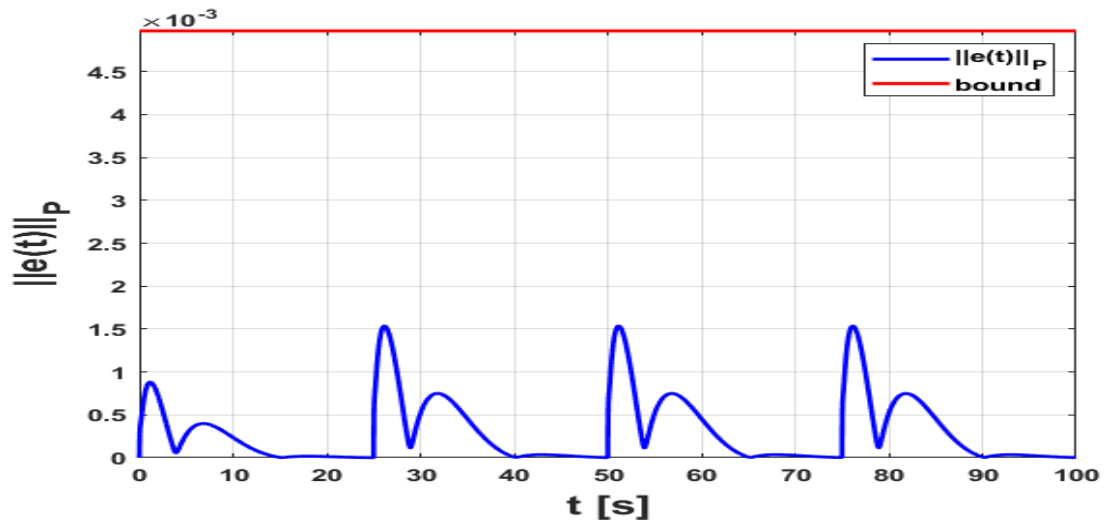


Figure 6. Histories of norm of error and bounds for tracking problem case 1

4.2.2. Case 2. The threshold ϵ is set to 5×10^{-4} , in this example. The reference model is designed to be a function of time, $r(t) = 0.1 \sin(0.1t)$.

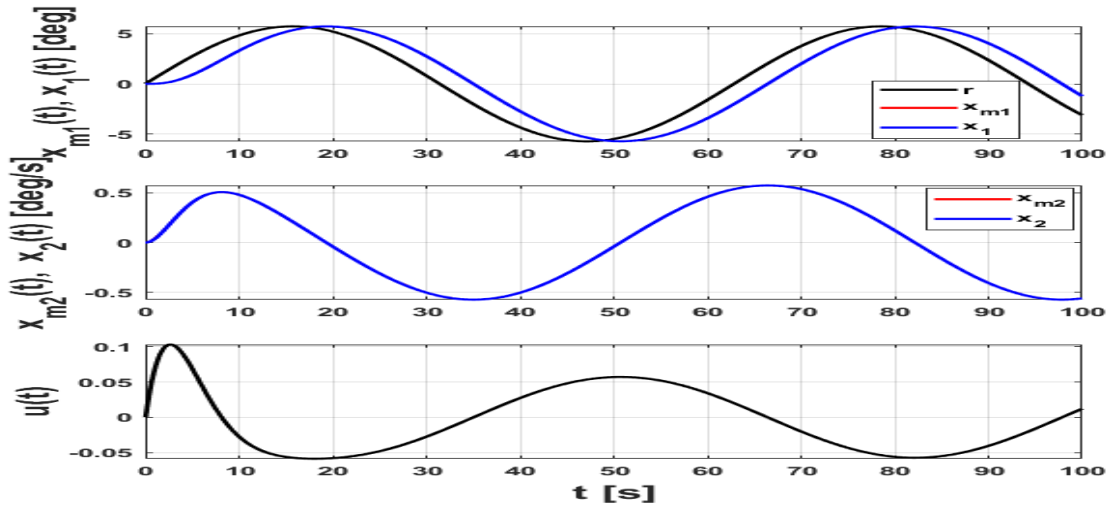


Figure 7. Histories of the states and the references states and controller for tracking problem case 2

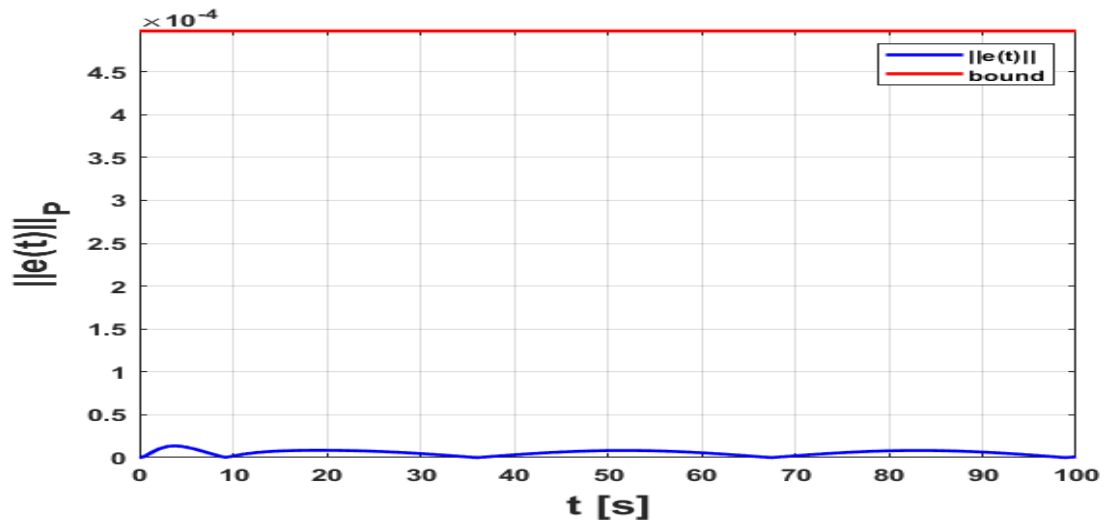


Figure 8. Histories of norm of error and bounds for tracking problem case 2

Figure 7 depicts the actual states and the reference models and the designed controller. In this figure, the actual states are following the model reference trajectories successfully like in Case 1. Similar to the previous cases, the proposed controller keeps error under the bound in this example also as can be seen in Figure 8.

5. CONCLUSION

The state constraint inequality is a challenging task to include in a traditional optimal controller design. An inverse optimal controller design with an STBLF that simplifies the controller design was presented in this work. Representative simulation results were shown for both the regulator and the tracking problems. These results seem to indicate that the developed inverse optimal controller has good potential for applications.

ACKNOWLEDGEMENTS

This study was supported in part by the NASA grants NNX15AM51A and NNX15AN04A.

The first author would like to thank the Republic of Turkey for the supporting her Ph.D. studies.

REFERENCES

- [1] Moylan, P. and Anderson, B., 'Nonlinear regulator theory and an inverse optimal control problem,' *IEEE Transactions on Automatic Control*, 1973, **18**(5), pp. 460–465.
- [2] Wan, C.-J. and Bernstein, D. S., 'Nonlinear feedback control with global stabilization,' *Dynamics and Control*, 1995, **5**(4), pp. 321–346.
- [3] Krstic, M. and Tsiotras, P., 'Inverse optimal stabilization of a rigid spacecraft,' *IEEE Transactions on Automatic Control*, 1999, **44**(5), pp. 1042–1049.
- [4] Luo, W., Chu, Y.-C., and Ling, K.-V., 'Inverse optimal adaptive control for attitude tracking of spacecraft,' *IEEE Transactions on Automatic Control*, 2005, **50**(11), pp. 1639–1654.
- [5] Cloutier, J. R., 'State-dependent riccati equation techniques: an overview,' in 'American Control Conference,' volume 2, 1997 pp. 932–936.
- [6] Heydari, A. and Balakrishnan, S., 'Optimal online path planning for approach and landing guidance,' in 'Proc. AIAA Atmospheric Flight Mechanics Conference, Portland, OR,' 2011 .

- [7] Arabi, E., Gruenwald, B. C., Yucelen, T., and Nguyen, N. T., 'A set-theoretic model reference adaptive control architecture for disturbance rejection and uncertainty suppression with strict performance guarantees,' *International Journal of Control*, 2018, **91**(5), pp. 1195–1208.
- [8] Tee, K. P., Ge, S. S., and Tay, E. H., 'Barrier Lyapunov functions for the control of output-constrained nonlinear systems,' *Automatica*, 2009, **45**(4), pp. 918–927.
- [9] Muse, J., 'A method for enforcing state constraints in adaptive control,' in 'AIAA Guidance, Navigation, and Control Conference,' 2011 p. 6205.
- [10] Bryson, A. E., Denham, W. F., and Dreyfus, S. E., 'Optimal programming problems with inequality constraints,' *AIAA journal*, 1963, **1**(11), pp. 2544–2550.
- [11] McIntyre, J. and Paiewonsky, B., 'On optimal control with bounded state variables,' in 'Advances in Control Systems,' volume 5, pp. 389–419, Elsevier, 1967.
- [12] Kreindler, E., 'Additional necessary conditions for optimal control with state-variable inequality constraints,' *Journal of Optimization theory and applications*, 1982, **38**(2), pp. 241–250.
- [13] Jacobson, D. H., Lele, M. M., and Speyer, J. L., 'New necessary conditions of optimality for control problems with state-variable inequality constraints,' *Journal of mathematical analysis and applications*, 1971, **35**(2), pp. 255–284.
- [14] Han, D. and Balakrishnan, S., 'State-constrained agile missile control with adaptive-critic-based neural networks,' *IEEE Transactions on Control Systems Technology*, 2002, **10**(4), pp. 481–489.
- [15] Haddad, W. M. and Chellaboina, V., *Nonlinear dynamical systems and control: a Lyapunov-based approach*, Princeton university press, 2011.
- [16] Heydari, A. and Balakrishnan, S., 'Path planning using a novel finite horizon sub-optimal controller,' *Journal of guidance, control, and dynamics*, 2013, **36**(4), pp. 1210–1214.
- [17] Çimen, T., 'State-dependent riccati equation (sdre) control: A survey,' *IFAC Proceedings Volumes*, 2008, **41**(2), pp. 3761–3775.
- [18] Lewis, F., Jagannathan, S., and Yesildirak, A., *Neural network control of robot manipulators and non-linear systems*, CRC Press, 1998.

IV. ADAPTIVE CONTROL OF UNCERTAIN DYNAMICAL SYSTEMS WITH AN OPTIMAL NONLINEAR REFERENCE MODEL

Meryem Deniz¹, Tansel Yucelen², S. N. Balakrishnan¹

¹Department of Mechanical & Aerospace Engineering
Missouri University of Science and Technology
Rolla, Missouri 65409–0050, United States of America

²Department of Mechanical Engineering
University of South Florida
Tampa, Florida 33620, United States of America

ABSTRACT

In this paper, we study the adaptive control of uncertain dynamical systems. Specifically, we use the Θ -D method to establish an optimal nonlinear reference model based on the known system dynamics. We then design the adaptive control algorithm for suppressing the unknown system dynamics, where it drives the trajectories of the uncertain dynamical system to that of the optimal nonlinear reference model. Two illustrative numerical examples are also given to complement our theoretical contribution.

1. INTRODUCTION

There is an ever-increasing interest in optimal control of nonlinear dynamical systems. Yet, due to the presence of unavoidable real-world exogenous disturbances and system uncertainties, achieving optimality is a challenge. Motivated by this standpoint, the authors of [1, 2, 3, 4, 5, 6, 7, 8, 9, 10, 11] study various feedback control algorithms with an approximate optimality (that is, suboptimality) guarantee. Building on the results in [12] and [13], the authors of [14] also propose a concurrent learning-based approximate optimal regulation. The authors of [15] and [16] then generalize the results of [14] to multiagent

systems and approximate optimal tracking problem, respectively. Finally, the authors of [17] utilize a max-min Hamiltonian Jacobi Bellman equation for uncertain nonlinear dynamical systems.

For uncertain nonlinear dynamical systems, the other approach toward optimality is the actor-critic-identifier (ACI) method. In particular, this method approximates the Hamilton–Jacobi–Bellman equation using three neural network (NN) layers. An advantage of using the ACI architecture is that learning by the actor, critic, and identifier is simultaneous without requiring knowledge of system dynamics. The online actor-critic algorithm is developed with policy iteration for infinite horizon optimal control problem [18]. The authors of [19] establish an online adaptive optimal control method for continuous time uncertain nonlinear dynamical systems. This method is based on the identifier-critic approximation dynamic programming with two NN layers (that is, there is no need for actor NN with this method). The authors of [20] propose an optimal control approach predicated on the adaptive-critic NNs for the aircraft systems. The key aspect of this method is that the NN does not need any priori knowledge of the controller. The optimal control based on a single network adaptive critic is also developed for nonlinear dynamical systems in [21], where this method has an advantage on computational complexity.

In the current literature, a method called as the Θ -D method [22] achieves effective suboptimal solutions for nonlinear dynamical systems. The advantage of this method is that it involves reduced nonlinear computations and control signals with initially small magnitudes. Yet, the authors of [22] does not focus on the presence of uncertainties. Motivated by this standpoint, this paper uses the Θ -D method to establish an optimal nonlinear reference model based on the known system dynamics. Building on the key ideas on nonlinear reference model based adaptive control architectures [23], we then design the adaptive control algorithm for suppressing the unknown system dynamics. Specifically, we show that the trajectories of the uncertain dynamical system converges to the trajectories of the optimal nonlinear reference model.

The rest of the paper is organized as follows. For completeness, an overview of the Θ -D method is presented in Section 2. Our theoretical contribution is then given in Section 3. Section 4 then shows the two illustrative numerical examples to complement our theoretical contribution. In Section 5, the conclusion is provided.

2. AN OVERVIEW ON $\Theta - D$ SUBOPTIMAL CONTROL METHOD

An overview of the $\Theta - D$ method [22] is now presented. Specifically, consider the nonlinear dynamical system given by

$$\dot{x}(t) = f(x(t)) + Bu(t), \quad x(0) = x_0, \quad (1)$$

along with the cost function

$$J(x(t), u(t)) = \frac{1}{2} \int_0^{\infty} (x^T(t)Qx(t) + u^T(t)Ru(t))dt. \quad (2)$$

Here, $x(t) \in \mathbb{R}^n$ is the state vector, $u(t) \in \mathbb{R}^m$ is the control input, and $f(x(t)) \in \mathbb{R}^n$ and $B \in \mathbb{R}^{n \times m}$ are known function and input matrix, respectively. In addition, $R \in \mathbb{R}_+^{m \times m}$ and $Q \in \mathbb{R}_+^{n \times n}$ in (2) are positive definite matrices. The optimal control is then given by

$$u^*(t) = -R^{-1}B^T \frac{\partial V}{\partial x} \quad (3)$$

The optimal solution of the above infinite-horizon nonlinear regulator problem can be obtained by solving the Hamiltonian-Jacobi-Bellman (HJB) given by

$$\frac{\partial V^T}{\partial x} f(x(t)) - \frac{1}{2} \frac{\partial V^T}{\partial x} BR^{-1}B^T \frac{\partial V}{\partial x} + \frac{1}{2} x^T Qx = 0. \quad (4)$$

Specifically, let

$$\dot{x}(t) = A_0x(t) + \Theta \left(\frac{A(x(t))}{\Theta} \right) x(t) + Bu(t), \quad x(0) = x_0, \quad (5)$$

and

$$J(x(t), u(t)) = \frac{1}{2} \int_0^\infty [x^T(t)(Q + \sum_{i=0}^\infty D_i \Theta^i)x(t) + u^T(t)Ru(t)] dt \quad (6)$$

be the rewritten versions of (1) and (2), respectively [22].

In addition, define the co-state λ as

$$\lambda = \frac{\partial V}{\partial x}, \quad (7)$$

and assume a power series expansion of λ in terms of Θ as

$$\lambda(t) = \sum_{i=0}^\infty T_i \Theta^i x(t). \quad (8)$$

Now, choosing the costate as

$$\lambda(t) = [T_0 \Theta^0 + T_1 \Theta^1 + T_2 \Theta^2] x(t), \quad (9)$$

one can rewrite the HJB equation in (4) as

$$\begin{aligned} & x^T(t) \left([T_0 + T_1 \Theta + T_2 \Theta^2] \right) \left(A_0 x(t) + \Theta \left(\frac{A(x(t))}{\Theta} \right) x(t) \right) \\ & - \frac{1}{2} x^T(t) \left([T_0 + T_1 \Theta + T_2 \Theta^2] \right) B R^{-1} B^T \left([T_0 + T_1 \Theta + T_2 \Theta^2] \right) x(t) \\ & + \frac{1}{2} x^T(t) \left(Q + \sum_{i=0}^\infty D_i \Theta^i \right) x(t) = 0. \end{aligned} \quad (10)$$

Finally, equating the coefficient of powers of Θ in (10) to zero yields to the following series of equation

$$T_0 A_0 + A_0^T T_0 - T_0 B R^{-1} B^T T_0 + Q = 0, \quad (11)$$

$$T_1(A_0 - BR^{-1}B^T T_0) + T_1(A_0^T - T_0 BR^{-1}B^T) = -\frac{T_0 A(x)}{\Theta} - \frac{T_0 A(x)}{\Theta} - D_1, \quad (12)$$

$$T_2(A_0 - BR^{-1}B^T T_0) + T_2(A_0^T - T_0 BR^{-1}B^T) = -\frac{T_1 A(x)}{\Theta} - \frac{T_1 A(x)}{\Theta} + T_1 BR^{-1}B^T T_1 - D_2. \quad (13)$$

The overview of the $\Theta - D$ method is now completed, where solving (11), (12), and (13) gives the feedback control signal (4) for the known nonlinear dynamical system in (1).

3. ADAPTIVE CONTROL WITH THE $\Theta - D$ NONLINEAR REFERENCE MODEL

In this section, we focus on uncertain nonlinear dynamical systems, where we use the $\Theta - D$ method to establish our nominal control signal based on the known system dynamics. In turn, it results in an optimal nonlinear reference model structure. Mathematically speaking, consider the uncertain nonlinear dynamical system given by

$$\dot{x}(t) = A_0 x(t) + A(x(t))x(t) + Bu(t) + Bd(x(t)), \quad x(0) = x_0, \quad (14)$$

where $d(x(t))$ is the uncertainty. The control algorithm is then separated into nominal and adaptive parts as

$$u(t) = u_n(t) + u_{ad}(t). \quad (15)$$

Using the $\Theta - D$ method overviewed in the previous section, the nominal controller is chosen as

$$u_n(t) = -R^{-1}B^T \left[T_0 \Theta^0 + T_1 \Theta^1 + T_2 \Theta^2 \right] x(t). \quad (16)$$

Substituting control algorithm (15) into (14) and choosing $\Theta = 1$, we have

$$\dot{x}(t) = A_0 x(t) + A(x(t))x(t) + B(u_n(t) + u_{ad}(t)) + Bd(x(t)), \quad x(0) = x_0. \quad (17)$$

In addition, substituting (16) into (17), we get

$$\begin{aligned}\dot{x}(t) &= A_0x(t) + A(x(t))x(t) - BR^{-1}B^T[T_0 + T_1 + T_2]x(t) + Bu_{ad}(t) + Bd(x(t)) \\ &= \left(A_0 - BR^{-1}B^T T_0\right)x(t) + \left(A(x(t)) - BR^{-1}B^T [T_1 + T_2]\right)x(t) + Bu_{ad}(t) + Bd(x(t))\end{aligned}\quad (18)$$

The optimal nonlinear reference model is now given as

$$\begin{aligned}\dot{x}_m(t) &= \left(A_0 - BR^{-1}B^T T_0\right)x_m(t) + \left(A(x_m(t)) - BR^{-1}B^T [T_1 + T_2]\right)x_m(t) \\ &= A_{m_1}x_m(t) + h(x_m(t)) - BK(x_m(t)), \quad x_m(0) = x_{m_0},\end{aligned}\quad (19)$$

where $A_{m_1} \triangleq A_0 - BR^{-1}B^T T_0$, $h(x_m(t)) \triangleq A(x_m(t))x_m(t)$, and $K(x_m(t)) \triangleq R^{-1}B^T [T_1 + T_2]x_m(t)$ (asymptotic stability of this reference model is considered based on the results overviewed in the previous section). Defining

$$h_m(x_m(t)) \triangleq h(x_m(t)) - BK(x_m(t)), \quad (20)$$

(19) can be rewritten as

$$\dot{x}_m(t) = A_{m_1}x_m(t) + h_m(x_m(t)), \quad x_m(0) = x_{m_0}. \quad (21)$$

We can now write

$$\dot{x}(t) = A_{m_1}x(t) + h_m(x(t)) + Bu_{ad}(t) + BW_2^T \phi_2(x(t)), \quad (22)$$

where $d(x(t)) = W_2^T \phi_2(x(t))$ represents the matched system uncertainty. Next, let

$$e(t) \triangleq x(t) - x_m(t), \quad e(0) = e_0 \triangleq x_0 - x_{m_0} \quad (23)$$

be the system error subject to

$$\begin{aligned}\dot{e}(t) &= A_{m_1}x(t) + h_m(x(t)) + Bu_{ad}(t) + BW_2^T\phi_2(x(t)) - A_{m_1}x_m(t) - h_m(x_m(t)), \\ &= A_{m_1}e(t) + h_m(x(t)) - h_m(x_m(t)) + Bu_{ad}(t) + BW_2^T\phi_2(x(t))\end{aligned}\quad (24)$$

From [23], the following assumption is needed for the main results of this paper.

Assumption 3.1. *There exists two vector fields $\mu : \mathbb{R}^n \rightarrow \mathbb{R}^n$ and $v : \mathbb{R}^n \times \mathbb{R}^n \times \mathbb{R}^m \rightarrow \mathbb{R}^m$ such that $\mu(0) = 0$ and*

$$\mu(e(t)) = A_{m_1}e(t) + h_m(x(t)) - h_m(x_m(t)) + Bv(e(t), x(t), x_m(t)), \quad (25)$$

holds. Furthermore, for the dynamical system $\dot{e}(t) = \mu(e(t))$ there exists a continuously differentiable function $\Phi : \mathbb{R}^n \rightarrow \mathbb{R}$ and a continuous vector field $l : \mathbb{R}^n \rightarrow \mathbb{R}^p$ such that $\Phi(\cdot)$ is positive definite, radially unbounded, $\Phi(0) = 0$, $l(0) = 0$, and

$$0 = \Phi'(e(t))\mu(e(t)) + l^T(e(t))l(e(t)), \quad (26)$$

holds for all $e \in \mathbb{R}$, where $\Phi'(e) = \frac{\partial\Phi}{\partial e}$ (we refer to [23] for additional details).

Finally, we use (25) into (24) and it is written as

$$\begin{aligned}\dot{e}(t) &= \mu(e(t)) - Bv(e(t), x(t), x_m(t)) + Bu_{ad}(t) + BW_2^T\phi_2(x(t)) \\ &= \mu(e(t)) + B[u_{ad}(t) + W_1^T\phi_1(x(t))]\end{aligned}\quad (27)$$

where the weight (W_1) and basis (ϕ_1) functions satisfy

$$\begin{aligned}W_1 &\triangleq [W_2^T \quad -\mathbb{I}]^T, \\ \phi_1(x(t), x_m(t), e(t)) &\triangleq [\phi_2^T(x(t)) \quad v^T(e(t), x(t), x_m(t))]^T.\end{aligned}\quad (28)$$

The adaptive control is then chosen as

$$u_{\text{ad}}(t) = -\hat{W}_1^T(t)\phi_1(x(t), x_m(t), e(t)). \quad (29)$$

By substituting (29) into (27), we get

$$\dot{e}(t) = \mu(e(t)) + B[-\hat{W}_1^T(t)\phi_1(x(t), x_m(t), e(t)) + W_1^T\phi_1(x(t), x_m(t), e(t))], \quad (30)$$

or equivalently

$$\dot{e}(t) = \mu(e(t)) + B[\tilde{W}_1^T(e(t))\phi_1(x(t), x_m(t), e(t))], \quad e(0) = e_0, \quad (31)$$

where $\tilde{W}_1(t) \triangleq W_1 - \hat{W}_1(t)$. The weight update rule now satisfies

$$\dot{\hat{W}}_1(t) = \gamma_1\phi_1(x(t), x_m(t), e(t))\Phi'(e(t))B, \quad \hat{W}_1(0) = \hat{W}_{10}, \quad (32)$$

where $\gamma_1 \in \mathbb{R}_+$ is the learning rate. Finally, the weight error dynamics satisfies

$$\dot{\tilde{W}}_1(t) = \gamma_1\phi_1(x(t), x_m(t), e(t))\Phi'(e(t))B, \quad \tilde{W}_1(0) = \tilde{W}_{10}. \quad (33)$$

We are now ready to present the main result of this paper.

Theorem 3.1. *Consider the closed-loop error dynamics given by (31) and (33). In addition, consider that Assumption 1 holds. Then, the pair $(e(t), \tilde{W}_1(t))$ is Lyapunov stable for all initial conditions and $\lim_{t \rightarrow \infty} e(t) = 0$.*

Proof. Consider the Lyapunov function given by

$$V(e(t), \tilde{W}_1(t)) = \Phi(e(t)) + \gamma_1^{-1} \text{tr}(\tilde{W}_1^T(t)\tilde{W}_1(t)). \quad (34)$$

Note that $V(e(t), \tilde{W}_1(t))$ is positive definite for all $(e(t), \tilde{W}_1(t))$ excluding (e_0, \tilde{W}_{10}) , radially unbounded, and $V(0, 0) = 0$. The time derivative of (34) can be calculated as

$$\begin{aligned}
\dot{V}(e(t), \tilde{W}_1(t)) &= \Phi'(e(t))\dot{e}(t) - 2\gamma_1^{-1}tr(\tilde{W}_1^T(t)\dot{\tilde{W}}_1(t)) \\
&= \Phi'(e(t))[\mu(e(t)) + B[\tilde{W}_1^T(t)\phi_1(x(t), x_m(t), e(t))]] \\
&\quad - 2tr(\tilde{W}_1^T(t)\phi_1(x(t), x_m(t), e(t))\Phi'(e(t))B) \\
&= \Phi'(e(t))\mu(e(t)) \\
&= -l^T(e(t))l(e(t)) \\
&\leq 0.
\end{aligned} \tag{35}$$

From (35) it is clear that the pair $(e(t), \tilde{W}_1(t))$ is Lyapunov stable for all initial conditions. Now, note that $l^T(e(t))l(e(t))$ is positive when $e(t) \neq 0$. Therefore, $\lim_{t \rightarrow \infty} e(t) = 0$ is immediate from [23, 24]. The proof is now complete. ■

4. ILLUSTRATIVE NUMERICAL EXAMPLES

In this section, two illustrative numerical examples are given to show the efficacy of the proposed method.

4.1. FIRST EXAMPLE

As our first example, consider the scalar dynamical system given by

$$\dot{x}(t) = -x^3(t) + x(t) + u(t) + d, \tag{36}$$

where d is selected as 0.1 and the value of the learning rate (γ_1) given in (32) is chosen as 250. The Q and R given in cost function (2) are chosen as 15 and 20, respectively. The initial state and the reference state of system are chosen as $x(0) = 1.5$ and $x_m(0) = 1$. In addition, the $\mu(e(t))$ in (25) is set as $A_r e(t)$, which is selected as $A_r = -3$. With these

selections, we have

$$v(t) = (-3 + \sqrt{2})e(t) - \frac{1}{\sqrt{2}}(x^3(t) - x_m^3(t)) + \frac{1}{4\sqrt{2}}(x^5(t) - x_m^5(t)) \quad (37)$$

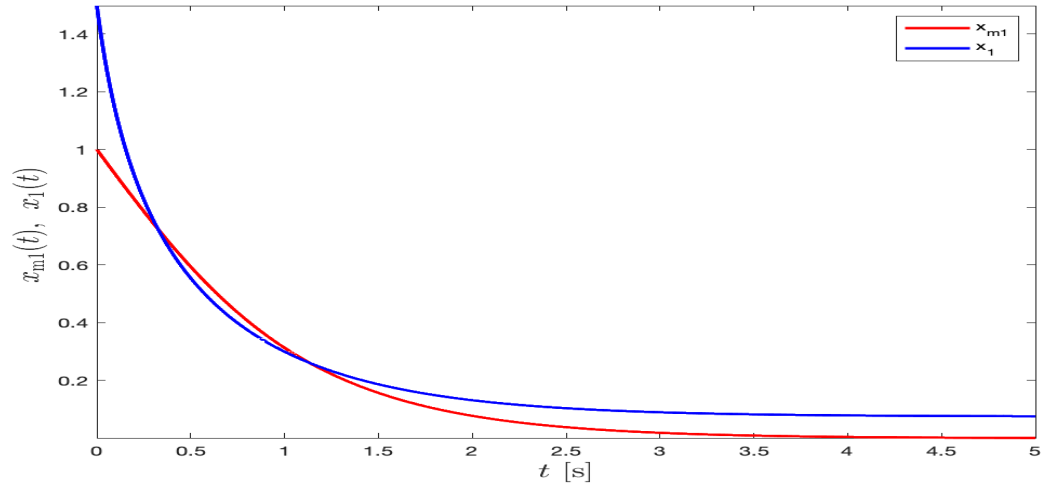


Figure 1. Histories of the actual and reference states without adaptive control

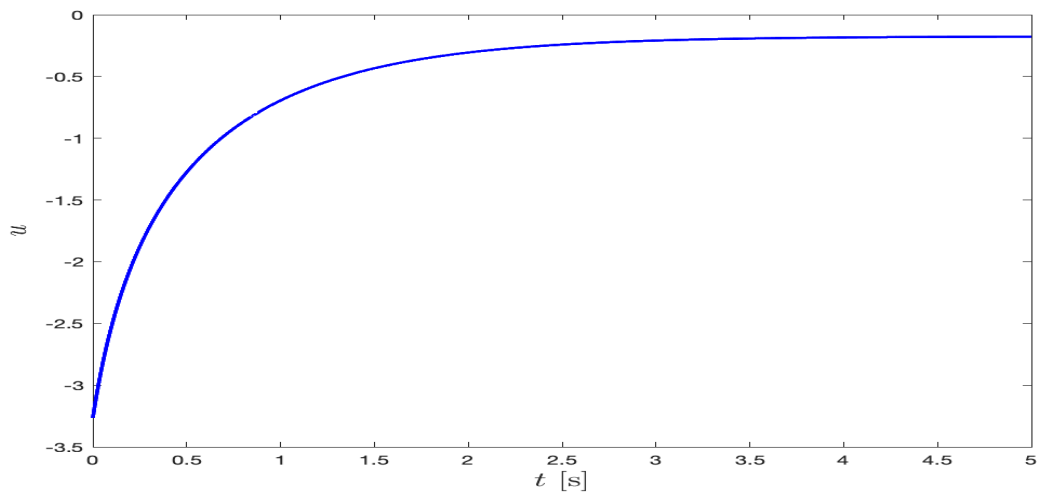


Figure 2. History of controller without adaptive control

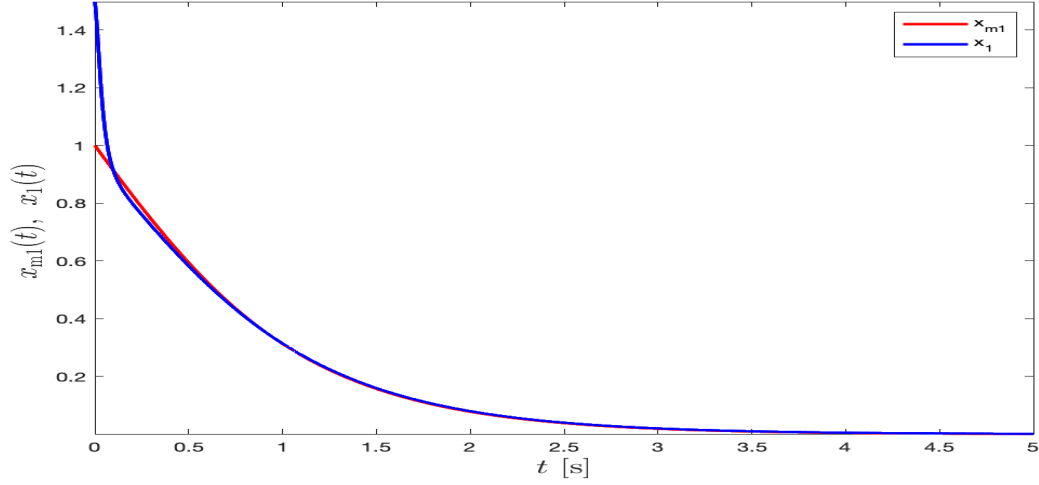


Figure 3. Histories of the actual and reference states with adaptive control

Figures 1 and 2 present the results for proposed method without the adaptive control input. Then, the adaptive control is added, where the system performance gets improved and shown in Figures 3 and 4.

4.2. SECOND EXAMPLE

The dynamics given in [25] is used in our second example to demonstrate the efficacy of the proposed adaptive control algorithm predicted on the optimal nonlinear reference model. Specifically, consider

$$\dot{x}_1(t) = x_1(t) - x_1^3(t) + x_2(t) + u_1(t) + d_1(x_1(t), x_2(t)) \quad (38)$$

$$\dot{x}_2(t) = x_1(t) - x_1^2(t)x_2(t) - x_2(t) + u_2(t) + d_2(x_1(t), x_2(t)), \quad (39)$$

where $d_1(x_1(t), x_2(t))$ is selected as $x_1(t) + 2x_2(t)$, and $d_2(x_1(t), x_2(t))$ is selected as $x_1(t) + 2x_2(t)$. In addition, the initial states and the reference states of the dynamic system are chosen as $x(0) = [1, 2]^T$ and $x_m(0) = [0.75, 2.25]^T$. The learning rate (γ_1) given in

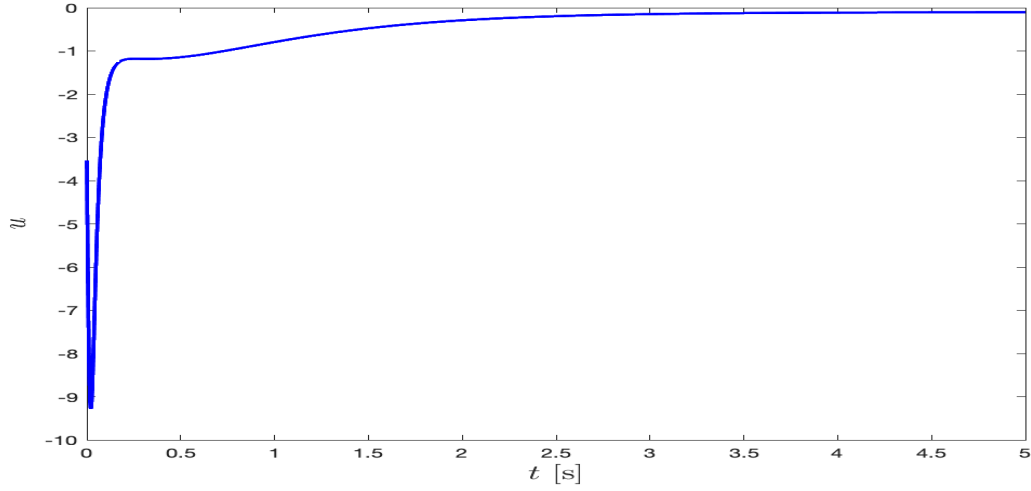


Figure 4. History of controller with adaptive control

(32) is set to 5. The Q and R from cost function are chosen as

$$Q = \begin{bmatrix} 1 & 0 \\ 0 & 10 \end{bmatrix}, \quad R = \begin{bmatrix} 20 & 0 \\ 0 & 20 \end{bmatrix}.$$

To find $v(t)$ given in (25), we select the $\mu(e(t))$ as $A_r e(t)$, where

$$A_r = \begin{bmatrix} 0 & 1 \\ -1 & -1.5 \end{bmatrix}.$$

Based on the above discussion, $v(t)$ takes the form given by

$$v(t) = \begin{bmatrix} v_1(t) \\ v_2(t) \end{bmatrix},$$

where $v_1(t) = 1.5811e_1(t) + e_2(t) - 0.6325x_1^3(t) + 0.1898x_1^5(t) + 0.6325x_{m_1}^3(t) - 0.1898x_{m_1}^5(t)$

and $v_2(t) = -e_1(t) + 0.0811e_2(t) - 0.6325x_1^2(t)x_2(t) + 0.1898x_1^4(t)x_2(t) + 0.6325x_{m_1}^2(t)x_{m_2}(t) - 0.1898x_{m_1}^4(t)x_{m_2}(t)$.

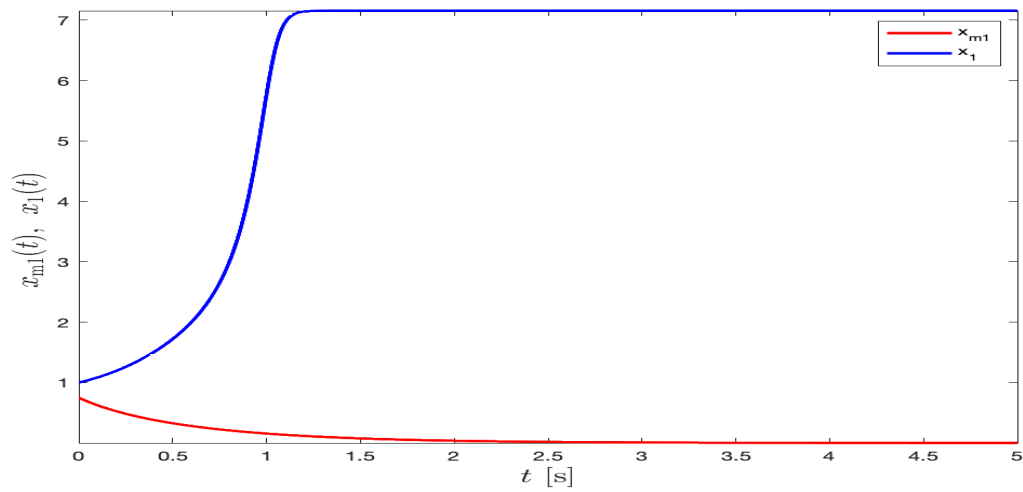


Figure 5. Histories of the actual and model reference state one without adaptive control

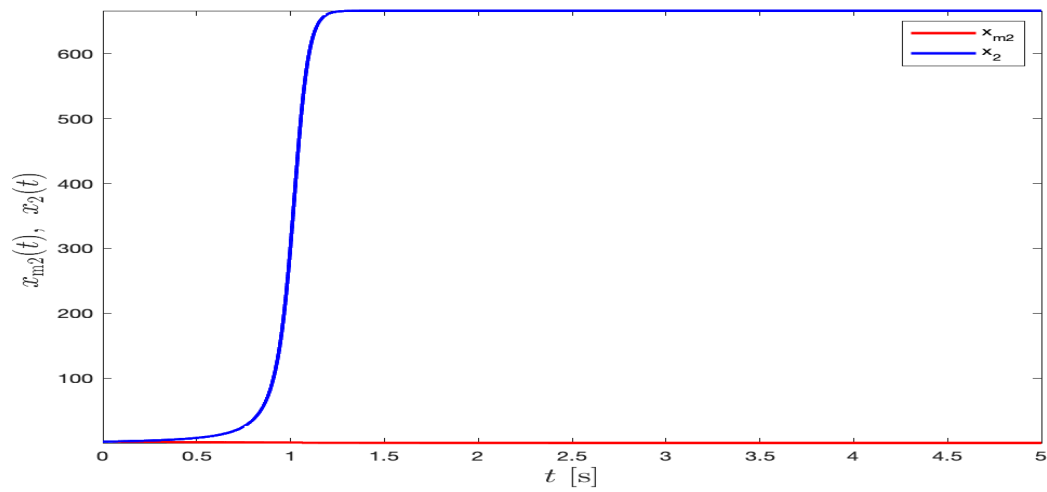


Figure 6. Histories of the actual and model reference state two without adaptive control

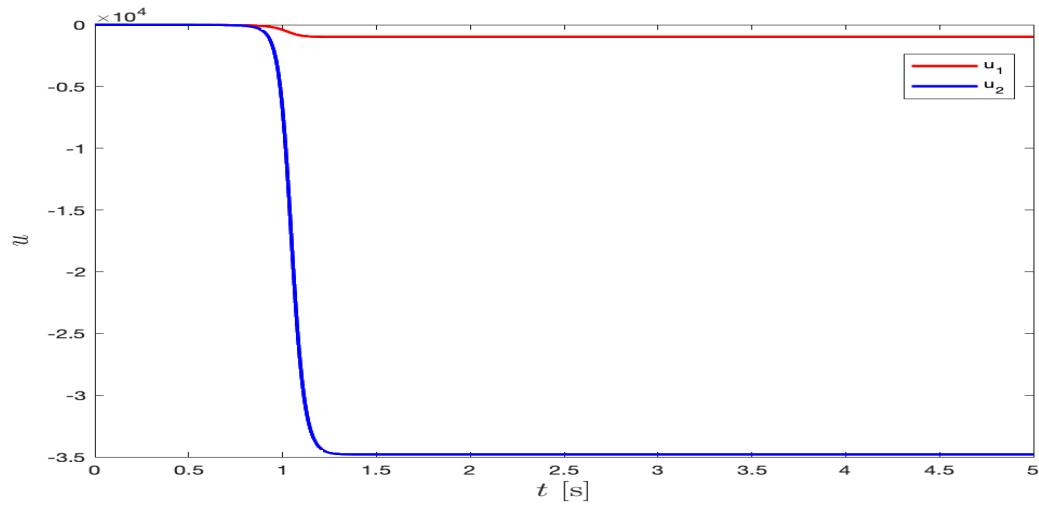


Figure 7. Histories of controller without adaptive control

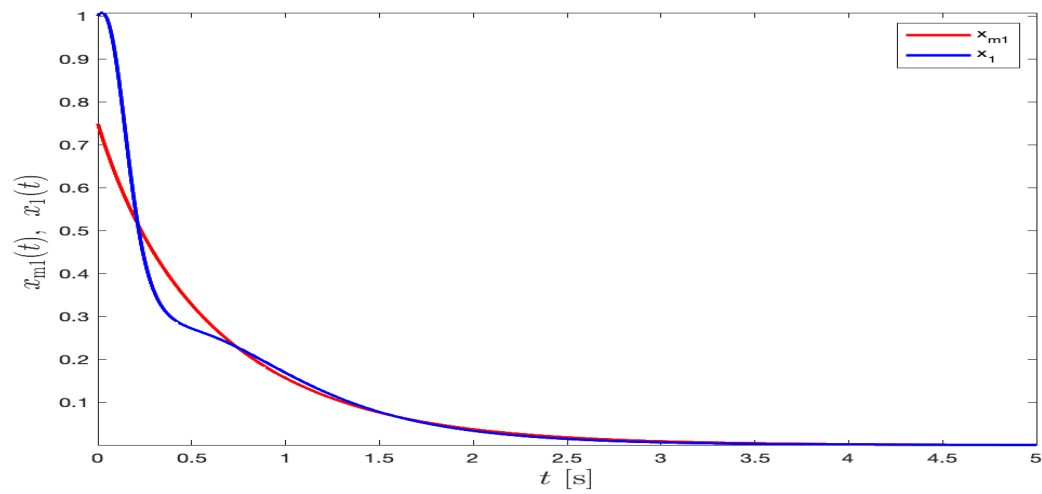


Figure 8. Histories of the actual and model reference state one with adaptive control

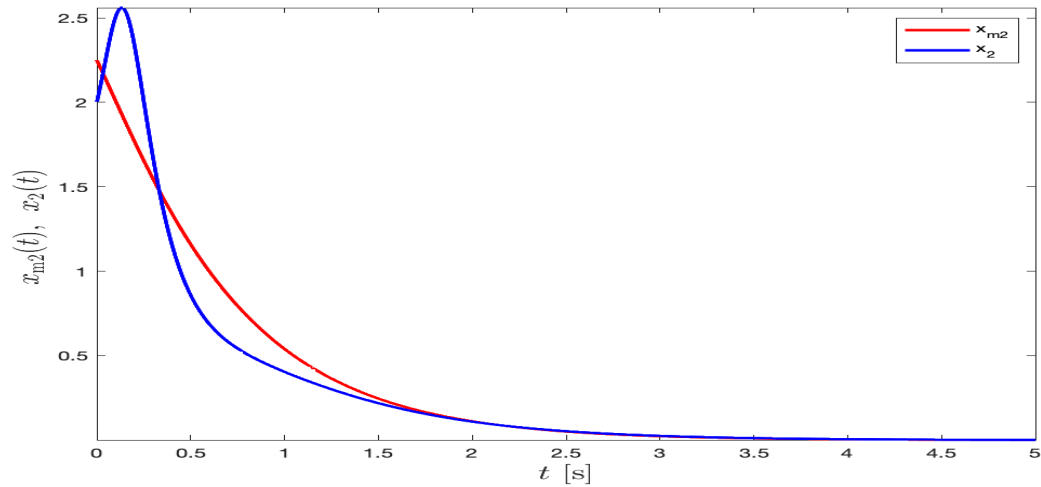


Figure 9. Histories of the actual and model reference state two with adaptive control

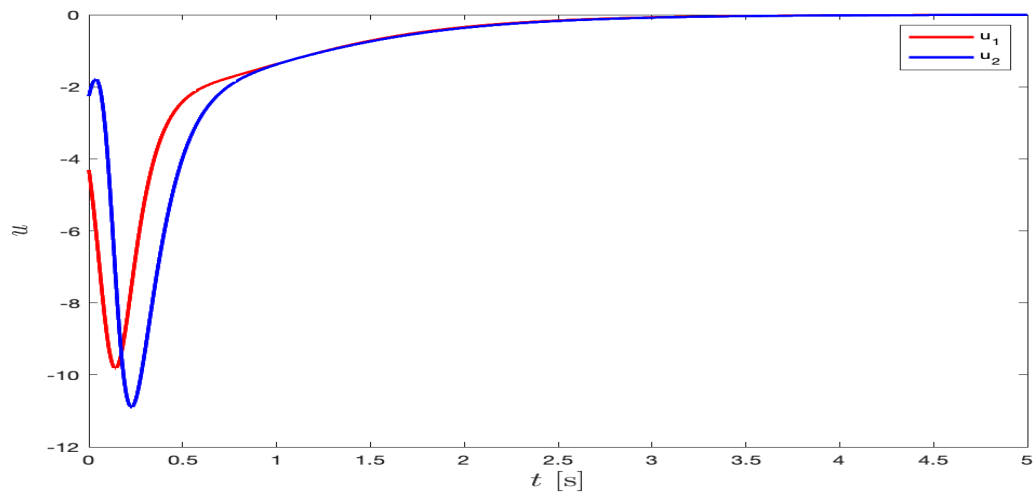


Figure 10. Histories of controller with adaptive control

Figures 5 to 7 show the results of the uncertain system without the adaptive controller. Figures 8 to 10 show the performance of the proposed method with the adaptive control input. Comparing these figures with and without adaptive control, it is clear that adding adaptive control input significantly improves the performance.

5. CONCLUSION

For adaptive control of uncertain dynamical systems, Θ -D method was used first to establish an optimal reference model in nonlinear form. Then, adaptive control input was designed to suppress the effect of system uncertainties. Two examples were demonstrated the efficacy of the proposed approach.

REFERENCES

- [1] Herty, M. and Kalise, D., 'Suboptimal nonlinear feedback control laws for collective dynamics,' in '2018 IEEE 14th International Conference on Control and Automation (ICCA),' IEEE, 2018 pp. 556–561.
- [2] Burghart, J., 'A technique for suboptimal feedback control of nonlinear systems,' IEEE Transactions on Automatic Control, 1969, **14**(5), pp. 530–533.
- [3] Eller, D. and Aggarwal, J., 'Sub-optimal control of non-linear single input systems,' International Journal of Control, 1968, **8**(2), pp. 113–121.
- [4] Garrard, W., McClamroch, N., and Clark, L., 'An approach to sub-optimal feedback control of non-linear systems,' International Journal of Control, 1967, **5**(5), pp. 425–435.
- [5] Garrard, W. L., 'Suboptimal feedback control for nonlinear systems,' Automatica, 1972, **8**(2), pp. 219–221.
- [6] Sannomiya, N., Itakura, H., *et al.*, 'A method for suboptimal design of nonlinear feedback systems,' Automatica, 1971, **7**(6), pp. 703–712.
- [7] Pearson, J., 'Approximation methods in optimal control i. sub-optimal control,' International Journal of Electronics, 1962, **13**(5), pp. 453–469.
- [8] Rosen, G. and Wismer, D., 'A sub-optimal feedback controller for on-line computer applications,' International Journal of Control, 1972, **15**(1), pp. 115–128.
- [9] Weber, A. and Lapidus, L., 'Suboptimal control of nonlinear systems: I. unconstrained,' AIChE Journal, 1971, **17**(3), pp. 641–648.
- [10] Weber, A. and Lapidus, L., 'Suboptimal control of nonlinear systems: II. constrained,' AIChE Journal, 1971, **17**(3), pp. 649–658.
- [11] Wernli, A. and Cook, G., 'Suboptimal control for the nonlinear quadratic regulator problem,' Automatica, 1975, **11**(1), pp. 75–84.

- [12] Chowdhary, G. and Johnson, E., ‘Concurrent learning for convergence in adaptive control without persistency of excitation,’ in ‘49th IEEE Conference on Decision and Control (CDC),’ IEEE, 2010 pp. 3674–3679.
- [13] Chowdhary, G., Yucelen, T., Mühlegg, M., and Johnson, E. N., ‘Concurrent learning adaptive control of linear systems with exponentially convergent bounds,’ *International Journal of Adaptive Control and Signal Processing*, 2013, **27**(4), pp. 280–301.
- [14] Kamalapurkar, R., Walters, P., and Dixon, W., ‘Concurrent learning-based approximate optimal regulation,’ in ‘52nd IEEE Conference on Decision and Control,’ IEEE, 2013 pp. 6256–6261.
- [15] Klotz, J., Kamalapurkar, R., and Dixon, W. E., ‘Concurrent learning-based network synchronization,’ in ‘2014 American Control Conference,’ IEEE, 2014 pp. 796–801.
- [16] Kamalapurkar, R., Andrews, L., Walters, P., and Dixon, W. E., ‘Model-based reinforcement learning for infinite-horizon approximate optimal tracking,’ *IEEE transactions on neural networks and learning systems*, 2016, **28**(3), pp. 753–758.
- [17] Ballesteros, M., Chairez, I., and Poznyak, A., ‘Robust optimal feedback control design for uncertain systems based on artificial neural network approximation of the bellman’s value function,’ *Neurocomputing*, 2020, **413**, pp. 134–144.
- [18] Vamvoudakis, K. G. and Lewis, F. L., ‘Online actor–critic algorithm to solve the continuous-time infinite horizon optimal control problem,’ *Automatica*, 2010, **46**(5), pp. 878–888.
- [19] Lv, Y., Na, J., Yang, Q., Wu, X., and Guo, Y., ‘Online adaptive optimal control for continuous-time nonlinear systems with completely unknown dynamics,’ *International Journal of Control*, 2016, **89**(1), pp. 99–112.
- [20] Balakrishnan, S. and Biega, V., ‘Adaptive-critic-based neural networks for aircraft optimal control,’ *Journal of Guidance, Control, and Dynamics*, 1996, **19**(4), pp. 893–898.
- [21] Padhi, R., Unnikrishnan, N., Wang, X., and Balakrishnan, S., ‘A single network adaptive critic (snac) architecture for optimal control synthesis for a class of nonlinear systems,’ *Neural Networks*, 2006, **19**(10), pp. 1648–1660.
- [22] Xin, M. and Balakrishnan, S., ‘A new method for suboptimal control of a class of nonlinear systems,’ in ‘Proceedings of the 41st IEEE Conference on Decision and Control, 2002.’, volume 3, IEEE, 2002 pp. 2756–2761.
- [23] Gruenwald, B. C., Yucelen, T., De La Torre, G., and Muse, J. A., ‘Adaptive control for uncertain dynamical systems with nonlinear reference systems,’ *International Journal of Systems Science*, 2020, **51**(4), pp. 687–703.
- [24] Haddad, W. M. and Chellaboina, V., *Nonlinear dynamical systems and control: a Lyapunov-based approach*, Princeton university press, 2011.

- [25] Cloutier, J. R., D'Souza, C. N., and Mracek, C. P., 'Nonlinear regulation and nonlinear h_∞ control via the state-dependent riccati equation technique: Part2, examples,' ”
Inrerna. Conf: On Nonlinear Problems in Aviation and Aerospace, 1996.

V. SET-THEORETIC MODEL REFERENCE ADAPTIVE CONTROL OF UNCERTAIN DYNAMICAL SYSTEMS WITH STATE CONSTRAINTS

Meryem Deniz¹, Tansel Yucelen², Ehsan Arabi³
¹Department of Mechanical & Aerospace Engineering
Missouri University of Science and Technology
Rolla, Missouri 65409–0050, United States of America
²Department of Mechanical Engineering
University of South Florida
Tampa, Florida 33620, United States of America
³Ford Research and Advanced Engineering
Ford Motor Company
Dearborn, MI 48121, United States of America

ABSTRACT

Many engineering systems are forced to operate in bounded state-space domains and therefore techniques to incorporate state constraints play an essential role for feedback controller designs. Yet, especially in the presence of system uncertainties, incorporating these constraints becomes a challenge. Motivated by this standpoint, a set-theoretic model reference adaptive control approach is proposed in this paper for uncertain nonlinear systems to keep the state values within the desired bounds. This paper also presents experimental results of set-theoretic barrier Lyapunov function (STBLF) to handle state constraints and uncertainties on a Quanser 3 DOF Hover system. Specifically, three different restricted potential functions are explored to demonstrate that much attention should be shown in the selection of the restricted potential functions in order to result in effective constrained control and also obtain a desirable closed-loop system performance. Illustrative numerical and experimental examples are also provided to demonstrate the efficacy of our contributions.

1. INTRODUCTION

Many engineering systems have bounds on the states of the system, otherwise possibly resulting in system failures. Consequently, designing a controller for uncertain systems with state constraints is a critical problem. The main functions of a controller are: 1) to ensure that the states of a system do not violate the state limits, 2) to guarantee stability, and 3) to account for uncertainties in the system in the case that they exist.

In the current literature, there exist notable methods to handle the state variable constraints. Muse developed an adaptive control method that forced the state of the system to stay in a given region [1]. The reason for the chosen region is to show stability analysis for nonlinear systems. The bounding functions are used to limit the states of a system. These bounding functions keep the states under the limit when the growth rate of the bounding functions is sufficiently large. Arabi *et al.* develop set-theoretic barrier Lyapunov function (STBLF) approach to constrain the tracking error between the actual uncertain system state and reference model state [2]. They illustrate the efficacy of the proposed method on different linear and nonlinear reference models. A barrier Lyapunov function for the control of output constrained nonlinear systems is proposed by Tee *et al.* [3]. The intended barrier Lyapunov function shows asymptotic tracking without violation of the constraint. In addition, the same authors relax the initial conditions using an asymmetric barrier Lyapunov function. Lavretsky and Gadiant design a baseline dynamic inversion based controller to prevent the system trajectory from leaving an acceptable subset [4]. The short period dynamics of fixed-wing aircraft is used to show the performance of the proposed method. An STBLF is developed with inverse optimal control to handle state constraints [5]. This method helps to design the optimal controller when the states have some constraints. Optimal control formulations also have been used in problems with state (inequality) constraints in [6, 7, 8, 9, 10]. Typically, it is challenging to incorporate the state constraints with an optimal control formulation because the corresponding mathematics is highly involved.

In this paper, the objectives are to keep the state under a prescribed limit, to guarantee stability, and to suppress the effect of uncertainty. To handle these problems, a new adaptive controller with the (STBLF) approach is designed. The method in [1] uses bounding functions for constraint enforcement, which only handle the soft constraint. Yet, the proposed method is designed for the hard constraint. Specifically, three different restricted potential functions are used to handle the state constraints and their performance is evaluated through illustrative numerical examples.

Throughout this paper, \mathbb{R} denotes set of real numbers, \mathbb{R}^n denotes the set of real column vectors, and $\mathbb{R}^{n \times m}$ denotes the set of real matrices. Also, we use \mathbb{R}_+ , $\mathbb{R}_+^{n \times n}$ respectively for the sets of positive real numbers, positive-definite matrices. We use \triangleq for the equality by definition. In addition, $(\cdot)^T$, $(\cdot)^{-1}$, $tr(\cdot)$, $\|\cdot\|_2$ denote transpose operator, inverse operator, trace operator, Euclidean norm, respectively. $\|\cdot\|_P = \sqrt{x^T P x}$ is written for the weighted Euclidean norm of $x(t) \in \mathbb{R}^n$ with the matrix $P \in \mathbb{R}_+^{n \times n}$. The minimum eigenvalue of the matrix $P \in \mathbb{R}^{n \times n}$ is used as $\lambda_{min}(P)$ and the maximum eigenvalue of the matrix $P \in \mathbb{R}^{n \times n}$ is used as $\lambda_{max}(P)$. Finally, the projection operator definition is introduced. Let $\Omega \in \mathbb{R}^n$ be a convex hypercube defined as $\Omega = \{\theta \in \mathbb{R}^n : (\theta_i^{min} \leq \theta_i \leq \theta_i^{max})_{i=1,2,\dots,n}\}$ with θ_i^{min} and θ_i^{max} respectively denoting the minimum and maximum bounds for the i^{th} component of the parameter vector $\theta \in \mathbb{R}^n$. In addition, with a sufficiently small constant $\epsilon_0 \in \mathbb{R}_+$, let $\Omega_{\epsilon_0} = \{\theta \in \mathbb{R}^n : (\theta_i^{min} + \epsilon_0 \leq \theta_i \leq \theta_i^{max} - \epsilon_0)_{i=1,2,\dots,n}\}$ be an another convex hypercube (i.e., $\Omega_{\epsilon_0} \subset \Omega$). Then the component-wise projection operator is defined $\text{Proj} : \mathbb{R}^n \times \mathbb{R}^n \rightarrow \mathbb{R}^n$ as $\text{Proj}(\theta, y) = (\theta_i^{max} - \theta_i)y_i/\epsilon_0$ when $\theta_i > \theta_i^{max} - \epsilon_0$ and $y_i > 0$, $\text{Proj}(\theta, y) = (\theta_i - \theta_i^{min})y_i/\epsilon_0$ when $\theta_i < \theta_i^{min} + \epsilon_0$ and $y_i < 0$, and $\text{Proj}(\theta, y) = y_i$ otherwise, where $y \in \mathbb{R}^n$. Then, from previous definition, we have $(\theta - \theta^*)^T(\text{Proj}(\theta, y) - y) \leq 0$, where $\theta^* \in \Omega_{\epsilon_0}$ (e.g., see [11, 12]). Also, one can generalize the projection operator definition to matrices using $\text{Proj}_m(\Theta, Y) = (\text{Proj}(\text{col}_1(\Theta), \text{col}_1(Y)), \dots, \text{Proj}(\text{col}_m(\Theta), \text{col}_m(Y)))$ that gives $\text{tr}[(\Theta - \Theta^*)^T(\text{Proj}_m(\Theta, Y) - Y)] = \sum_{i=1}^m [\text{col}_i(\Theta - \Theta^*)^T(\text{Proj}(\text{col}_i(\Theta), \text{col}_i(Y)) - \text{col}_i(Y))] \leq 0$ with $n \times m$ dimensional matrices Y , Θ , and Θ^* .

2. SET-THEORETIC BARRIER LYAPUNOV FUNCTION WITH STATE CONSTRAINTS

In this study, we focus on uncertain nonlinear systems with the form given by

$$\dot{x}(t) = Ax(t) + B\Lambda u(t) + Bf(x(t)), \quad x(0) = x_0, \quad (1)$$

where $x(t) \in \mathbb{R}^n$, $t \geq 0$, is the state vector, $u(t) \in \mathbb{R}^m$, $t \geq 0$, is the control input, $A \in \mathbb{R}^{n \times n}$ and $B \in \mathbb{R}^{n \times m}$ is a known system matrix and a known input matrix, respectively, $\Lambda \in \mathbb{R}^{m \times m}$ is a constant unknown positive definite matrix, and $f(x(t)) : \mathbb{R}^n \rightarrow \mathbb{R}^m$ is an unknown function. In this case, Λ is assumed to be of the form

$$\Lambda = I + \lambda, \quad (2)$$

where $\lambda < I$.

Assumption 2.1. *The unknown function $f(x)$ given in (1) satisfies*

$$f(x(t)) = W^T \beta(x(t)), \quad (3)$$

where $\beta : \mathbb{R}^n \rightarrow \mathbb{R}^l$ is a basis function and $W \in \mathbb{R}^{l \times m}$ is a set of constant unknown weights with an upper bound $\|W\|_2 \leq w$.

Let the nominal controller be defined as

$$u_n(t) = -K_n x(t) + K_r r(t), \quad (4)$$

where $K_n \in \mathbb{R}^{m \times n}$ is the nominal feedback gain matrix, $K_r \in \mathbb{R}^{m \times n_r}$ is the nominal feed-forward gain matrix and $r(t) \in \mathbb{R}^{n_r}$ is a given bounded piecewise continuous command. Assuming $\Lambda = I$ and $f(x(t)) = 0$, this nominal controller yields to the reference model

given by

$$\dot{x}_m(t) = A_m x_m(t) + B_m r(t), \quad (5)$$

where $A_m \triangleq A - BK_n$ is a Hurwitz matrix, and $B_m \triangleq BK_r$.

The controller is then designed as

$$u(t) = u_n(t) - u_{ad}(t) - u_c(t), \quad (6)$$

where $u_n(t)$ is the nominal controller which yields the desired performance for the unconstrained nominal system without uncertainties, $u_{ad}(t)$ represents the adaptive controller which accounts for the uncertainty in the system, and $u_c(t)$ is the controller that enforces the state constraints.

The definition of the barrier Lyapunov function is given next to handle the state constraints.

Definition 2.1. A restricted potential function $\phi(\|a\|_P)$, $\phi : \mathbb{R} \rightarrow \mathbb{R}$ can be defined on the set given by

$$\mathcal{D}_\epsilon \triangleq \{a : \|a\|_P \in [0, \epsilon)\}, \quad (7)$$

where $\epsilon \in \mathbb{R}_+$ is a user-defined constant, when following conditions are satisfied [2]:

i) If $\|a\|_P = 0$, then $\phi(\|a\|_P) = 0$.

ii) If $a \in \mathcal{D}_\epsilon$ and $\|a\|_P \neq 0$, then $\phi(\|a\|_P) > 0$.

iii) If $\|a\|_P \rightarrow \epsilon$, then $\phi(\|a\|_P) \rightarrow \infty$.

iv) $\phi(\|a\|_P)$ is continuously differentiable on \mathcal{D}_ϵ .

v) If $a \in \mathcal{D}_\epsilon$, then $D_\phi(\|a\|_P) > 0$, where $D_\phi(\|a\|_P) \triangleq \frac{d\phi(\|a\|_P)}{d\|a\|_P^2}$.

vi) If $a \in \mathcal{D}_\epsilon$, then $D_\phi(\|a\|_P)\|a\|_P^2 - \phi(\|a\|_P) > 0$.

We now present three different generalized restricted potential function candidates ($\phi(\|a\|_P)$) that satisfy the above definition.

2.1. CASE 1

The first generalized restricted potential function is given by

$$\phi(\|a\|_P) = \frac{\|a\|_P^2}{\epsilon - \|a\|_P}, \quad \|a\|_P \in \mathcal{D}_\epsilon. \quad (8)$$

By taking the partial derivative of (8) with respect to $\|a\|_P^2$, we get

$$D_\phi(\|a\|_P) = \frac{\epsilon - \frac{1}{2}\|a\|_P}{(\epsilon - \|a\|_P)^2} > 0, \quad \|a\|_P \in \mathcal{D}_\epsilon. \quad (9)$$

2.2. CASE 2

The second generalized restricted potential function is defined as

$$\phi(\|a\|_P) = \frac{\epsilon^2 \|a\|_P^2}{\epsilon^2 - \|a\|_P^2}, \quad \|a\|_P \in \mathcal{D}_\epsilon, \quad (10)$$

and the partial derivative of (10) with respect to $\|a\|_P^2$ is given by

$$D_\phi(\|a\|_P) = \frac{\epsilon^4}{(\epsilon^2 - \|a\|_P^2)^2} > 0, \quad \|a\|_P \in \mathcal{D}_\epsilon. \quad (11)$$

2.3. CASE 3

The last generalized restricted potential function is given as

$$\phi(\|a\|_P) = \frac{\epsilon^4 \|a\|_P^2}{\epsilon^2 - \|a\|_P^2}, \quad \|a\|_P \in \mathcal{D}_\epsilon, \quad (12)$$

and the partial derivative of (12) with respect to $\|a\|_{\mathbb{P}}^2$ is

$$D_{\phi}(\|a\|_{\mathbb{P}}) = \frac{\epsilon^6}{(\epsilon^2 - \|a\|_{\mathbb{P}}^2)^2} > 0, \quad \|a\|_{\mathbb{P}} \in \mathcal{D}_{\epsilon}. \quad (13)$$

The adaptive control law ($u_{\text{ad}}(t)$) used in this study is given by

$$u_{\text{ad}}(t) = (I + \hat{\lambda}(t))^{-1} [\hat{W}^T(t)\beta(x(t)) + \hat{\lambda}(t)(u_n(t) - u_c(t))], \quad (14)$$

where $\hat{\lambda}(t)$ is the estimate of the unknown coefficients in the control effectiveness matrix and $\hat{W}(t)$ is the estimate of the weight matrix and the control law for constraint ($u_c(t)$) is given as

$$u_c(t) = \frac{D_{\phi}(\|x(t)\|_{\mathbb{P}})}{1 + D_{\phi}(\|x(t)\|_{\mathbb{P}})} K_r r(t). \quad (15)$$

The update laws of $\hat{W}(t)$ and $\hat{\lambda}(t)$ are given as

$$\dot{\hat{W}}(t) = -\gamma_1 \text{Proj}(\hat{W}(t), \beta(e^T(t) - D_{\phi}(\|x(t)\|_{\mathbb{P}})x^T(t))PB), \quad (16)$$

$$\dot{\hat{\lambda}}(t) = -\gamma_2 \text{Proj}(\hat{\lambda}(t), B^T P(e(t) - D_{\phi}(\|x(t)\|_{\mathbb{P}})x(t))u(t)). \quad (17)$$

Note that since we use the projection operator in (16) and (17), it follows that $\|\hat{W}\|_2 \leq \bar{w}$, $\|\hat{\lambda}\|_2 \leq \bar{\lambda}_{\max}$. In addition, $\gamma_1 \in \mathbb{R}_+$ and $\gamma_2 \in \mathbb{R}_+$ are the learning rates, and $P \in \mathbb{R}^{n \times n}$ and $P = P^T > 0$ is the solution of the Lyapunov equation given by

$$A_m^T P + P A_m + Q = 0, \quad (18)$$

where $Q \in \mathbb{R}^{n \times n}$ is a positive definite matrix. Using (2) and (3) in (1), we get

$$\dot{x}(t) = Ax(t) + B(I + \lambda)u(t) + BW^T\beta(x(t)), \quad x(0) = x_0, \quad (19)$$

and substituting (6) into (19), one can write

$$\dot{x}(t) = Ax(t) + B[u_n(t) - u_{ad}(t) - u_c(t)] + B\lambda u(t) + BW^T\beta(x(t)). \quad (20)$$

Now, using (4) into (20), the system dynamics becomes

$$\begin{aligned} \dot{x}(t) &= Ax(t) + B[-K_n x(t) + K_r r(t)] - B[u_{ad}(t) + u_c(t)] + B\lambda u(t) + BW^T\beta(x(t)) \\ &= A_m x(t) + B_m r(t) - B[u_{ad}(t) + u_c(t)] + B\lambda u(t) + BW^T\beta(x(t)). \end{aligned} \quad (21)$$

Next, arranging (14) and substituting into (21) yield

$$\begin{aligned} \dot{x}(t) &= A_m x(t) + B_m r(t) - B\hat{\lambda}(t)u(t) - B\hat{W}^T(t)\beta(x(t)) - Bu_c(t) + B\lambda u(t) + BW^T\beta(x(t)) \\ &= A_m x(t) + B_m r(t) - B[\hat{\lambda}(t) - \lambda]u(t) - B[\hat{W}^T(t) - W^T]\beta(x(t)) - Bu_c(t) \\ &= A_m x(t) + B_m r(t) - B\tilde{\lambda}(t)u(t) - B\tilde{W}^T(t)\beta(x(t)) - Bu_c(t), \end{aligned} \quad (22)$$

where $\tilde{\lambda} = \hat{\lambda} - \lambda$ is the control effectiveness estimation error and $\tilde{W} = \hat{W} - W$ is the weight estimation error. Finally, defining the reference model tracking error as $e \triangleq x_m - x$, the error dynamics can be expressed as

$$\dot{e}(t) = A_m e(t) + B\tilde{\lambda}(t)u(t) + B\tilde{W}^T(t)\beta(x(t)) + Bu_c(t). \quad (23)$$

Assumption 2.2. *The command $r(t) \in \mathbb{R}^{n_r}$ exponentially converges to a steady state value, i.e., $\exists r_{ss} \in \mathbb{R}^{n_r}$, $\alpha^*, \beta^* \in \mathbb{R}_+$ such that*

$$\|r(t) - r_{ss}\| \leq \alpha^* e^{-\beta^* t}, \quad t \in [0, \infty) \quad (24)$$

holds. In addition, we let $x_{m_{ss}} \in \mathbb{R}^n$ be the steady state value of the reference system state given by $x_{m_{ss}} = -A_m^{-1} B_m r_{ss}$.

Theorem 2.1. *Under the control input defined in (6) with nominal control (4), adaptive control (14) and control law for constraint (15) with update laws given in (16) and (17), the closed-loop systems dynamics is stable. If the initial weighted Euclidean norm is less than the user-defined constant, then the closed-loop systems states are bounded and the system weighted Euclidean norm strictly satisfies the user-defined constant given by*

$$\|x(t)\|_P < \epsilon, \quad t \geq 0. \quad (25)$$

Proof. Let the Lyapunov function candidate be

$$\begin{aligned} V(e(t), x(t), \tilde{W}(t), \tilde{\lambda}(t)) &= e^T(t)Pe(t) + \phi(\|x(t)\|_P) + tr(\tilde{W}^T(t)\gamma_1^{-1}\tilde{W}(t)) \\ &+ tr(\tilde{\lambda}(t)\gamma_2^{-1}\tilde{\lambda}^T(t)). \end{aligned} \quad (26)$$

Note that $V(0, 0, 0, 0) = 0$, and $V(e(t), x(t), \tilde{W}(t), \tilde{\lambda}(t)) > 0$ for all $(e(t), \|x(t)\|_P, \tilde{W}(t), \tilde{\lambda}(t)) \neq (0, 0, 0, 0)$. Boundedness of the closed-loop system states is proven using the Lyapunov candidate defined in (26). The time derivative of (26) is given as

$$\begin{aligned} \dot{V}(e(t), x(t), \tilde{W}(t), \tilde{\lambda}(t)) &= 2e^T(t)P\dot{e}(t) + \frac{d\phi(\|x(t)\|_P)}{dt} + 2 tr(\tilde{W}^T(t)\gamma_1^{-1}\dot{\tilde{W}}(t)) \\ &+ 2 tr(\tilde{\lambda}(t)\gamma_2^{-1}\dot{\tilde{\lambda}}^T(t)), \end{aligned} \quad (27)$$

where $\frac{d\phi(\|x(t)\|_P)}{dt}$ is given by

$$\frac{d\phi(\|x(t)\|_P)}{dt} = \frac{d\phi(\|x(t)\|_P)}{d\|x(t)\|_P} \frac{d\|x(t)\|_P}{dx(t)} \frac{dx(t)}{dt} = 2D_\phi(\|x\|_P)x^T(t)P\dot{x}(t). \quad (28)$$

By substituting (28) into (27), we get

$$\begin{aligned} \dot{V}(e(t), x(t), \tilde{W}(t), \tilde{\lambda}(t)) &= 2e^T(t)P\dot{e}(t) + 2D_\phi(\|x(t)\|_P)x^T(t)P\dot{x}(t) \\ &+ 2 tr(\tilde{W}^T(t)\gamma_1^{-1}\dot{\tilde{W}}(t)) + 2 tr(\tilde{\lambda}(t)\gamma_2^{-1}\dot{\tilde{\lambda}}^T(t)). \end{aligned} \quad (29)$$

By substituting (22) and (23) into (29), we get

$$\begin{aligned}
\dot{V}(e(t), x(t), \tilde{W}(t), \tilde{\lambda}(t)) &= 2e^T(t)P[A_m e(t) + Bu_c(t)] \\
&\quad + 2D_\phi(\|x(t)\|_P)x^T(t)P[A_mx(t) + B_mr(t) - Bu_c(t)] \\
&\quad + 2\text{tr}[\tilde{W}^T(t)(\gamma_1^{-1}\dot{\tilde{W}}(t) + \beta(e^T(t) - D_\phi(\|x(t)\|_P)x^T(t))PB)] \\
&\quad + 2\text{tr}[\tilde{\lambda}^T(t)(\gamma_2^{-1}\dot{\tilde{\lambda}}(t) + u(t)(e^T(t) - D_\phi(\|x(t)\|_P)x^T(t))PB)].
\end{aligned} \tag{30}$$

By using (16) and (17) into (30), and also using projection operator properties, we get

$$\begin{aligned}
\dot{V}(e(t), x(t), \tilde{W}(t), \tilde{\lambda}(t)) &\leq 2e^T(t)P[A_m e(t) + Bu_c(t)] \\
&\quad + 2D_\phi(\|x(t)\|_P)x^T(t)P[A_mx(t) + B_mr(t) - Bu_c(t)].
\end{aligned} \tag{31}$$

By using (18) and (15) into (31), we get

$$\begin{aligned}
\dot{V}(e(t), x(t), \tilde{W}(t), \tilde{\lambda}(t)) &\leq -e^T(t)Qe(t) + 2e^T(t)PBu_c(t) - D_\phi(\|x(t)\|_P)x^T(t)Qx(t) \\
&\quad + 2D_\phi(\|x(t)\|_P)x^T(t)P[B_mr(t) - Bu_c(t)].
\end{aligned} \tag{32}$$

By using (15) into (32), we get

$$\begin{aligned}
\dot{V}(e(t), x(t), \tilde{W}(t), \tilde{\lambda}(t)) &\leq -e^T(t)Qe(t) - D_\phi(\|x(t)\|_P)x^T(t)Qx(t) \\
&\quad + 2\frac{D_\phi(\|x(t)\|_P)}{1 + D_\phi(\|x(t)\|_P)}e^T(t)PBK_r r(t) \\
&\quad + 2D_\phi(\|x(t)\|_P)x^T(t)P[BK_r r(t) - B\frac{D_\phi(\|x(t)\|_P)}{1 + D_\phi(\|x(t)\|_P)}K_r r(t)] \\
&\leq -e^T(t)Qe(t) - D_\phi(\|x(t)\|_P)x^T(t)Qx(t) \\
&\quad + 2\frac{D_\phi(\|x(t)\|_P)}{1 + D_\phi(\|x(t)\|_P)}e^T(t)PBK_r r(t) \\
&\quad + 2\frac{D_\phi(\|x(t)\|_P)}{1 + D_\phi(\|x(t)\|_P)}x^T(t)PBK_r r(t).
\end{aligned} \tag{33}$$

Then, we use $e = x_m - x$, we get

$$\begin{aligned}
\dot{V}(e(t), x(t), \tilde{W}(t), \tilde{\lambda}(t)) &\leq -e^T(t)Qe(t) - D_\phi(\|x(t)\|_P)x^T(t)Qx(t) \\
&\quad + 2\frac{D_\phi(\|x(t)\|_P)}{1 + D_\phi(\|x(t)\|_P)}x^T(t)PBK_r r(t) \\
&\quad + 2\frac{D_\phi(\|x(t)\|_P)}{1 + D_\phi(\|x(t)\|_P)}(x_m(t) - x(t))^T PBK_r r(t) \quad (34) \\
&\leq -e^T(t)Qe(t) - D_\phi(\|x(t)\|_P)x^T(t)Qx(t) \\
&\quad + 2\frac{D_\phi(\|x(t)\|_P)}{1 + D_\phi(\|x(t)\|_P)}x_m^T(t)PBK_r r(t).
\end{aligned}$$

By adding and subtracting $2\frac{D_\phi}{1+D_\phi}x_{m_{ss}}^T PB_m r_{ss}$, we will have

$$\begin{aligned}
\dot{V}(e(t), x(t), \tilde{W}(t), \tilde{\lambda}(t)) &\leq -e^T(t)Qe(t) - D_\phi(\|x(t)\|_P)x^T(t)Qx(t) \\
&\quad + 2\frac{D_\phi(\|x(t)\|_P)}{1 + D_\phi(\|x(t)\|_P)}x_m^T(t)PBK_r r(t) \quad (35) \\
&\quad + 2\frac{D_\phi(\|x(t)\|_P)}{1 + D_\phi(\|x(t)\|_P)}[x_{m_{ss}}^T PB_m r_{ss} - x_{m_{ss}}^T PB_m r_{ss}].
\end{aligned}$$

By rearranging (35), we get

$$\begin{aligned}
\dot{V}(e(t), x(t), \tilde{W}(t), \tilde{\lambda}(t)) &\leq -e^T(t)Qe(t) - D_\phi(\|x(t)\|_P)x^T(t)Qx(t) \\
&\quad + 2\frac{D_\phi(\|x(t)\|_P)}{1 + D_\phi(\|x(t)\|_P)}x_{m_{ss}}^T PB_m r_{ss} \quad (36) \\
&\quad + 2\frac{D_\phi(\|x(t)\|_P)}{1 + D_\phi(\|x(t)\|_P)}[x_m^T(t)PBK_r r(t) - x_{m_{ss}}^T PB_m r_{ss}],
\end{aligned}$$

where $x_{m_{ss}} = -A_m^{-1}B_m r_{ss}$. Since, $B_m r_{ss} = -A_m x_{m_{ss}}$, this can be expressed as

$$\begin{aligned}
\dot{V}(e(t), x(t), \tilde{W}(t), \tilde{\lambda}(t)) &\leq -e^T(t)Qe(t) - D_\phi(\|x(t)\|_P)x^T(t)Qx(t) \\
&\quad - 2\frac{D_\phi(\|x(t)\|_P)}{1 + D_\phi(\|x(t)\|_P)}x_{m_{ss}}^T PA_m x_{m_{ss}} \quad (37) \\
&\quad + 2\frac{D_\phi(\|x(t)\|_P)}{1 + D_\phi(\|x(t)\|_P)}[x_m^T(t)PBK_r r(t) - x_{m_{ss}}^T PB_m r_{ss}].
\end{aligned}$$

By using $A_m^T P + P A_m + Q = 0$, we get

$$\begin{aligned} \dot{V}(e(t), x(t), \tilde{W}(t), \tilde{\lambda}(t)) &\leq -e^T(t) Q e(t) - D_\phi(\|x(t)\|_P) x^T(t) Q x(t) \\ &\quad + \frac{D_\phi(\|x(t)\|_P)}{1 + D_\phi(\|x(t)\|_P)} x_{m_{ss}}^T Q x_{m_{ss}} \\ &\quad + 2 \frac{D_\phi(\|x(t)\|_P)}{1 + D_\phi(\|x(t)\|_P)} [x_m^T(t) P B K_r r(t) - x_{m_{ss}}^T P B_m r_{ss}]. \end{aligned} \quad (38)$$

Since $D_\phi > 0$, it implies $\frac{D_\phi}{1+D_\phi} < D_\phi$, we get

$$\begin{aligned} \dot{V}(e(t), x(t), \tilde{W}(t), \tilde{\lambda}(t)) &\leq -e^T(t) Q e(t) - D_\phi(\|x(t)\|_P) [x^T(t) Q x(t) - x_{m_{ss}}^T Q x_{m_{ss}}] \\ &\quad + 2 \|(x_m^T(t) P B K_r r(t) - x_{m_{ss}}^T P B_m r_{ss})\|. \end{aligned} \quad (39)$$

Since $\exists \alpha^*, \beta^* \in \mathbb{R}_+$ such that

$$\|r(t) - r_{ss}\| \leq \alpha^* e^{-\beta^* t}, \quad t \in [0, \infty), \quad (40)$$

and the reference dynamics in (5) are exponentially stable, it is straight forward to show that there exist positive constants α_0 and β_0 such that

$$\|(x_m^T(t) P B K_r r(t) - x_{m_{ss}}^T P B_m r_{ss})\| \leq \alpha_0 e^{-\beta_0 t}, \quad t \in [0, \infty). \quad (41)$$

Then, (39) becomes

$$\begin{aligned} \dot{V}(e(t), x(t), \tilde{W}(t), \tilde{\lambda}(t)) &\leq -e^T(t) Q e(t) - D_\phi(\|x(t)\|_P) [x^T(t) Q x(t) - x_{m_{ss}}^T Q x_{m_{ss}}] \\ &\quad + 2\alpha_0 e^{-\beta_0 t}. \end{aligned} \quad (42)$$

There are three conditions for proof. These are

i) If $x^T Q x > x_{\text{mss}}^T Q x_{\text{mss}}$,

$$\begin{aligned} \dot{V}(e(t), x(t), \tilde{W}(t), \tilde{\lambda}(t)) &\leq -e^T(t) Q e(t) - D_\phi(\|x(t)\|_P) x^T(t) Q x(t) + 2\alpha_0 e^{-\beta_0 t} \\ &\leq -\lambda_{\min}(Q) \|e(t)\|^2 - D_\phi(\|x(t)\|_P) \lambda_{\min}(Q) \|x(t)\|^2 \\ &\quad + 2\alpha_0 e^{-\beta_0 t}. \end{aligned} \tag{43}$$

By adding and subtracting $\rho\phi(\|x(t)\|_P)$, $\rho \text{tr}(\tilde{W}^T(t)\gamma_1^{-1}\tilde{W}(t))$, and $\rho \text{tr}(\tilde{\lambda}(t)\gamma_2^{-1}\tilde{\lambda}^T(t))$ to the right hand side of (43), which we define $\rho \triangleq \frac{\lambda_{\min}(Q)}{\lambda_{\max}(P)}$, and we get

$$\begin{aligned} \dot{V}(e(t), x(t), \tilde{W}(t), \tilde{\lambda}(t)) &\leq -\lambda_{\min}(Q) \|e(t)\|^2 - D_\phi(\|x(t)\|_P) \lambda_{\min}(Q) \|x(t)\|^2 + 2\alpha_0 e^{-\beta_0 t} \\ &\quad + \rho\phi(\|x(t)\|_P) - \rho\phi(\|x(t)\|_P) + \rho \text{tr}(\tilde{W}^T(t)\gamma_1^{-1}\tilde{W}(t)) \\ &\quad - \rho \text{tr}(\tilde{W}^T(t)\gamma_1^{-1}\tilde{W}(t)) + \rho \text{tr}(\tilde{\lambda}(t)\gamma_2^{-1}\tilde{\lambda}^T(t)) \\ &\quad - \rho \text{tr}(\tilde{\lambda}(t)\gamma_2^{-1}\tilde{\lambda}^T(t)). \end{aligned} \tag{44}$$

By arranging (44), we get

$$\begin{aligned} \dot{V}(e(t), x(t), \tilde{W}(t), \tilde{\lambda}(t)) &\leq \rho [e^T(t) P e(t) + \phi(\|x(t)\|_P) + \text{tr}(\tilde{W}^T(t)\gamma_1^{-1}\tilde{W}(t))] \\ &\quad - \rho [\text{tr}(\tilde{\lambda}(t)\gamma_2^{-1}\tilde{\lambda}^T(t))] \\ &\quad - \rho [D_\phi(\|x(t)\|_P) x^T(t) P x(t) - \phi(\|x(t)\|_P)] \\ &\quad + \rho \text{tr}(\tilde{W}^T(t)\gamma_1^{-1}\tilde{W}(t)) + \rho \text{tr}(\tilde{\lambda}(t)\gamma_2^{-1}\tilde{\lambda}^T(t)) + 2\alpha_0 e^{-\beta_0 t}. \end{aligned} \tag{45}$$

Since $\tilde{W} = \hat{W} - W$, the upper bound of $\|\tilde{W}\|$ is $\tilde{w} = w + \bar{w}$, and $\tilde{\lambda} = \lambda - \hat{\lambda}$, the upper bound of $\|\tilde{\lambda}\|$ is $\tilde{\lambda}_{\max} = \lambda_{\max} + \bar{\lambda}_{\max}$. Therefore, the upper bounds of $\|\tilde{W}\|$ and $\|\tilde{\lambda}\|$ are utilized \tilde{w} and $\tilde{\lambda}_{\max}$, respectively. Also, $2\alpha_0 e^{-\beta_0 t} \leq 2\alpha_0$. By defining

$d = \rho\gamma_1^{-1}\tilde{w}^2 + \rho\gamma_2^{-1}\tilde{\lambda}_{\max}^2 + 2\alpha_0$, (45) reduces to

$$\begin{aligned} \dot{V}(e(t), x(t), \tilde{W}(t), \tilde{\lambda}(t)) &\leq -\rho[e^T(t)Pe(t) + \phi(\|x(t)\|_P) + \text{tr}(\tilde{W}^T(t)\gamma_1^{-1}\tilde{W}(t))] \\ &\quad - \rho[\text{tr}(\tilde{\lambda}(t)\gamma_2^{-1}\tilde{\lambda}^T(t))] \\ &\quad - \rho[D_\phi(\|x(t)\|_P)x^T(t)Px(t) - \phi(\|x(t)\|_P)] + d. \end{aligned} \quad (46)$$

By using vi from the Definition 1, (46) can be rewritten as

$$\dot{V}(e(t), x(t), \tilde{W}(t), \tilde{\lambda}(t)) \leq -\rho V(e(t), x(t), \tilde{W}(t), \tilde{\lambda}(t)) + d. \quad (47)$$

ii) If $x^T Qx = x_{m_{ss}}^T Qx_{m_{ss}}$,

$$\dot{V}(e(t), x(t), \tilde{W}(t), \tilde{\lambda}(t)) \leq -e^T(t)Qe(t) + 2\alpha_0 e^{-\beta_0 t} \quad (48)$$

The detail of proof is given in [1].

iii) If $x^T Qx < x_{m_{ss}}^T Qx_{m_{ss}}$, let use (38), and since $\frac{D_\phi}{1+D_\phi} < 1$, it implies $\frac{D_\phi}{1+D_\phi} < D_\phi$, we get

$$\begin{aligned} \dot{V}(e(t), x(t), \tilde{W}(t), \tilde{\lambda}(t)) &\leq -e^T(t)Qe(t) - D_\phi(\|x(t)\|_P)x^T(t)Qx(t) + \|x_{m_{ss}}^T Qx_{m_{ss}}\| \\ &\quad + 2\|(x_m^T(t)PBK_r r(t) - x_{m_{ss}}^T PB_m r_{ss})\| \end{aligned} \quad (49)$$

By rearranging (49), we get

$$\begin{aligned} \dot{V}(e(t), x(t), \tilde{W}(t), \tilde{\lambda}(t)) &\leq -e^T(t)Qe(t) - D_\phi(\|x(t)\|_P)x^T(t)Qx(t) + 2\alpha_0 e^{-\beta_0 t} \\ &\quad + \lambda_{\max}(Q)\|x_{m_{ss}}\|^2 \\ &\leq -\lambda_{\min}(Q)\|e(t)\|^2 - D_\phi(\|x(t)\|_P)\lambda_{\min}(Q)\|x(t)\|^2 + 2\alpha_0 e^{-\beta_0 t} \\ &\quad + \lambda_{\max}(Q)\|x_{m_{ss}}\|^2 \end{aligned} \quad (50)$$

By adding and subtracting $\rho\phi(\|x(t)\|_{\mathbb{P}})$, $\rho tr(\tilde{W}^T \gamma_1^{-1} \tilde{W})$, and $\rho tr(\tilde{\lambda} \gamma_2^{-1} \tilde{\lambda}^T)$ to the right hand side of (50), we get

$$\begin{aligned} \dot{V}(e(t), x(t), \tilde{W}(t), \tilde{\lambda}(t)) &\leq -\lambda_{\min}(Q)\|e(t)\|^2 - D_{\phi}(\|x(t)\|_{\mathbb{P}})\lambda_{\min}(Q)\|x(t)\|^2 + 2\alpha_0 e^{-\beta_0 t} \\ &\quad + \lambda_{\max}(Q)\|x_{\text{mss}}\|^2 + \rho\phi(\|x(t)\|_{\mathbb{P}}) - \rho\phi(\|x(t)\|_{\mathbb{P}}) \\ &\quad + \rho tr(\tilde{W}^T(t)\gamma_1^{-1}\tilde{W}(t)) - \rho tr(\tilde{W}^T(t)\gamma_1^{-1}\tilde{W}(t)) \\ &\quad + \rho tr(\tilde{\lambda}(t)\gamma_2^{-1}\tilde{\lambda}^T(t)) - \rho tr(\tilde{\lambda}(t)\gamma_2^{-1}\tilde{\lambda}^T(t)). \end{aligned} \quad (51)$$

By arranging (51), we get

$$\begin{aligned} \dot{V}(e(t), x(t), \tilde{W}(t), \tilde{\lambda}(t)) &\leq -\rho[e^T(t)Pe(t) + \phi(\|x(t)\|_{\mathbb{P}}) + tr(\tilde{W}^T(t)\gamma_1^{-1}\tilde{W}(t))] \\ &\quad - \rho[tr(\tilde{\lambda}(t)\gamma_2^{-1}\tilde{\lambda}^T(t))] \\ &\quad - \rho[D_{\phi}(\|x(t)\|_{\mathbb{P}})x^T(t)Px(t) - \phi(\|x(t)\|_{\mathbb{P}})] \\ &\quad + \rho tr(\tilde{W}^T(t)\gamma_1^{-1}\tilde{W}(t)) \\ &\quad + \rho tr(\tilde{\lambda}(t)\gamma_2^{-1}\tilde{\lambda}^T(t)) + 2\alpha_0 e^{-\beta_0 t} + \lambda_{\max}(Q)\|x_{\text{mss}}\|^2. \end{aligned} \quad (52)$$

By defining $d = \rho\gamma_1^{-1}\tilde{w}^2 + \rho\gamma_2^{-1}\tilde{\lambda}_{\max}^2 + 2\alpha_0 + \lambda_{\max}(Q)\|x_{\text{mss}}\|^2$, (52) reduces to

$$\begin{aligned} \dot{V}(e(t), x(t), \tilde{W}(t), \tilde{\lambda}(t)) &\leq -\rho[e^T(t)Pe(t) + \phi(\|x(t)\|_{\mathbb{P}}) + tr(\tilde{W}^T(t)\gamma_1^{-1}\tilde{W}(t))] \\ &\quad - \rho[tr(\tilde{\lambda}(t)\gamma_2^{-1}\tilde{\lambda}^T(t))] \\ &\quad - \rho[D_{\phi}(\|x(t)\|_{\mathbb{P}})x^T(t)Px(t) - \phi(\|x(t)\|_{\mathbb{P}})] + d. \end{aligned} \quad (53)$$

By using $[D_{\phi}x^T Px - \phi(\|x\|_{\mathbb{P}})] > 0$ from the properties, (53) can be rewritten as

$$\dot{V}(e(t), x(t), \tilde{W}(t), \tilde{\lambda}(t)) \leq -\rho V(e(t), x(t), \tilde{W}(t), \tilde{\lambda}(t)) + d. \quad (54)$$

Equations (47), (48) and (54) show that $V(e(t), x(t), \tilde{W}(t), \tilde{\lambda}(t))$ given by (26) is bounded. Since $\phi(\|x(t)\|_P)$ is contained inside $V(e(t), x(t), \tilde{W}(t), \tilde{\lambda}(t))$ then this implies that $\phi(\|x(t)\|_P)$ is also bounded for all $t \in [0, \infty)$. Hence, if $(\|x(0)\|_P) < \epsilon$, then $(\|x(t)\|_P) < \epsilon$ for all time is immediate. ■

3. ILLUSTRATIVE NUMERICAL AND EXPERIMENTAL EXAMPLES

The Quanser 3 DOF Hover shown in Figure 1 is used to demonstrate the practical and theoretical capabilities of the proposed set-theoretic barrier Lyapunov function for handling state constraints and uncertainties. The Quanser 3 DOF Hover is a laboratory setup resembling a simplified helicopter model with four propellers driven by DC motors. The Quanser 3 DOF Hover has four DC motors: front and back motors and right and left motors. The front and back motors mainly control the system about the pitch axis while the left and right motors primarily move it about the roll axis. Also, the total torque generated by the propeller motors causes the body to move about the yaw axis. The Quanser 3 DOF



Figure 1. Quanser 3 DOF Hover

Hover dynamics [13] is as follows:

$$J_p \ddot{\theta}_p(t) = K_f(V_f - V_b) \quad (55)$$

$$J_r \ddot{\theta}_r(t) = K_f(V_r - V_l) \quad (56)$$

$$J_y \ddot{\theta}_y(t) = K_t(V_r + V_l) - K_t(V_f + V_b), \quad (57)$$

where θ_p is the pitch angle, θ_r is the roll angle and θ_y is the yaw angle. K_f is the thrust-force constant, V_f is the front motor voltage, V_b is the back motor voltage. V_r is the right motor voltage, V_l is the left motor voltage. K_t is the thrust-torque constant. The equivalent of (55) to (57) is written as a state space model in the form

$$\dot{x}(t) = Ax(t) + Bu(t) \quad (58)$$

$$y(t) = Cx(t) + Du(t) \quad (59)$$

with

$$A = \begin{bmatrix} 0 & 0 & 0 & 1 & 0 & 0 \\ 0 & 0 & 0 & 0 & 1 & 0 \\ 0 & 0 & 0 & 0 & 0 & 1 \\ 0 & 0 & 0 & 0 & 0 & 0 \\ 0 & 0 & 0 & 0 & 0 & 0 \\ 0 & 0 & 0 & 0 & 0 & 0 \end{bmatrix}, \quad B = \begin{bmatrix} 0 & 0 & 0 & 0 \\ 0 & 0 & 0 & 0 \\ 0 & 0 & 0 & 0 \\ -\frac{K_t}{J_y} & -\frac{K_t}{J_y} & \frac{K_t}{J_y} & \frac{K_t}{J_y} \\ \frac{LK_f}{J_p} & -\frac{LK_f}{J_p} & 0 & 0 \\ 0 & 0 & \frac{LK_f}{J_r} & -\frac{LK_f}{J_r} \end{bmatrix}.$$

$$C = \begin{bmatrix} 1 & 0 & 0 & 0 & 0 & 0 \\ 0 & 1 & 0 & 0 & 0 & 0 \\ 0 & 0 & 1 & 0 & 0 & 0 \end{bmatrix}, \quad D = \begin{bmatrix} 0 & 0 & 0 & 0 \\ 0 & 0 & 0 & 0 \\ 0 & 0 & 0 & 0 \end{bmatrix}.$$

In the following problems, the state vector is of the form

$$x(t) = [\theta_y(t) \ \theta_p(t) \ \theta_r(t) \ \dot{\theta}_y(t) \ \dot{\theta}_p(t) \ \dot{\theta}_r(t)]^T, \quad (60)$$

the output vector form is given as

$$y(t) = [\theta_y(t) \ \theta_p(t) \ \theta_r(t)]^T, \quad (61)$$

also, the control vector form is given by

$$u(t) = [V_f(t) \ V_b(t) \ V_r(t) \ V_l(t)]^T. \quad (62)$$

Note that (58) and (59) are derived based on the ideal system conditions. However, in practical application scenarios where system uncertainties are present, one can alternatively consider the uncertain system dynamics in the form given by

$$\begin{aligned} \dot{x}(t) &= Ax(t) + B\Lambda u(t) + Bf(x(t)) \\ y(t) &= Cx(t) \end{aligned} \quad (63)$$

Linear quadratic regulator theory is used to design the nominal controller gain matrix with the weighting matrices as $Q = 0.001 \text{diag}([500, 350, 350, 0, 20, 20])$ and

$R = 0.00001 \text{diag}([1, 1, 1, 1])$. The feedback control gain defined in (4) are selected as

$$K_n = \begin{bmatrix} -111.8034 & 132.2876 & 0.0000 & -41.4128 & 36.2268 & 0.0000 \\ -111.8034 & -132.2876 & 0.0000 & -41.4128 & -36.2268 & -0.0000 \\ 111.8034 & 0.0000 & 132.2876 & 41.4128 & 0.0000 & 36.2268 \\ 111.8034 & 0.0000 & -132.2876 & 41.4128 & 0.0000 & -36.2268 \end{bmatrix}$$

The parameter Λ is the unknown control effectiveness gain and set at 0.1. In this example, the threshold ϵ is set to be 10 for all cases. Initial conditions of the states are chosen as $0 \text{ deg}, 0 \text{ deg}, 0 \text{ deg}$ and $0 \text{ deg/s}, 0 \text{ deg/s}, 0 \text{ deg/s}$, respectively. The value of the learning rate (γ_2) given in (17) is chosen as 0.001. To command a desired yaw step of ± 5 degrees at 0.04 Hz, pitch step of ± 4 degrees at 0.1 Hz frequency, and a roll angle step of ± 4 degrees at 0.08 Hz. The three generalized restricted potential functions are used.

3.1. ILLUSTRATIVE NUMERICAL RESULTS

In this section, the numerical simulation is considered on the Quanser 3 DOF hover system. The proposed method has three different restricted potential functions. The objective is to motivate the need for careful selection of an appropriate STBLF to result in proper system tracking while conforming to the state constraints.

3.1.1. Case 1. The generalized restricted potential function given in 2.1 in Definition 1 is used for this case. Figure 2 presents the histories of states. The actual state does

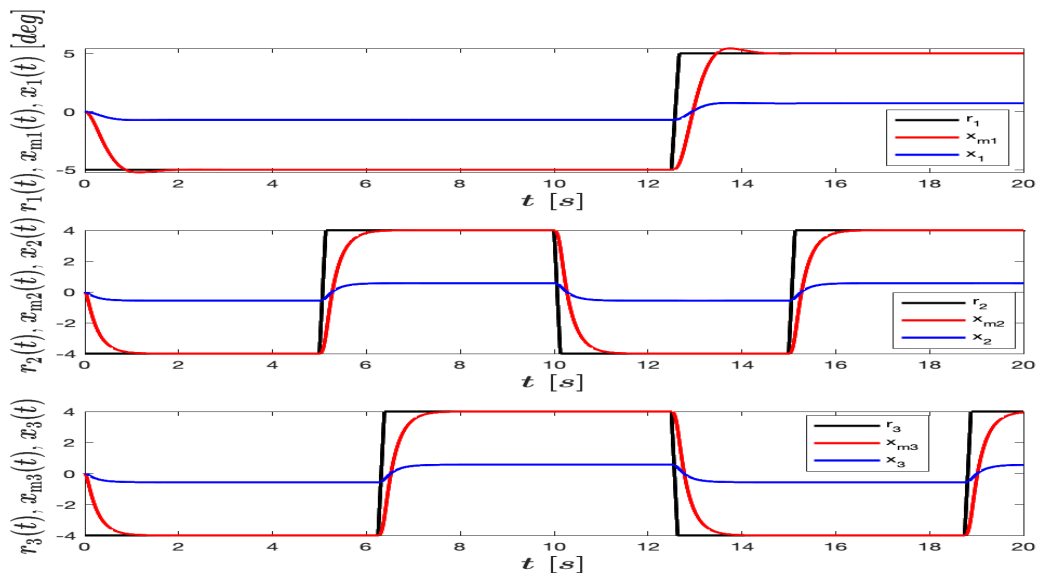


Figure 2. Histories of the actual and model reference states

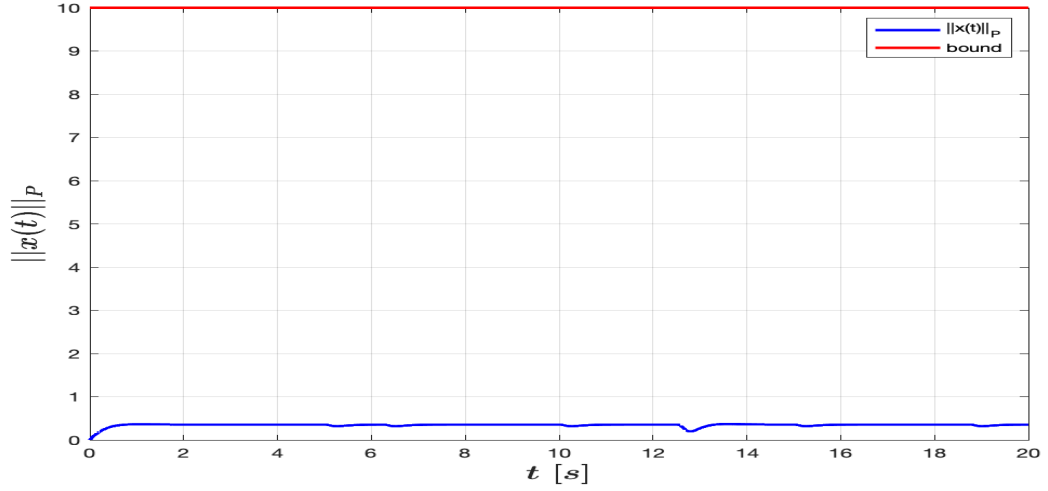


Figure 3. Histories of the norm of the states and the bound

not follow the reference trajectory properly because the controller law for constraint (u_c) is high and forces the state to be well under the bound. As we can be seen from Figure 3, the norm of the states is under the bound.

3.1.2. Case 2. In this case, the generalized restricted potential function defined in 2.2 in Definition 1 is used. Comparing Figure 4 with Figure 2, the tracking performance is better in Figure 4. The reason is that the restricted potential function given in (8) produces more control output to keep the norm of the states under the bound. Although the restricted potential function defined in (10) has even less control output, the proposed method still keeps the norm of the states under the user-defined constraint as shown in Figure 5.

3.1.3. Case 3. The generalized restricted potential function shown in 2.3 in Definition 1 is used for this case. Figure 6 presents the histories of the states. The results in Figure 6 have better tracking performance than the results shown in Figure 4 because the constraint controller magnitude is less than the nominal controller magnitude. It is seen that the tracking performance is improved with the restricted potential function defined in

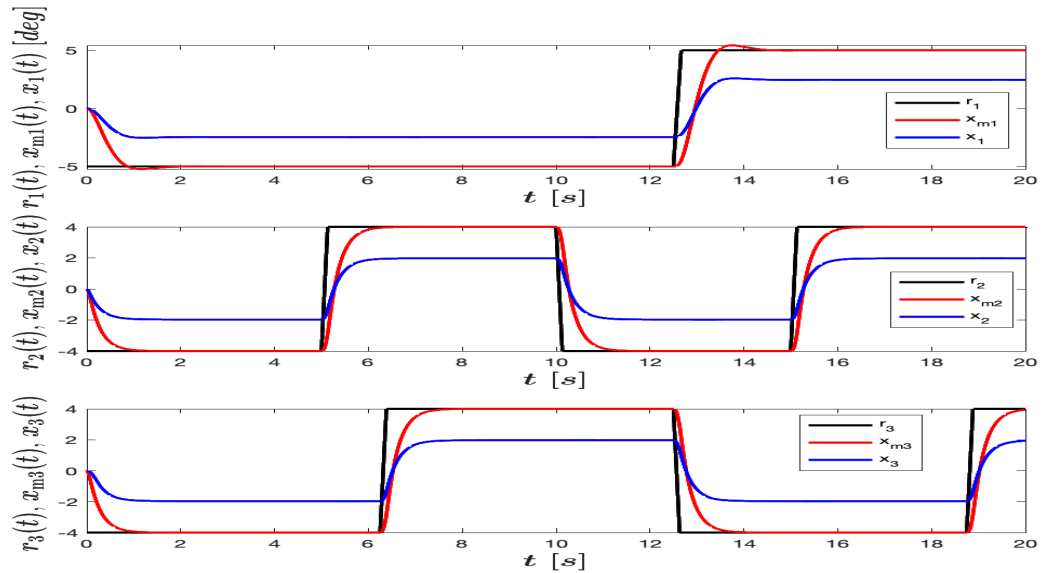


Figure 4. Histories of the actual and model reference states

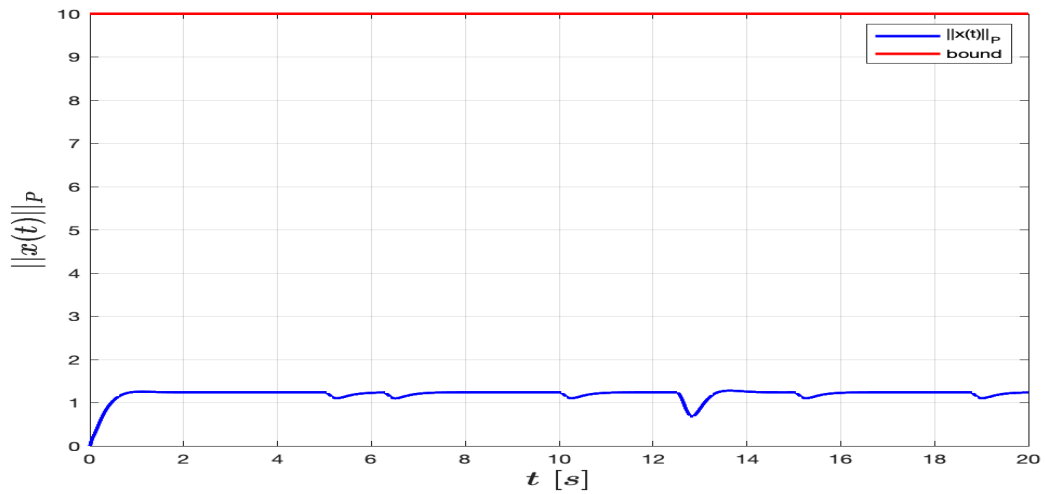


Figure 5. Histories of the norm of the states and the bound

(12) compared with the restricted potential function defined in (10). While improving the tracking performance, the proposed restricted potential function keeps the norm of the states under the user-defined constraint as shown in Figure 7.

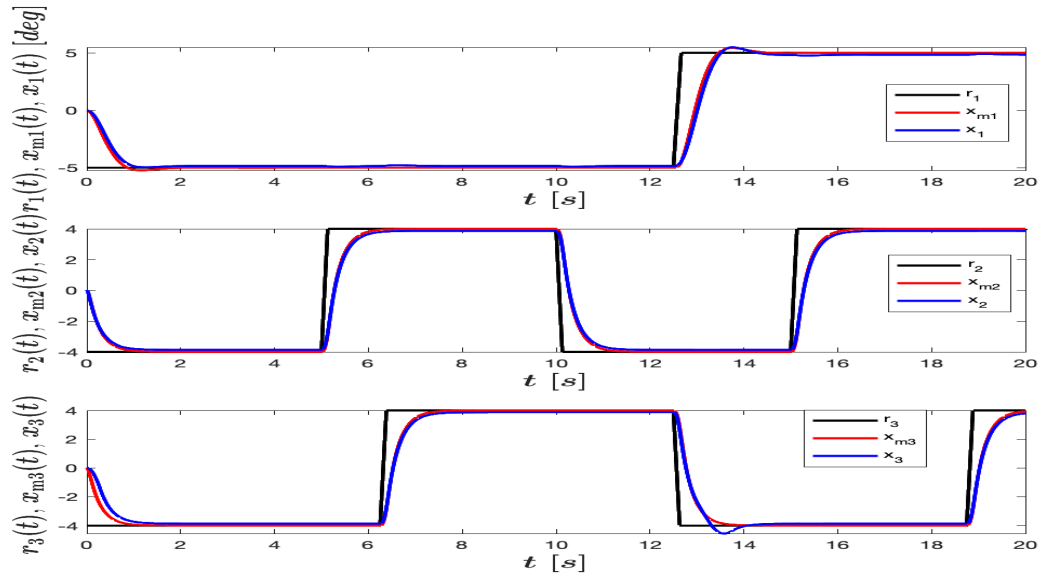


Figure 6. Histories of the actual and model reference states

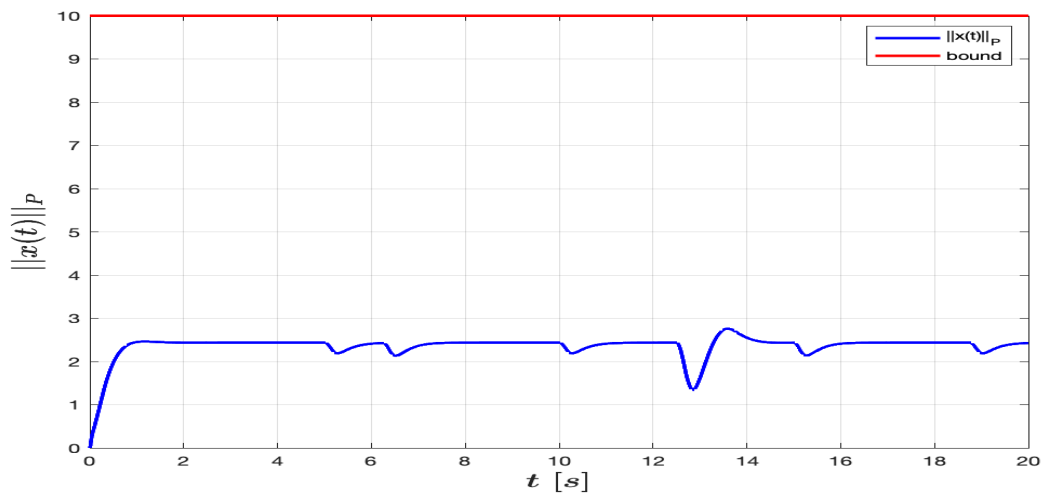


Figure 7. Histories of the norm of the states and the bound

3.2. ILLUSTRATIVE EXPERIMENTAL RESULTS

In this section, also same restricted potential functions are used as in numerical results.. The objective is to illustrate the efficiency of the proposed method with both theory and practical studies. The cases below were also used in the simulation results.

3.2.1. Case 1. The generalized restricted potential function given in 2.1 in Definition 1 is used for this case.

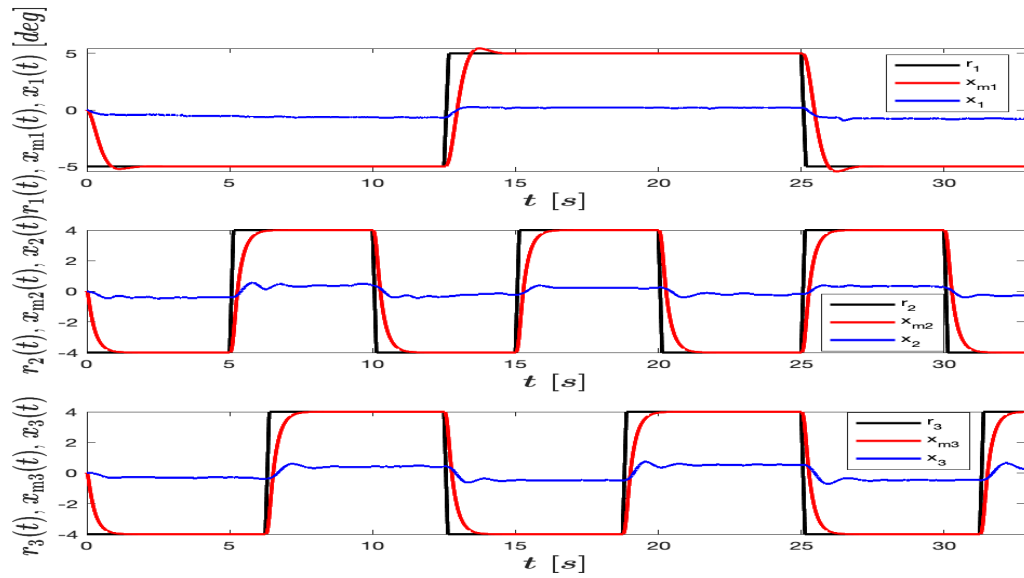


Figure 8. Histories of the actual and model reference states

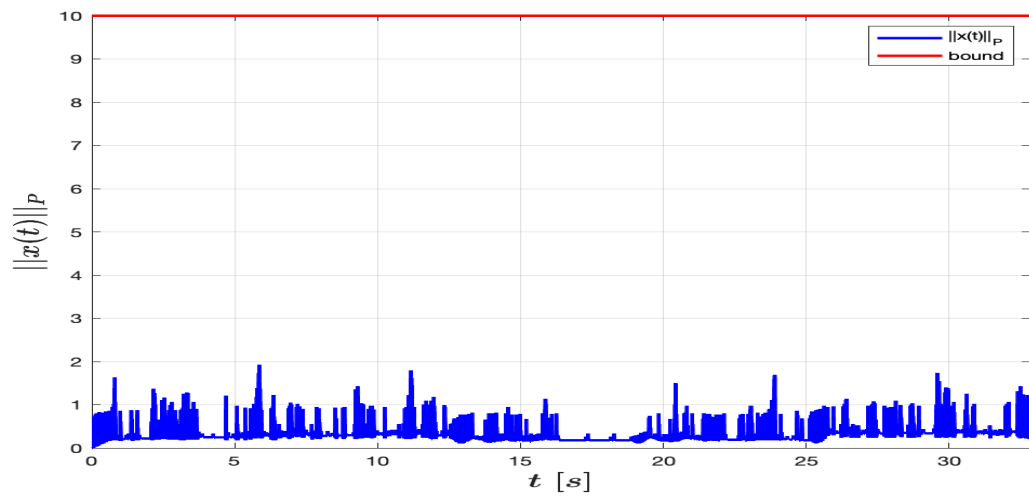


Figure 9. Histories of the norm of the states and the bound

Figures 8 and 9 show the performance of the Case 1 results. Note that the norm of the states are under the bound but not tracking the reference signal properly. Therefore, the design of the controller law for constraint (u_c) has important role for improving the tracking performance as well as the keep the norm of the states within a bound.

3.2.2. Case 2. In this case, the generalized restricted potential function defined in 2.2 in Definition 1 is used. The another design of the controller law for constraint is

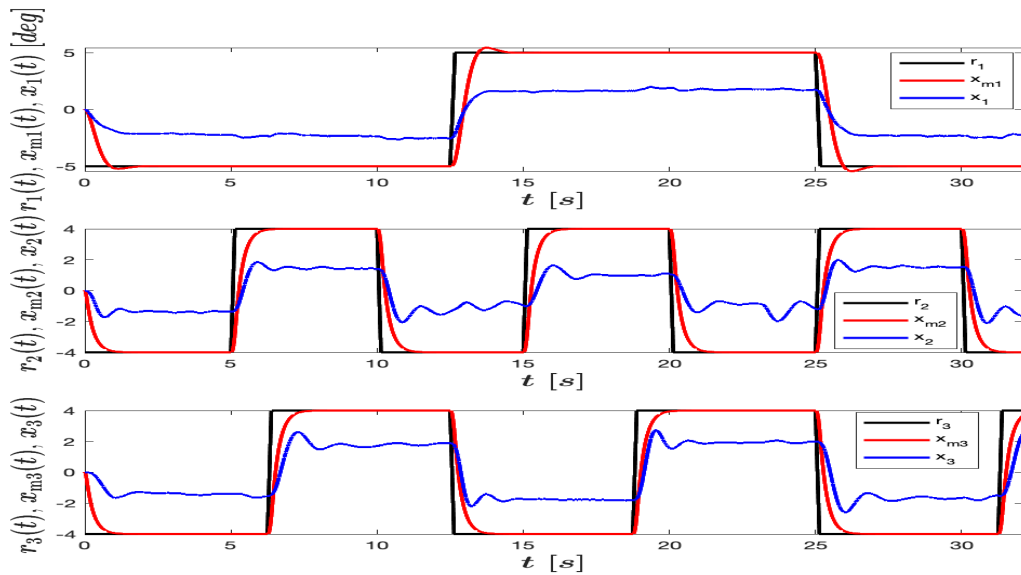


Figure 10. Histories of the actual and model reference states

designed for Case 2 which is given in 2.2 in Definition 1. Figures 10 and 11 keep the norm of the states under the user defined constraint and show improvement of tracking reference signal as comparing with Figure 8. However, it is still not enough to track the reference trajectory properly.

3.2.3. Case 3. The generalized restricted potential function shown in 2.3 in Definition 1 is used for this case. The last design of controller law for constraint in Case 3 given in 2.3 shows better tracking performance than the results shown in Figures 8 and 10. While improving the tracking performance, the proposed restricted potential function keeps the norm of the states under the user-defined constraint as shown in Figure 13.

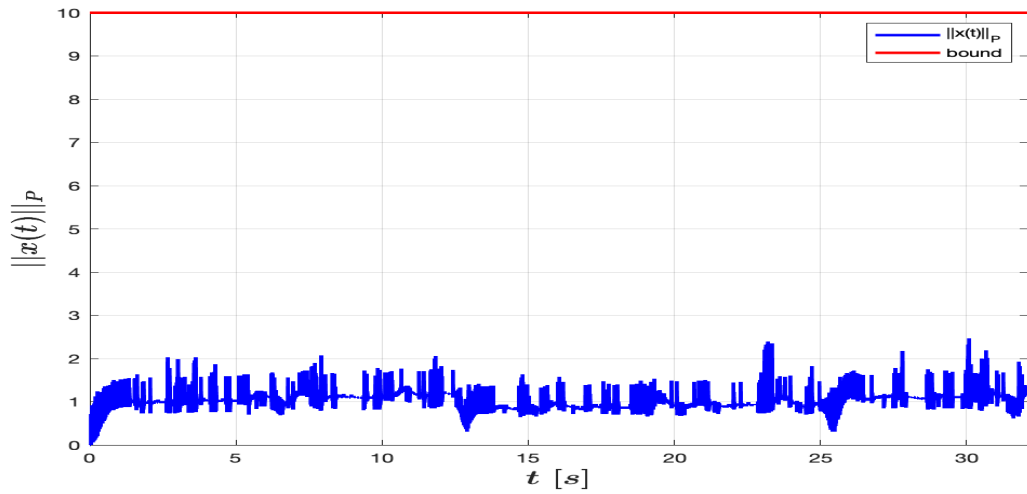


Figure 11. Histories of the norm of the states and the bound

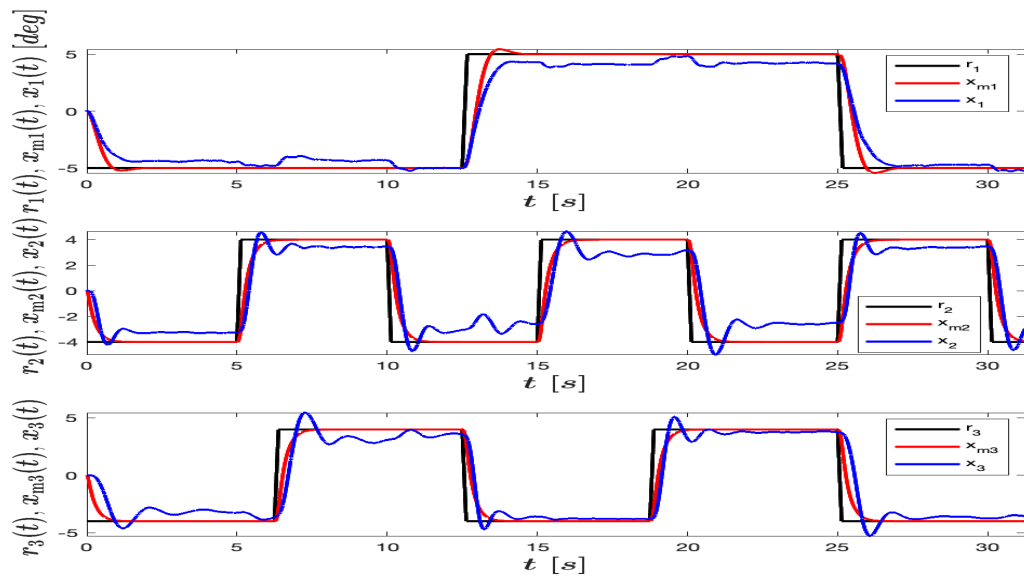


Figure 12. Histories of the actual and model reference states

4. CONCLUSION

This paper proposed three different STBLFs to handle state constraints in model reference adaptive control. Many STBLFs exist in the literature and this work shows that the choice of STBLF significantly affects the system performance. With a suitable STBLF,

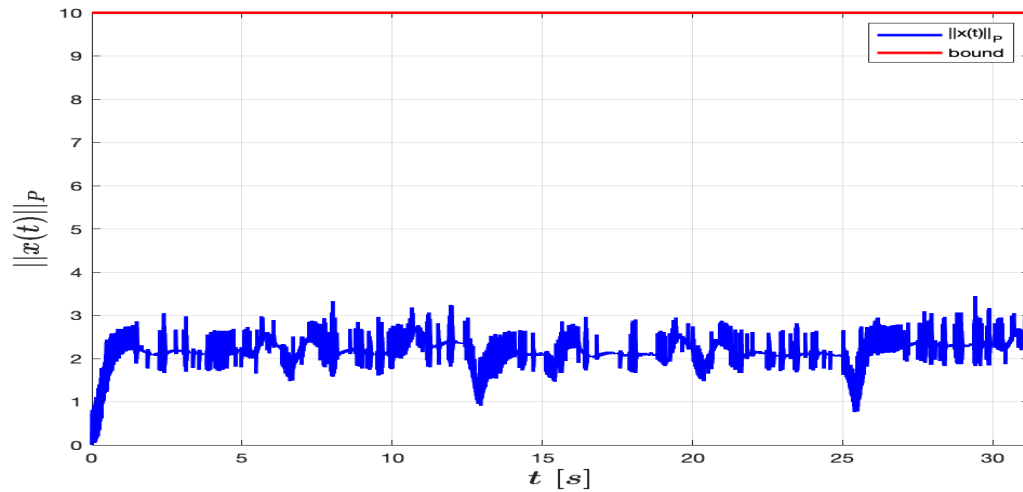


Figure 13. Histories of the norm of the states and the bound

not only is the state constraint satisfied but also desirable closed-loop system tracking performance can be achieved. Finally, the theoretical study was supported with numerical and experimental studies. These results appear to demonstrate that the developed STBLF has good potential for applications.

ACKNOWLEDGEMENTS

The first author would like to thank the Republic of Turkey for the supporting her Ph.D. studies.

REFERENCES

- [1] Muse, J., 'A method for enforcing state constraints in adaptive control,' in 'AIAA Guidance, Navigation, and Control Conference,' 2011 p. 6205.
- [2] Arabi, E., Gruenwald, B. C., Yucelen, T., and Nguyen, N. T., 'A set-theoretic model reference adaptive control architecture for disturbance rejection and uncertainty suppression with strict performance guarantees,' *International Journal of Control*, 2018, **91**(5), pp. 1195–1208.

- [3] Tee, K. P., Ge, S. S., and Tay, E. H., 'Barrier lyapunov functions for the control of output-constrained nonlinear systems,' *Automatica*, 2009, **45**(4), pp. 918–927.
- [4] Lavretsky, E. and Gadiant, R., 'Robust adaptive design for aerial vehicles with state-limiting constraints,' *Journal of guidance, control, and dynamics*, 2010, **33**(6), pp. 1743–1752.
- [5] Deniz, M., Devi, P., and Balakrishnan, S., 'Inverse optimal control with set-theoretic barrier lyapunov function for handling state constraints,' in '2020 American Control Conference (ACC),' IEEE, 2020 pp. 981–986.
- [6] Han, D. and Balakrishnan, S., 'State-constrained agile missile control with adaptive-critic-based neural networks,' *IEEE Transactions on Control Systems Technology*, 2002, **10**(4), pp. 481–489.
- [7] Bryson, A. E., Denham, W. F., and Dreyfus, S. E., 'Optimal programming problems with inequality constraints,' *AIAA journal*, 1963, **1**(11), pp. 2544–2550.
- [8] McIntyre, J. and Paiewonsky, B., 'On optimal control with bounded state variables,' in 'Advances in Control Systems,' volume 5, pp. 389–419, Elsevier, 1967.
- [9] Kreindler, E., 'Additional necessary conditions for optimal control with state-variable inequality constraints,' *Journal of Optimization theory and applications*, 1982, **38**(2), pp. 241–250.
- [10] Jacobson, D. H., Lele, M. M., and Speyer, J. L., 'New necessary conditions of optimality for control problems with state-variable inequality constraints,' *Journal of mathematical analysis and applications*, 1971, **35**(2), pp. 255–284.
- [11] Lavretsky, E. and Wise, K. A., 'Robust adaptive control,' in 'Robust and adaptive control,' pp. 317–353, Springer, 2013.
- [12] Pomet, J.-B. and Praly, L., 'Adaptive nonlinear regulation: estimation from the lyapunov equation,' *IEEE Transactions on Automatic Control*, 1992, **37**(6), pp. 729–740, doi:10.1109/9.256328.
- [13] Apkarian, J. and Lévis, M., 'Quanser 3 dof hover user manual,' in 'Quanser Laboratory Guide,' available at <https://www.quanser.com/products/3-dof-hover/>, 2013.

VI. A FINITE-TIME ARCHITECTURE FOR DISTRIBUTED ADAPTIVE CONTROL OF UNCERTAIN MULTIAGENT SYSTEMS

Meryem Deniz¹, K. Merve Dogan², Tansel Yucelen³

¹Department of Mechanical & Aerospace Engineering
Missouri University of Science and Technology
Rolla, Missouri 65409–0050, United States of America

²Department of Aerospace Engineering
Embry-Riddle Aeronautical University
Daytona Beach, Florida 32114, United States of America

³Department of Mechanical Engineering

University of South Florida
Tampa, Florida 33620, United States of America

ABSTRACT

In this paper, we present a distributed adaptive control approach that achieves finite-time stability of uncertain multiagent systems. Specifically, the proposed approach is predicated on agent-wise nonlinear reference models that capture the ideal finite-time behavior of the overall multiagent system. Utilizing the error signals between the states of agent dynamics and the states of these reference models, adaptive control signals are then developed in order to drive these error signals to zero in finite-time when agent dynamics are affected by system uncertainties. Therefore, each agent to achieve its ideal performance is guaranteed in finite-time. In addition to the presented rigorous system-theoretical analysis, we give an illustrative numerical example to demonstrate the efficacy of the proposed finite-time architecture.

1. INTRODUCTION

Teams of agents (e.g., unmanned aerial, ground, water, and underwater vehicles) operated through a network are called multiagent systems, where they will play a key role in a wide array of civilian and military applications such as surveillance and reconnaissance, ground and air traffic management, payload and passenger transportation, and emergency response; to name but a few examples. Whether civilian or military, however, there are important multiagent systems applications that require operations to be completed in a finite-time duration such as cooperative engagement, sequential execution of time-critical network operations (i.e., multiagent automation), and rendezvous. To this end, the authors of, for example, [1, 2, 3, 4, 5, 6, 7, 8, 9] focus on finite-time distributed control approaches for multiagent systems. Yet, the common denominator of these approaches is that they neither focus on disturbances nor system uncertainties that are unavoidable anomalies affecting agent dynamics.

As it is well-known, disturbances such as ground frictions and wind, and system uncertainties resulting from simplifying approximations, unknown agent parameters, and structural damages can significantly degrade the stability and performance of multiagent systems. Motivated by this standpoint, the authors of, for example, [10, 11, 12, 13] focus on how to address disturbances, while for example, [14, 15, 16, 17, 18, 19, 20, 21, 22, 23, 24, 25, 26, 27] focus on how to address system uncertainties in the finite time control of multiagent systems. In particular, the authors of [14, 15, 16, 17, 18] adopt distributed adaptive control methods, the authors of [19, 20] and [21, 22] also respectively consider input constraints and state constraints, the authors of [23, 24, 25] deal with unknown control inputs and control directions, and the authors of [26] and [27] respectively focus on nonlinear uncertainties and unmodeled dynamics.

Considering the aforementioned contributions addressing anomalies, note that none of these results utilize a reference model toward finite-time distributed control. Only the authors of [28] utilize a reference model for finite-time distributed control. However, their

reference model exchanges measurements that are affected by anomalies. From a safety standpoint, this implies that when a subset of agents does not satisfy the assumptions presented in [28], then this can result in an unstable reference model behavior, and therefore, an unstable closed-loop multiagent performance. While the focus is not finite-time distributed control, the authors of [29] present a new reference model architecture that allows exchange of measurements that are not affected by anomalies. In contrast to the one in [28], this new reference model ensures safety in the sense that agents always rely on stable reference model states in their adaptive control signals for suppressing the negative effect of system anomalies.

In this paper, we present a distributed adaptive control approach that achieves finite-time stability of uncertain multiagent systems. Specifically, the proposed approach is predicated on agent-wise nonlinear reference models, where they generalize their linear counterparts in [29] in order to capture the ideal finite-time behavior of the overall multiagent system while ensuring safety. Utilizing the error signals between the states of agent dynamics and the states of these reference models, adaptive control signals are then developed in order to drive these error signals to zero in finite-time when agent dynamics are affected by system uncertainties. Therefore, each agent to achieve its ideal performance is guaranteed in finite-time. In addition to the presented rigorous system-theoretical analysis of the proposed agent-wise nonlinear reference models as well as the closed-loop multiagent system, we give an illustrative numerical example to demonstrate the efficacy of the proposed finite-time architecture.

2. MATHEMATICAL PRELIMINARIES

The notation given below is used throughout this paper. In particular, \mathbb{R} denotes the set of real numbers, \mathbb{R}^n denotes the set of $n \times 1$ real column vectors, $\mathbb{R}^{n \times m}$ denotes the set of $n \times m$ real matrices. \mathbb{R}_+ and $\mathbb{R}_+^{n \times n}$ respectively denote the sets of positive real numbers and positive-definite matrices, \mathbb{Z} denotes the set of integers, \mathbb{Z}_+ and $\bar{\mathbb{Z}}_+$ respectively denote the

sets of positive integers and nonnegative integers, 0_n denotes the $n \times 1$ vector of all zeros, $\mathbf{1}_n$ denotes the $n \times 1$ vector of all ones, $0_{n \times n}$ denotes the $n \times n$ zero matrix, and I_n denotes the $n \times n$ identity matrix. We also write “ \triangleq ” for the equality by definition, $(\cdot)^T$ for the transpose, $(\cdot)^{-1}$ for the inverse, $\text{sgn}(x) = [\text{sgn}(x_1), \text{sgn}(x_2), \dots, \text{sgn}(x_n)]$ for a vector containing signum functions of scalars x_i , $i = 1 \dots, n$, and $\tanh(x) = [\tanh(x_1), \tanh(x_2), \dots, \tanh(x_n)]$ for a vector containing tangent hyperbolic functions of scalars x_i , $i = 1 \dots, n$. Finally, the minimum eigenvalue of the matrix $A \in \mathbb{R}^{n \times n}$ is represented by $\lambda_{\min}(A)$, the maximum eigenvalue of the matrix $A \in \mathbb{R}^{n \times n}$ is represented by $\lambda_{\max}(A)$, and the diagonal matrix with the vector a on its diagonal is represented by $\text{diag}(a)$.

The basic definitions from graph theory are now given, where we refer to excellent books [30] and [31]. Specifically, an undirected graph \mathcal{G} is defined by a set of nodes $\mathcal{V}_{\mathcal{G}} = \{1, \dots, N\}$ and a set of edges $\mathcal{E}_{\mathcal{G}} \subset \mathcal{V}_{\mathcal{G}} \times \mathcal{V}_{\mathcal{G}}$. When $(i, j) \in \mathcal{E}_{\mathcal{G}}$, the nodes i and j are said to be neighbors, where $i \sim j$ represents the neighboring relation. A path $i_0, i_1 \dots, i_L$ is a finite sequence of nodes such that $i_{k-1} \sim i_k$, $k = 1, \dots, L$ and a graph \mathcal{G} is connected when there is a path between any pair of distinct nodes. The degree of a node d_i is given by the number of its neighbors, where the degree matrix of a graph \mathcal{G} , $\mathcal{D}(\mathcal{G}) \in \mathbb{R}^{N \times N}$, is represented by $\mathcal{D}(\mathcal{G}) \triangleq \text{diag}(d)$ with $d = [d_1, \dots, d_N]^T$. In addition, $\mathcal{A}(\mathcal{G}) \in \mathbb{R}^{N \times N}$ represents the adjacency matrix of a graph \mathcal{G} and is defined by $[\mathcal{A}(\mathcal{G})]_{ij} = 1$ when $(i, j) \in \mathcal{E}_{\mathcal{G}}$ and $[\mathcal{A}(\mathcal{G})]_{ij} = 0$ otherwise. Finally, $\mathcal{L}(\mathcal{G}) \triangleq \mathcal{D}(\mathcal{G}) - \mathcal{A}(\mathcal{G})$ denotes the Laplacian matrix of a graph. For the results contained in this paper, we consider a connected and undirected graph \mathcal{G} and utilize the following lemma from [32].

Lemma 2.1. *For a connected and undirected graph \mathcal{G} , $\mathcal{F}(\mathcal{G}) \triangleq \mathcal{L}(\mathcal{G}) + \mathcal{K} \in \mathbb{R}_+^{N \times N}$ holds, where $\mathcal{K} = \text{diag}(k)$, $k = [k_1, k_2, \dots, k_N]^T$, $k_i \in \overline{\mathbb{Z}}_+$, $i = 1, \dots, N$, with at least one k_i being nonzero.*

3. PROBLEM FORMULATION

Consider an uncertain multiagent system consisting of N agents subject to an undirected and connected graph \mathcal{G} , where the dynamics of an agent is given by

$$\dot{x}_i(t) = u_i(t) + w_i^T(t)\delta_i(x_i(t)), \quad i = 1, \dots, N. \quad (1)$$

In (1), $x_i(t) \in \mathbb{R}$ is the state vector, $u_i(t) \in \mathbb{R}$ is the feedback control input, $w_i(t) \in \mathbb{R}^s$ is the unknown weight, and $\delta_i(\cdot) \in \mathbb{R} \rightarrow \mathbb{R}^s$ is the known basis function with the form $\delta_i(\cdot) = [\delta_{i1}(x), \delta_{i2}(x), \dots, \delta_{is}(x)]$ of agent i . Consider also agent-wide nonlinear reference models in the form given by

$$\begin{aligned} \dot{x}_{r_i}(t) = & - \sum_{i \sim j} (x_{r_i}(t) - x_{r_j}(t)) - k_i(x_{r_i}(t) - c(t)) \\ & - \sigma \operatorname{sgn} \left(\sum_{i \sim j} (x_{r_i}(t) - x_{r_j}(t)) - k_i(x_{r_i}(t) - c(t)) \right). \end{aligned} \quad (2)$$

In (2), $x_{r_i}(t) \in \mathbb{R}$ is the reference state vector, $k_i \in \{0, 1\}$ for all $i = 1, \dots, N$ with at least one k_i being one, $c(t) \in \mathbb{R}$ is the command that is available to leader agent(s) (i.e., the one(s) with $k_i = 1$), and $\sigma \in \mathbb{R}_+$ is a design variable.

Our *first objective* is *a*) to show that the reference state vector of an agent converges to the command in finite-time, where (2) then captures the ideal finite-time behavior of the overall multiagent system. In addition, our *second objective* is *b*) to drive the state vectors of agents to the state vectors of their reference models in finite-time. Motivated by this standpoint, consider the distributed control signal given by

$$\begin{aligned} u_i(t) = & - \sum_{i \sim j} (x_i(t) - x_{r_j}(t)) - k_i(x_i(t) - c(t)) \\ & - \sigma \operatorname{sgn} \left(\sum_{i \sim j} (x_i(t) - x_{r_j}(t)) - k_i(x_i(t) - c(t)) \right) \\ & - u_{a_i}(t) - u_{f_i}(t). \end{aligned} \quad (3)$$

In (3), $u_{a_i}(t) \in \mathbb{R}$ is the adaptive component and $u_{f_i}(t) \in \mathbb{R}$ is the component to achieve finite-time convergence of this distributed control signal (details in Section 4).

Now, substituting (3) into (1), one can rewrite the agent dynamics as

$$\begin{aligned} \dot{x}_i(t) = & - \sum_{i \sim j} (x_i(t) - x_{r_j}(t)) - k_i(x_i(t) - c(t)) \\ & - \sigma \operatorname{sgn} \left(\sum_{i \sim j} (x_i(t) - x_{r_j}(t)) - k_i(x_i(t) - c(t)) \right) \\ & - u_{a_i}(t) - u_{f_i}(t) + w_i^T(t) \delta_i(x_i(t)). \end{aligned} \quad (4)$$

This completes our problem formulation. The next section presents system-theoretical analyses to achieve the objectives *a*) and *b*) mentioned above.

4. SYSTEM-THEORETICAL ANALYSES

4.1. ANALYSIS FOR OBJECTIVE A)

Before presenting the first main result of this paper for achieving objective *a*), we make the following assumption.

Assumption 4.1. *An upper bound of the time rate of change of the command is known and given by $\dot{c}(t) \leq c^*$.*

For the following first main result of this paper, we define $\rho_1 \triangleq 2\lambda_{\min}(\mathcal{F}(\mathcal{G}))$, $\rho_2 \triangleq \alpha\sqrt{2\lambda_{\min}(\mathcal{F}(\mathcal{G}))}$, $\alpha \triangleq \sigma - \bar{c} \in \mathbb{R}_+$, and $V(t_0) = \frac{1}{2}\tilde{x}_r^T(t_0)\mathcal{F}(\mathcal{G})\tilde{x}_r(t_0)$. Here, $\bar{c} \in \mathbb{R}_+$ satisfies $\|\mathbf{1}_N \dot{c}(t)\|_2 \leq \bar{c}$, where existence of \bar{c} follows from the above assumption. We are now ready to present the following result.

Theorem 4.1. Consider the reference model dynamics of each agent given by (2) and Assumption 4.1. If $\sigma > \bar{c}$, then the states of the reference model approaches to $c(t)$ in finite-time T subject to the upper bound given by

$$T \leq \frac{2}{\rho_1} \ln \left(\frac{\rho_1 \sqrt{V(t_0)} + \rho_2}{\rho_2} \right). \quad (5)$$

Proof. Let $\tilde{x}_{r_i}(t) \triangleq x_{r_i}(t) - c(t)$ be the tracking error between the reference model of an agent and the given command. Let also $x_r(t) \triangleq [x_{r_1}(t), x_{r_2}(t), \dots, x_{r_N}(t)]^T \in \mathbb{R}^N$ and $\tilde{x}_r(t) = [\tilde{x}_{r_1}(t), \tilde{x}_{r_2}(t), \dots, \tilde{x}_{r_N}(t)]^T \in \mathbb{R}^N$. One can now compactly write

$$\dot{x}_r(t) = -\mathcal{F}(\mathcal{G})x_r(t) - \sigma \operatorname{sgn}(\mathcal{F}(\mathcal{G})x_r(t)) + \mathcal{K}\mathbf{1}_N c(t) + \sigma \operatorname{sgn}(\mathbf{1}_N c(t)), \quad (6)$$

$$\dot{\tilde{x}}_r(t) = -\mathcal{F}(\mathcal{G})\tilde{x}_r(t) - \sigma \operatorname{sgn}(\mathcal{F}(\mathcal{G})\tilde{x}_r(t)) - \mathbf{1}_N \dot{c}(t). \quad (7)$$

To show the convergence of the reference model to tracking command, consider the Lyapunov function candidate given by

$$V(\tilde{x}_r) = \frac{1}{2} \tilde{x}_r^T \mathcal{F}(\mathcal{G}) \tilde{x}_r. \quad (8)$$

Since $\mathcal{F}(\mathcal{G}) \in \mathbb{R}_+^{N \times N}$ by Lemma 2.1, $V(0) = 0$ and $V(\tilde{x}_r) > 0$ for all $\tilde{x}_r \neq 0$, and $V(\tilde{x}_r)$ is radially unbounded. Now, the time derivative of (8) yields

$$\begin{aligned} \dot{V}(\tilde{x}_r(t)) &= -\tilde{x}_r^T(t) \mathcal{F}(\mathcal{G}) \mathcal{F}(\mathcal{G}) \tilde{x}_r(t) \\ &\quad - \sigma \tilde{x}_r^T(t) \mathcal{F}(\mathcal{G}) \operatorname{sgn}(\mathcal{F}(\mathcal{G}) \tilde{x}_r(t)) \\ &\quad - \tilde{x}_r^T(t) \mathcal{F}(\mathcal{G}) \mathbf{1}_N \dot{c}(t) \\ &\leq -\|\mathcal{F}(\mathcal{G}) \tilde{x}_r(t)\|_2^2 - \sigma \|\mathcal{F}(\mathcal{G}) \tilde{x}_r(t)\|_1 \\ &\quad + \|\mathcal{F}(\mathcal{G}) \tilde{x}_r(t)\|_2 \bar{c} \\ &\leq -\|\mathcal{F}(\mathcal{G}) \tilde{x}_r(t)\|_2^2 - (\sigma - \bar{c}) \|\mathcal{F}(\mathcal{G}) \tilde{x}_r(t)\|_2. \end{aligned} \quad (9)$$

From the statement of the theorem, (9) yields

$$\begin{aligned}
\dot{V}(\tilde{x}_r(t)) &\leq -\|\mathcal{F}(\mathcal{G})\tilde{x}_r(t)\|_2^2 - \alpha\|\mathcal{F}(\mathcal{G})\tilde{x}_r(t)\|_2 \\
&= -\tilde{x}_r^\top(t)\mathcal{F}(\mathcal{G})\mathcal{F}(\mathcal{G})\tilde{x}_r(t) \\
&\quad - \alpha\sqrt{\tilde{x}_r^\top(t)\mathcal{F}(\mathcal{G})\mathcal{F}(\mathcal{G})\tilde{x}_r(t)} \\
&\leq -\lambda_{\min}(\mathcal{F}(\mathcal{G}))\tilde{x}_r^\top(t)\mathcal{F}(\mathcal{G})\tilde{x}_r(t) \\
&\quad - \alpha\sqrt{\lambda_{\min}(\mathcal{F}(\mathcal{G}))}\sqrt{\tilde{x}_r^\top(t)\mathcal{F}(\mathcal{G})\tilde{x}_r(t)} \\
&\leq -2\lambda_{\min}(\mathcal{F}(\mathcal{G}))V - \alpha\sqrt{2\lambda_{\min}(\mathcal{F}(\mathcal{G}))}\sqrt{V} \\
&= -\rho_1V - \rho_2\sqrt{V}.
\end{aligned} \tag{10}$$

Next, using (10), we show that (5) holds. To this end, one can write

$$\begin{aligned}
-(\rho_1V + \rho_2\sqrt{V}) &\geq \frac{dV}{dt} \\
-dt &\geq \frac{dV}{(\rho_1V + \rho_2\sqrt{V})}.
\end{aligned} \tag{11}$$

Note that one can define $\sqrt{V} = v$ such that V becomes $V = v^2$. Taking the derivative of V now yields $dV = 2vdv$. Rearranging now (11) results in

$$-dt \geq \frac{2vdv}{(\rho_1v^2 + \rho_2v)}. \tag{12}$$

By taking the integral of both sides of the above inequality, one can get

$$\begin{aligned}
-\int_{t_0}^T dt &\geq \int_{t_0}^T \frac{2vdv}{(\rho_1v^2 + \rho_2v)} \\
&= \frac{2\ln(\rho_1v + \rho_2)}{\rho_1} \Big|_{t_0}^T.
\end{aligned} \tag{13}$$

Then, using the variable of change $\sqrt{V} = v$ over the time interval $[t_0, T]$, (13) becomes

$$\begin{aligned} - \int_{t_0}^T dt &\geq \frac{2\ln(\rho_1\sqrt{V} + \rho_2)}{\rho_1} \Big|_{t_0}^T \\ &= \frac{2\ln(\rho_1\sqrt{V(T)} + \rho_2)}{\rho_1} \\ &\quad - \frac{2\ln(\rho_1\sqrt{V(t_0)} + \rho_2)}{\rho_1}. \end{aligned} \tag{14}$$

Finally, when $V(T) = 0$ and $t_0 = 0$, with the quotient rule for natural logarithms (i.e., $\ln(a/b) = \ln a - \ln b$, where $a \in \mathbb{R}_+$ and $b \in \mathbb{R}_+$), the finite-time can be calculated as in (5). The proof is now complete. \blacksquare

4.2. ANALYSIS FOR OBJECTIVE B)

We next present the second main result of this paper for achieving objective *b*). To this end, let $\tilde{x}_i(t) \triangleq x_i(t) - x_{r_i}(t)$ be the tracking error of agent i , $i = 1, \dots, N$, that satisfies the dynamics given by

$$\begin{aligned} \dot{\tilde{x}}_i(t) &= \dot{x}_i(t) - \dot{x}_{r_i}(t) \\ &= -(d_i + k_i)\tilde{x}_i - \sigma(\text{sgn}(z_{1_i}(t)) - \text{sgn}(z_{2_i}(t))) \\ &\quad - (u_{a_i}(t) - w_i^T \delta_i(x_i(t))) - u_{f_i}(t), \end{aligned} \tag{15}$$

where $z_{1_i}(t) \triangleq \sum_{i \sim j} (x_i(t) - x_{r_j}(t)) - k_i(x_i(t) - c(t))$ and $z_{2_i}(t) \triangleq \sum_{i \sim j} (x_{r_i}(t) - x_{r_j}(t)) - k_i(x_{r_i}(t) - c(t))$. Since (15) contains the nonlinear term “ $\text{sgn}(z_{1_i}(t)) - \text{sgn}(z_{2_i}(t))$ ” that do not produce a term depending on $\tilde{x}_i(t)$, we now utilize adaptive control theory with nonlinear reference models [gruenwald2020adaptive]. Specifically, consider $\mu_i(\tilde{x}_i(t)) \triangleq \tilde{x}_i$ and a locally Lipschitz function $\beta_i(\cdot) \in \mathbb{R}$ such that

$$\mu_i(\tilde{x}_i(t)) = \text{sgn}(z_{1_i}(t)) - \text{sgn}(z_{2_i}(t)) + \beta_i(\cdot) \tag{16}$$

holds $(\beta_i(\cdot))$ can be readily calculated; see, for example, (32), (33), and (34) in Section 5).

One can now rewrite (15) as

$$\begin{aligned}
\dot{\tilde{x}}_i(t) &= -(d_i + k_i)\tilde{x}_i(t) - \sigma(\tilde{x}_i(t) - \beta_i) \\
&\quad - (u_{a_i}(t) - w_i^T \delta_i(x_i(t))) - u_{f_i}(t) \\
&= -(d_i + k_i + \sigma)\tilde{x}_i(t) \\
&\quad - u_{a_i}(t) + w_{a_i}^T(\cdot)\delta_{a_i}(\cdot) - u_{f_i}(t)
\end{aligned} \tag{17}$$

with $w_{a_i}(\cdot) \triangleq [w_i^T, \sigma]^T \in \mathbb{R}^{s+1}$ and $\delta_{a_i}(\cdot) \triangleq [\delta_i^T(x_i), \beta_i]^T \in \mathbb{R}^{s+1}$.

Next, let the adaptive component of the distributed controller given by (3) be

$$u_{a_i}(t) = -\hat{w}_{a_i}^T(t)\delta_{a_i}(\cdot) \tag{18}$$

with the weight update rule

$$\dot{\hat{w}}_{a_i}(t) = \gamma_i^{-1}\delta_{a_i}(\cdot)\tilde{x}_i(t), \tag{19}$$

where $\gamma_i \in \mathbb{R}_+$ is the learning rate. Now, substituting (18) into the (17), we have

$$\dot{\tilde{x}}_i(t) = -(d_i + k_i + \sigma)\tilde{x}_i(t) - \tilde{w}_{a_i}^T(t)\delta_{a_i}(\cdot) - u_{f_i}(t), \tag{20}$$

where $\tilde{w}_{a_i}(t) \triangleq \hat{w}_{a_i}(t) - w_{a_i} \in \mathbb{R}^{s+1}$ is the weight estimation error that satisfies the dynamics given by

$$\dot{\tilde{w}}_{a_i}(t) = \gamma_i^{-1}\delta_{a_i}(\cdot)\tilde{x}_i(t). \tag{21}$$

Finally, let the finite-time component of the distributed controller given by (3) be

$$u_{f_i}(t) = b_i \text{sgn}(\tilde{x}_i(t)), \tag{22}$$

where $b_i \in \mathbb{R}_+$ is a design parameter. From (20), we arrive

$$\dot{\tilde{x}}_i(t) = -(d_i + k_i + \sigma)\tilde{x}_i(t) - \tilde{w}_{a_i}^T \delta_{a_i} - b_i \text{sgn}(\tilde{x}_i(t)). \quad (23)$$

We are now ready to present the second main result of this paper for achieving objective b), where $a_i \triangleq d_i + k_i + \sigma$ and $p_i(t_0) \triangleq \tilde{x}_i^2(t_0)$ in the next theorem.

Theorem 4.2. *Consider the uncertain multiagent system consisting of N agents given by (1), the reference model given by (2) subject to Assumption 4.1 and $\sigma > \bar{c}$, and the distributed control signal given by (3) with adaptive and finite-time components respectively given by (18) and (19), and (22). Then the pair $(\tilde{x}_i(t), \tilde{w}_{a_i})$ is bounded for all $i = 1, \dots, N$, and the tracking error $\tilde{x}_i(t)$ vanishes in finite-time T_i for all $i = 1, \dots, N$ subject to the upper bound given by*

$$T_i \leq \frac{1}{a_i} \ln \left(\frac{a_i \sqrt{p_i(t_0)} + b_i}{b_i} \right). \quad (24)$$

Proof. Consider the Lyapunov candidate be given by

$$V_i(\tilde{x}_i, \tilde{w}_{a_i}) = \frac{1}{2} \tilde{x}_i^2 + \frac{1}{2} \gamma_i \tilde{w}_{a_i}^2. \quad (25)$$

Here, $V_i(0, 0) = 0$ and $V_i(\tilde{x}_i, \tilde{w}_{a_i}) > 0$ for all $(\tilde{x}_i, \tilde{w}_{a_i}) \neq 0$, and $V_i(\tilde{x}_i, \tilde{w}_{a_i})$ is radially unbounded. Now, the time derivative of (25) yields

$$\begin{aligned} \dot{V}_i(\cdot) &= \tilde{x}_i(t) \dot{\tilde{x}}_i(t) + \gamma_i \tilde{w}_{a_i}(t) \dot{\tilde{w}}_{a_i}(t) \\ &= -(d_i + k_i + \sigma) \tilde{x}_i^2(t) - \tilde{x}_i(t) \tilde{w}_{a_i}^T \delta_{a_i} \\ &\quad - \tilde{x}_i(t) b_i \text{sgn}(\tilde{x}_i(t)) + \gamma_i \tilde{w}_{a_i} \gamma_i^{-1} \delta_{a_i} \tilde{x}_i(t) \\ &\leq -(d_i + k_i + \sigma) \tilde{x}_i^2(t) - \tilde{x}_i(t) b_i \text{sgn}(\tilde{x}_i(t)) \\ &\leq -a_i \tilde{x}_i^2(t) - b_i |\tilde{x}_i(t)|. \end{aligned} \quad (26)$$

This implies that the pair $(\tilde{x}_i(t), \tilde{w}_{a_i}(t))$ is bounded for all $i = 1, \dots, N$.

To show finite-time convergence of the tracking error $\tilde{x}_i(t)$, one can write

$$V_i(\cdot) \leq - \int (a_i \tilde{x}_i^2(t) + b_i |\tilde{x}_i(t)|) + V_0 \quad (27)$$

by integrating (26). Using the inequality $\frac{1}{2}\tilde{x}_i^2(t) \leq V_i(\cdot)$ that follows from (25), (27) can now be rewritten as

$$\frac{1}{2}\tilde{x}_i^2(t) \leq - \int (a_i \tilde{x}_i^2(t) + b_i |\tilde{x}_i(t)|) + V_0. \quad (28)$$

Next, let $p_i(t) \triangleq \tilde{x}_i^2(t) > 0$. Thus, we arrive

$$\frac{1}{2}p_i(t) \leq - \int (a_i p_i(t) + b_i \sqrt{p_i(t)}) + V_0. \quad (29)$$

Finally, taking the time derivative of (29) yields

$$\dot{p}_i(t) \leq -(2a_i p_i(t) + 2b_i \sqrt{p_i(t)}). \quad (30)$$

Since a_i and b_i are positive, the finite-time convergence for all agents follows similar to the proof of Theorem 4.1. The calculation of T_i also follows similar to the proof of the same theorem. The proof is now complete. \blacksquare

Remark 4.1. *As it is well-known, $\text{sgn}(\cdot)$ can cause chattering in the control inputs of each agent. In this case, it is of practice to approximate this function with $\text{sgn}(x) \approx \tanh(kx)$ for a large value of $k \in \mathbb{R}_+$.*

We refer to the next section for details.

5. ILLUSTRATIVE NUMERICAL EXAMPLE

To illustrate the proposed distributed adaptive control approach in Theorem 4.2, which is predicated on the agent-wise nonlinear reference model in Theorem 4.1, consider the group of three agents on the connected and undirected graph \mathcal{G} shown in Figure 1 with

the first agent being the leader. For this graph, the resulting $\mathcal{L}(\mathcal{G})$ and \mathcal{K} matrices become

$$\mathcal{L}(\mathcal{G}) = \begin{bmatrix} 2 & -1 & -1 \\ -1 & 1 & 0 \\ -1 & 0 & 1 \end{bmatrix}, \quad \mathcal{K} = \begin{bmatrix} 1 & 0 & 0 \\ 0 & 0 & 0 \\ 0 & 0 & 0 \end{bmatrix}. \quad (31)$$

For the dynamics of each agent, we use $\delta_i(x_i(t)) = x_i(t)$ and $w_i = 5$ respectively for the basis functions and the unknown weights. In addition, the initial states and the reference states of agents are randomly chosen over the interval $[-5, 5]$ respectively as $x(0) = [0.90, -1.15, -3.80]^T$ and $x_r(0) = [-0.80, -2.80, -0.10]^T$. To satisfy (16), $\beta_i(\cdot)$ values are also calculated as

$$\begin{aligned} \beta_1(\cdot) = & -(x_1(t) - x_{r_1}(t)) - \operatorname{sgn}\left((x_1(t) - x_{r_2}(t)) \right. \\ & \left. + (x_1(t) - x_{r_3}(t)) + (x_1(t) - c(t))\right) \\ & + \operatorname{sgn}\left((x_{r_1}(t) - x_{r_2}(t)) + (x_{r_1}(t) - x_{r_3}(t)) \right. \\ & \left. + (x_{r_1}(t) - c(t))\right), \end{aligned} \quad (32)$$

$$\begin{aligned} \beta_2(\cdot) = & -(x_2(t) - x_{r_2}(t)) - \operatorname{sgn}\left((x_2(t) - x_{r_1}(t)) \right. \\ & \left. + \operatorname{sgn}\left((x_{r_2}(t) - x_{r_1}(t))\right), \end{aligned} \quad (33)$$

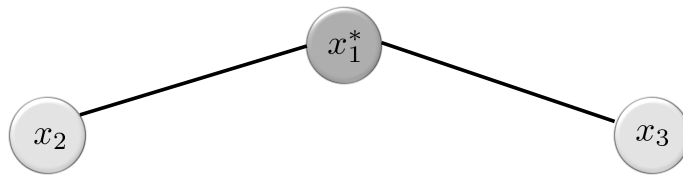


Figure 1. Three agents on the connected and undirected graph \mathcal{G} with the first agent being the leader (i.e., $k_1 = 1$) and the second and the third agents being followers (i.e., $k_2 = 0$ and $k_3 = 0$).

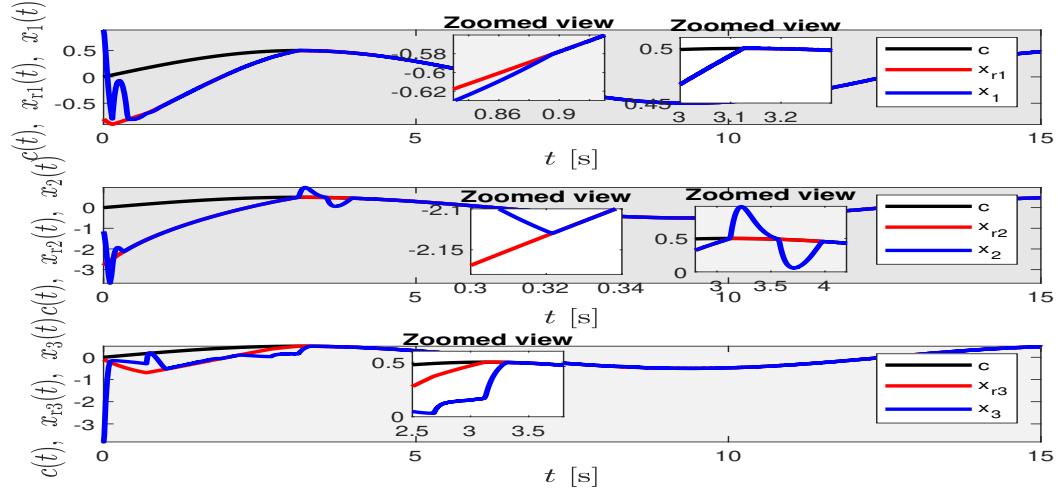


Figure 2. Performance of the states and the references states of each agent (the command available to the first agent is shown in all figures).

$$\begin{aligned} \beta_3(\cdot) = & -(x_3(t) - x_{r_3}(t)) - \operatorname{sgn}\left((x_3(t) - x_{r_1}(t))\right) \\ & + \operatorname{sgn}\left((x_{r_3}(t) - x_{r_1}(t))\right). \end{aligned} \quad (34)$$

Finally, we use a sinusoidal wave command $c(t)$ with an amplitude of 0.5 and a frequency of 0.08 Hz, and we choose $b_i = 2.5$, $\gamma_i = 100$, and $\sigma = 0.5$, where $\sigma > \bar{c}$ holds in this case (i.e., $\|\mathbf{1}_N \dot{c}(t)\|_2 \leq \bar{c}$ is calculated with $\bar{c} = 0.35$ such that $\sigma = 0.5 > 0.35$ holds).

Figures 2 and 3 show the performance of the proposed distributed control approach predicated on the agent-wise nonlinear reference models. Note that the reference state of each agent approach to the time-varying command in finite-time, which numerically validates the theory presented in Theorem 4.1, and the state of each agent also approach to their corresponding reference state in finite-time, which further numerically validates the theory presented in Theorem 4.2. Following the discussion in Remark 4.1, however, chattering happens in the control signals of each agent. To provide a remedy to this problem by following the discussion in the same remark, “ $\operatorname{sgn}(\cdot)$ ” is replaced with “ $\tanh(1000(\cdot))$ ”

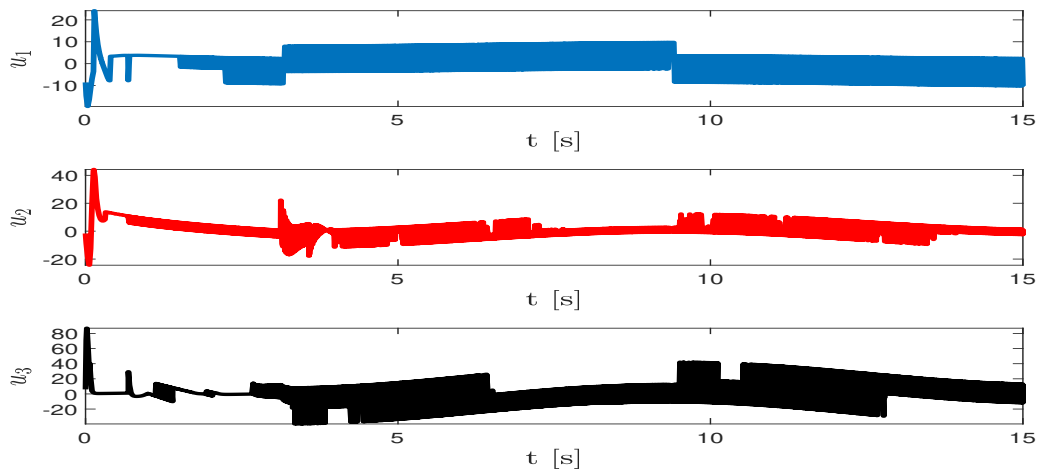


Figure 3. History of the control signals of each agent.

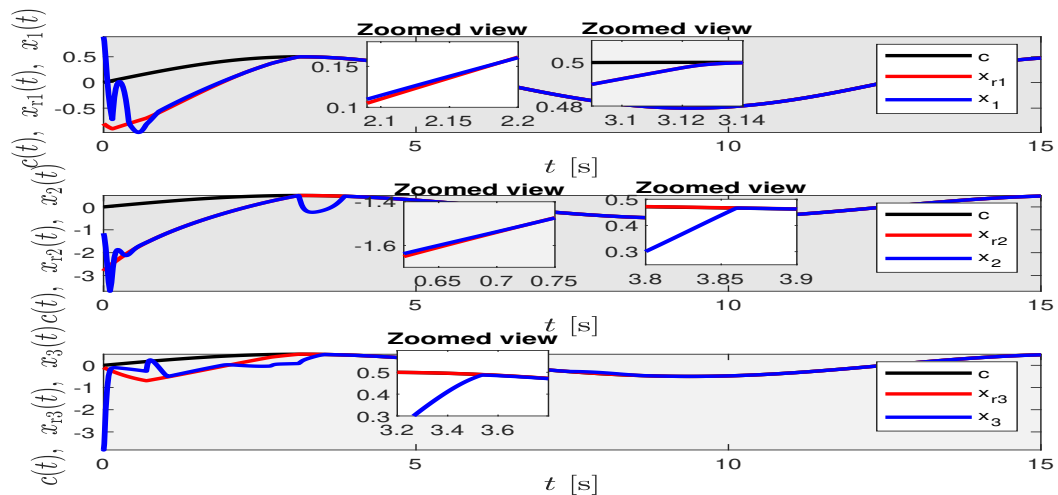


Figure 4. Performance of the states and the references states of each agent when “sgn(·)” is replaced with “tanh(1000(·))” by following the discussion in Remark 4.1 (the command available to the first agent is shown in all figures).

in Figures 4 and 5. Compared to the performance in Figure 2, in particular, a similar closed-loop multiagent system performance is achieved in Figure 4, where no chattering happens in this case in the control signals of each agent, as clearly seen from Figure 5.

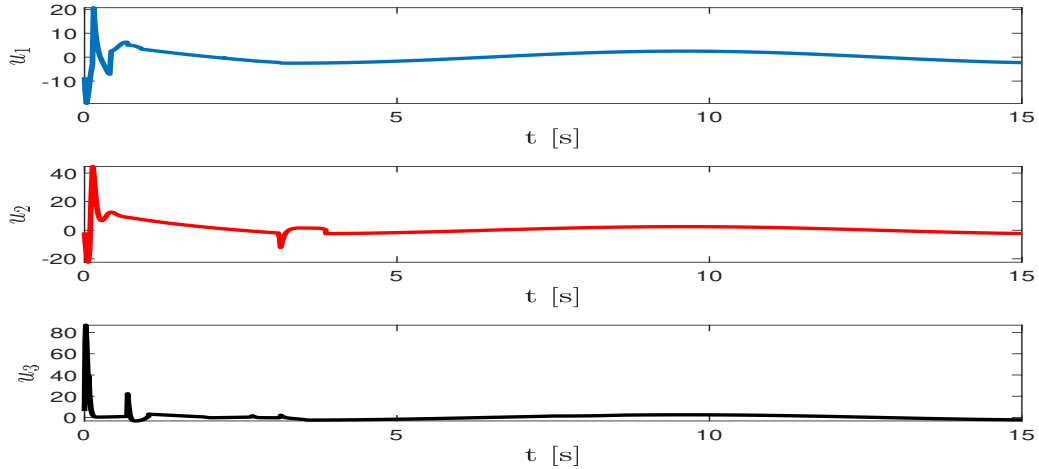


Figure 5. History of the control signals of each agent when “ $\text{sgn}(\cdot)$ ” is replaced with “ $\text{tanh}(1000(\cdot))$ ” by following the discussion in Remark 4.1.

6. CONCLUSION

A finite-time distributed adaptive control approach was presented for uncertain multiagent systems, where it was predicated on agent-wise nonlinear reference models. Specifically, these reference models generalized their linear counterparts in [29] for capturing the ideal finite-time behavior of the overall multiagent system while ensuring safety in the sense that agents always rely on stable reference model states in their adaptive control signals for suppressing the negative effect of system anomalies. Utilizing the error signals between the states of agent dynamics and the states of these reference models, we showed that adaptation allows us to drive these error signals of each agent subject to uncertainties to zero in finite-time; that is, each agent achieved its ideal performance in finite-time. Finally, an illustrative numerical example demonstrated the efficacy of the proposed control approach. Future research can involve extending the results of this paper presented in Theorems 4.1 and 4.2 to high-order uncertain agent dynamics as well as to agents over directed and switching graph topologies.

REFERENCES

- [1] Li, Z., Zhan, A., Yang, C., Qiu, J., and Wen, Y., 'Finite-time coordination of a class of second-order nonlinear multi-agent systems,' in '4th International Conference on Information, Cybernetics and Computational Social Systems (ICCSS),' 2017 pp. 512–516.
- [2] Li, Z. and Ji, H., 'Finite-time consensus and tracking control of a class of nonlinear multiagent systems,' *IEEE transactions on automatic control*, 2018, **63**(12), pp. 4413–4420.
- [3] Systems, M.-A., Li, Z., Chen, X., Wen, Y., and Qiu, J., 'Finite-time tracking consensus control for a class of nonlinear,' in 'IECON 2017 - 43rd Annual Conference of the IEEE Industrial Electronics Society,' 2017 pp. 5803–5808.
- [4] Wang, H., Yu, W., Yao, L., and Chen, G., 'Fully-distributed finite-time consensus of second-order multi-agent systems on a directed network,' in '2018 IEEE International Symposium on Circuits and Systems (ISCAS),' 2018 pp. 1–4.
- [5] Yu, S., Long, X., and Guo, G., 'Homogeneous finite-time consensus tracking of high-order-integrator agents by parametric approach,' *International Journal of Control*, 2017, **90**(12), pp. 2655–2666.
- [6] Cao, Y., Ren, W., and Meng, Z., 'Decentralized finite-time sliding mode estimators and their applications in decentralized finite-time formation tracking,' *Systems & Control Letters*, 2010, **59**(9), pp. 522–529.
- [7] Gao, J. and Zheng, M., 'Distributed adaptive event-triggered protocol for tracking control of leader-following multi-agent systems,' *Journal of the Franklin Institute*, 2019, **356**(17), pp. 10466–10479.
- [8] Cortés, J., 'Finite-time convergent gradient flows with applications to network consensus,' *Automatica*, 2006, **42**(11), pp. 1993–2000.
- [9] Xiao, F., Wang, L., Chen, J., and Gao, Y., 'Finite-time formation control for multi-agent systems,' *Automatica*, 2009, **45**(11), pp. 2605–2611.
- [10] Tian, B., Lu, H., Zuo, Z., and Yang, W., 'Fixed-time leader–follower output feedback consensus for second-order multiagent systems,' *IEEE transactions on cybernetics*, 2018, **49**(4), pp. 1545–1550.
- [11] Li, S., Du, H., and Lin, X., 'Finite-time consensus algorithm for multi-agent systems with double-integrator dynamics,' *Automatica*, 2011, **47**(8), pp. 1706–1712.
- [12] Yu, S. and Long, X., 'Finite-time consensus tracking of perturbed high-order agents with relative information by integral sliding mode,' *IEEE Transactions on Circuits and Systems II: Express Briefs*, 2016, **63**(6), pp. 563–567.

- [13] Yu, Z., Yu, S., Jiang, H., and Hu, C., ‘Distributed consensus for multi-agent systems via adaptive sliding mode control,’ *International Journal of Robust and Nonlinear Control*, 2021.
- [14] Huang, J., Wen, C., Wang, W., and Song, Y.-D., ‘Adaptive finite-time consensus control of a group of uncertain nonlinear mechanical systems,’ *Automatica*, 2015, **51**, pp. 292–301.
- [15] Jin, X., Zhao, X., Qin, J., Zheng, W. X., and Kang, Y., ‘Adaptive finite-time consensus of a class of disturbed multi-agent systems,’ *Journal of the Franklin Institute*, 2018, **355**(11), pp. 4644–4664.
- [16] Tu, Z., Yu, H., and Xia, X., ‘Decentralized finite-time adaptive consensus of multiagent systems with fixed and switching network topologies,’ *Neurocomputing*, 2017, **219**, pp. 59–67.
- [17] Wang, W., Long, J., Wen, C., and Huang, J., ‘Recent advances in distributed adaptive consensus control of uncertain nonlinear multi-agent systems,’ *Journal of Control and Decision*, 2020, **7**(1), pp. 44–63.
- [18] Sun, C., Hu, G., and Xie, L., ‘Robust consensus tracking for a class of high-order multi-agent systems,’ *International Journal of Robust and Nonlinear Control*, 2016, **26**(3), pp. 578–598.
- [19] Cai, M. and Xiang, Z., ‘Adaptive finite-time consensus tracking for multiple uncertain mechanical systems with input saturation,’ *International Journal of Robust and Nonlinear Control*, 2017, **27**(9), pp. 1653–1676.
- [20] Zhou, Y. and Zhang, G., ‘Adaptive finite-time consensus for multi-agent systems with input constraints,’ in ‘2019 Chinese Control Conference (CCC),’ 2019 pp. 5952–5957.
- [21] Liu, D. and Zhao, L., ‘Adaptive finite-time consensus tracking control for nonlinear multiagent systems in nonstrict feedback form with full-state constraints,’ *International Journal of Adaptive Control and Signal Processing*, 2021.
- [22] Ji, Q., Chen, G., and He, Q., ‘Neural network-based distributed finite-time tracking control of uncertain multi-agent systems with full state constraints,’ *IEEE Access*, 2020, **8**, pp. 174365–174374.
- [23] Yu, H., Shen, Y., and Xia, X., ‘Adaptive finite-time consensus in multi-agent networks,’ *Systems & Control Letters*, 2013, **62**(10), pp. 880–889.
- [24] Liu, G., Zhao, L., and Yu, J., ‘Adaptive finite-time consensus tracking for nonstrict feedback nonlinear multi-agent systems with unknown control directions,’ *IEEE Access*, 2019, **7**, pp. 155262–155269.
- [25] Radenkovic, M. and Tadi, M., ‘Multi-agent adaptive consensus of networked systems on directed graphs,’ *International Journal of Adaptive Control and Signal Processing*, 2016, **30**(1), pp. 46–59.

- [26] Zhao, L., Liu, Y., Li, F., and Man, Y., ‘Fully distributed adaptive finite-time consensus for uncertain nonlinear multiagent systems,’ *IEEE Transactions on Cybernetics*, 2020.
- [27] Sun, C., Hu, G., and Xie, L., ‘Fast finite-time consensus tracking for first-order multi-agent systems with unmodelled dynamics and disturbances,’ in ‘11th IEEE International Conference on Control & Automation (ICCA),’ 2014 pp. 249–254.
- [28] Arabi, E. and Yucelen, T., ‘Control of uncertain multiagent systems with spatiotemporal constraints,’ *IEEE Transactions on Control of Network Systems*, 2021.
- [29] Dogan, K. M., Yucelen, T., Ristevki, S., and Muse, J. A., ‘Distributed adaptive control of uncertain multiagent systems with coupled dynamics,’ in ‘2020 American Control Conference,’ 2020 pp. 3497–3502.
- [30] Godsil, C. D. and Royle, G., *Algebraic graph theory*, Springer, New York, 2001.
- [31] Mesbahi, M. and Egerstedt, M., *Graph theoretic methods in multiagent networks*, Princeton University Press, 2010.
- [32] Lewis, F. L., Zhang, H., Hengster-Movric, K., and Das, A., *Cooperative control of multi-agent systems: Optimal and adaptive design approaches*, Springer Science & Business Media, 2013.

SECTION

2. SUMMARY AND CONCLUSIONS

The purpose of this dissertation was to develop new optimal and adaptive control methods for uncertain dynamical systems. Overall, the proposed methods improve the system stability, performance of trajectory tracking, handle state constraints, and suppress the uncertainties.

Specifically, integrated path planning and control architecture for impaired aircraft was used in Paper I. This paper considered engine failure ($T=0$) and landing. The integrated path planning and control equations are used in conjunction with the SDRE method to successfully produce the elevator deflection histories to land the aircraft. Also, an adaptive controller-based modified state observer was used to estimate uncertainties.

In Paper II, path planning and control were used for impaired aircraft but with sliding mode control. The second-order sliding mode control was used to control the aircraft, and the higher-order sliding mode was used to estimate the system uncertainties. This paper also considered the impaired aircraft with elevator deflection stuck at some angle.

After using optimal control with uncertainties, the state constraint problem was introduced. The state constraint inequality is not an easy task with the optimal solution. The inverse optimal control with the set-theoretic barrier Lyapunov function was considered in Paper III. Highly mathematics involved in the optimal solution of state constraints. Therefore, the inverse optimal based set-theoretic barrier Lyapunov function was developed to overcome the highly involved mathematical solutions.

Paper IV introduced the adaptive control of uncertain dynamical systems with an optimal nonlinear reference model. After focusing on the importance of optimal control and nonlinear reference model of the dynamical system, the Θ -D based optimal nonlinear

reference model was developed with adaptive control for uncertain dynamical systems. As a result, the state of the uncertain dynamical system converged to the state of the optimal nonlinear reference model.

When the state constraint with optimal control was studied, the uncertainties were not considered. Paper V introduced the set-theoretic model reference adaptive control method for an uncertain dynamical system with state constraints. In this method, the norm of the states did not violate the state limits, and desirable closed-loop system tracking performance was achieved. The efficacy of the proposed method was demonstrated with simulation and experimental studies.

Finally, the finite-time method for distributed adaptive control was presented for uncertain multiagent systems in Paper VI. Specifically, the agent-wise nonlinear reference model was considered. The nonlinear reference model ensured the safety of agents. Also, the adaptive control method was introduced to converge error signals to zero in finite time. The simulation results demonstrated the efficacy of the proposed approach.

APPENDIX A.

PROOF OF THE THEOREM OF THE PAPER I

1. PROOF OF THE THEOREM OF THE PAPER I

The proof of the Theorem 1 of the Paper I is utilized with Lyapunov stability analysis.

The Lyapunov candidate is chosen as

$$V(e_a, \tilde{W}) = e_a^T P e_a + \text{tr}(\tilde{W} \Gamma^{-1} \tilde{W}). \quad (1)$$

Note that $v(0, 0) = 0$ and $V(e_a, \tilde{W}) > 0$ for all $(e_a, \tilde{W}) \neq (0, 0)$. Taking the derivate of (1) yields

$$\dot{V} = \dot{e}_a^T P e_a + e_a^T P \dot{e}_a + \text{tr}(\dot{\tilde{W}}^T \Gamma^{-1} \tilde{W}) + \text{tr}(\tilde{W}^T \Gamma^{-1} \dot{\tilde{W}}). \quad (2)$$

By substituting (8) into (2), we arrive

$$\dot{V} = e_a^T (-K_2^T P - P K_2) e_a + 2e_a^T P (\tilde{W}^T \phi(x) + \varepsilon) + 2\text{tr}(\tilde{W}^T \Gamma^{-1} \dot{\tilde{W}}). \quad (3)$$

Then, we use the error between the actual weight and the estimated weight of the neural network in (3) as

$$\dot{V} = e_a^T (-K_2^T P - P K_2) e_a + 2e_a^T P (\tilde{W}^T \phi(x) + \varepsilon) - 2\text{tr}(\tilde{W}^T \Gamma^{-1} \dot{\hat{W}}). \quad (4)$$

Using (9) into (4), we now get

$$\dot{V} = e_a^T (-K_2^T P - P K_2) e_a + 2e_a^T P \varepsilon + 2\text{tr}(\sigma \tilde{W}^T \hat{W}). \quad (5)$$

From the solution of the Lyapunov equation $-K_2^T P - P K_2 = -Q$, the (5) becomes

$$\dot{V} = -e_a^T Q e_a + 2e_a^T P \varepsilon + 2\text{tr}(\sigma \tilde{W}^T \hat{W}). \quad (6)$$

When we take the norms on the right hand side of the equality, (6) can be upper bounded as

$$\dot{V} \leq -\lambda_{\min}(Q) \|e_a\|^2 + 2 \|e_a\| \lambda_{\max}(P) \|\varepsilon\| + 2\sigma \|\tilde{W}\| \|\hat{W}\|. \quad (7)$$

The neural network approximation error ε is assumed to be bounded such that $\|\varepsilon\| \leq \varepsilon_m$.

The norm of the error between the actual weight and the estimated weight of the neural network is defined as $\|\tilde{W}\| = \|W - \hat{W}\|$. Now (7) becomes

$$\begin{aligned} \dot{V} &\leq -\lambda_{\min}(Q) \|e_a\|^2 + 2 \|e_a\| \lambda_{\max}(P) \varepsilon_m + 2\sigma \|W - \hat{W}\| \|\hat{W}\| \\ &\leq -\lambda_{\min}(Q) \|e_a\|^2 + 2 \|e_a\| \lambda_{\max}(P) \varepsilon_m + 2\sigma (\|W\| \|\hat{W}\| - \|\hat{W}\| \|\hat{W}\|). \end{aligned}$$

The upper bound of the norm of the actual weight is W_{max} . Substituting W_{max} into (8), we get

$$\dot{V} \leq -\lambda_{\min}(Q) \|e_a\|^2 + 2 \|e_a\| \lambda_{\max}(P) \varepsilon_m + 2\sigma (W_{max} \|\hat{W}\| - \|\hat{W}\| \|\hat{W}\|). \quad (8)$$

1.1. UPPER BOUND ON ESTIMATION ERROR

To find the upper bound on the estimation error, (8) can be rearranged as

$$\dot{V} \leq -\lambda_{\min}(Q) \|e_a\|^2 + 2 \|e_a\| \lambda_{\max}(P) \varepsilon_m - 2\sigma \left(\|\hat{W}\| - \frac{W_{max}}{2} \right)^2 + 2\sigma \left(\frac{W_{max}}{2} \right)^2. \quad (9)$$

We assume that the estimation error has an upper bound β satisfying

$$\beta = \frac{\lambda_{\max}(P) \varepsilon_m + \sqrt{\left((\lambda_{\max}(P) \varepsilon_m)^2 + \sigma \lambda_{\min}(Q) \frac{W_{max}^2}{2} \right)^2}}{\lambda_{\min}(Q)} \quad (10)$$

1.2. UPPER BOUND OF THE NEURAL NETWORK WEIGHTS

To find the upper bound on the $\|\hat{W}\|$, the following derivations need to be solved.

$$\dot{V} \leq -\lambda_{\min}(Q) \|e_a\|^2 + 2 \|e_a\| \lambda_{\max}(P) \varepsilon_m + 2\sigma(W_{max} \|\hat{W}\| - \|\hat{W}\| \|\hat{W}\|). \quad (11)$$

$$\dot{V} \leq -\lambda_{\min}(Q) \left(\|e_a\|^2 + \frac{2 \|e_a\| \lambda_{\max}(P) \varepsilon_m}{\lambda_{\min}(Q)} \right) + 2\sigma(W_{max} \|\hat{W}\| - \|\hat{W}\|^2). \quad (12)$$

Using the first part of the right side of the equation, we can write

$$\dot{V} \leq -\lambda_{\min}(Q) \left[\left(\|e_a\| - \frac{\lambda_{\max}(P) \varepsilon_m}{\lambda_{\min}(Q)} \right)^2 - \left(\frac{\lambda_{\max}(P) \varepsilon_m}{\lambda_{\min}(Q)} \right)^2 \right] + 2\sigma(W_{max} \|\hat{W}\| - \|\hat{W}\|^2) \quad (13)$$

Then, the terms are considered separately as given by $a_1 = -\lambda_{\min}(Q) \left[\left(\|e_a\| - \frac{\lambda_{\max}(P) \varepsilon_m}{\lambda_{\min}(Q)} \right)^2 \right]$, $a_2 = \lambda_{\min}(Q) \left(\frac{\lambda_{\max}(P) \varepsilon_m}{\lambda_{\min}(Q)} \right)^2$, $a_3 = 2\sigma(W_{max} \|\hat{W}\|)$ and $a_4 = -2\sigma(W_{max} \|\hat{W}\|^2)$. From the above definitions, a_1 is negative definite and the other equations are considered as

$$-\lambda_{\min}(Q) \left(\frac{\lambda_{\max}(P) \varepsilon_m}{\lambda_{\min}(Q)} \right)^2 - 2\sigma(W_{max} \|\hat{W}\|) + 2\sigma(W_{max} \|\hat{W}\|^2) \geq 0, \quad (14)$$

where this inequality yields to the bound using a quadratic equation. Therefore, the bound is satisfies as

$$\|\hat{W}\| \geq \frac{2\sigma W_{max} + \sqrt{4\sigma^2 W_{max}^2 + 8\sigma \left(\frac{\lambda_{\max}(P)^2 \varepsilon_m^2}{\lambda_{\min}(Q)} \right)}}{4\sigma}, \quad (15)$$

where $\|\hat{W}\| \geq \mathcal{L}$. We now get

$$\mathcal{L} = \frac{W_{max} + \sqrt{W_{max}^2 + 2 \left(\frac{\lambda_{\max}(P)^2 \varepsilon_m^2}{\sigma \lambda_{\min}(Q)} \right)}}{2}. \quad (16)$$

The conclusion is that both estimation error and neural network weights are uniformly bounded.

APPENDIX B.

PROOF OF THE THEOREM OF THE PAPER III

1. PROOF OF THE THEOREM OF THE PAPER III

The proof of the Theorem 3.1 of the Paper III is utilized with Lyapunov stability analysis. The Lyapunov candidate is chosen as

$$V(e) = \phi(\|e\|_P) \quad (1)$$

Taking the time derivative of (1) we get,

$$\begin{aligned} \dot{V}(e) &= \frac{d\phi(\|e(t)\|_P)}{dt} = \frac{d\phi(\|e(t)\|_P)}{d\|e(t)\|_P^2} \frac{d\|e(t)\|_P^2}{dt} = \frac{d\phi(\|e(t)\|_P)}{d\|e(t)\|_P^2} \frac{d\|e(t)\|_P^2}{de} \frac{de}{dt} \\ &= \frac{1}{2} D_\phi(\|e(t)\|_P) e^T(t) P \dot{e}(t). \end{aligned} \quad (2)$$

where

$$\begin{aligned} \dot{V}(e) &= \frac{1}{2} D_\phi(\|e(t)\|_P) e^T(t) P \dot{e}(t) \\ &= \frac{1}{2} D_\phi(\|e(t)\|_P) e^T(t) P (Ae - Bu - BR_2^{-1} B^T D_\phi(\|e(t)\|_P) P (x_m - C^T r)) \end{aligned} \quad (3)$$

where we can use $D_\phi(\|e(t)\|_P)$ as D_ϕ . By using the equation (31) in equation (3), the above equation becomes,

$$\begin{aligned} \dot{V}(e) &= \frac{1}{2} D_\phi e^T(t) P (Ae(t) - \frac{1}{2} BR_2^{-1} B^T D_\phi P e(t) - BR_2^{-1} B^T D_\phi P (x_m(t) - Cr(t))) \\ &= \frac{1}{2} D_\phi e^T(t) P A e(t) - \frac{1}{4} D_\phi e^T(t) P BR_2^{-1} B^T D_\phi P e(t) \\ &\quad - \frac{1}{2} D_\phi e^T(t) P BR_2^{-1} B^T D_\phi P (x_m(t) - Cr(t)) \\ &= \frac{1}{2} D_\phi e^T(t) P [A - \frac{1}{2} BR_2^{-1} B^T D_\phi P] e(t) - \frac{1}{2} D_\phi e^T(t) P BR_2^{-1} B^T D_\phi P (x_m(t) - Cr(t)) \end{aligned} \quad (4)$$

where $A_H = A - \frac{1}{2} BR_2^{-1} B^T D_\phi P$ where P is chosen such that A_H is point-wise stable. Then

$$\begin{aligned} \dot{V}(e) &= \frac{1}{2} D_\phi e^T(t) P A_H e(t) + -\frac{1}{2} D_\phi e^T(t) P BR_2^{-1} B^T D_\phi P (x_m(t) - Cr(t)) \\ &= \frac{1}{4} e^T(t) D_\phi [P A_H + A_H^T P] e(t) - \frac{1}{2} D_\phi e^T(t) P BR_2^{-1} B^T D_\phi P (x_m(t) - Cr(t)) \end{aligned} \quad (5)$$

where $PA_H + A_H^T P = -Q$.

$$\begin{aligned}
\dot{V}(e) &= -\frac{1}{4}D_\phi e^T(t)Qe(t) - \frac{1}{2}D_\phi^2 e^T(t)PBR_2^{-1}B^T D_\phi P(x_m(t) - Cr(t)) \\
&\leq -\frac{1}{4}D_\phi \lambda_{\min}(Q) \|e(t)\|^2 - \frac{1}{2}D_\phi^2 \|e(t)\|^2 \|PBR_2^{-1}B^T D_\phi P\| \\
&\quad - \frac{1}{2}D_\phi^2 \|PBR_2^{-1}B^T D_\phi P\| \|(x_m(t) - Cr(t))\|^2
\end{aligned} \tag{6}$$

By adding and subtracting $\frac{1}{8}\lambda_{\min}(Q)\phi(\|e\|_P)$,

$$\begin{aligned}
\dot{V}(e) &\leq -\frac{1}{8}\lambda_{\min}(Q)\phi(\|e\|_P) - \lambda_{\min}(Q)\left[\frac{1}{4}D_\phi e^T P e \right. \\
&\quad \left. - \frac{1}{8}\phi(\|e\|_P)\right].
\end{aligned} \tag{7}$$

By using the property given in (11) in paper III, $[\frac{1}{4}D_\phi e^T P e - \frac{1}{8}\phi(\|e\|_P)] > 0$. Therefore, it is proved that

$$\dot{V}(e) \leq -\frac{1}{8}\lambda_{\min}(Q)\phi(\|e\|_P). \tag{8}$$

REFERENCES

- [1] Baba, Y., Takano, H., and Sano, M., 'Desired trajectory and guidance force generators for an aircraft,' in 'Guidance, Navigation, and Control Conference,' 1996 p. 3873.
- [2] Menon, P., Badgett, M., Walker, R., and Duke, E., 'Nonlinear flight test trajectory controllers for aircraft,' *Journal of Guidance, Control, and Dynamics*, 1987, **10**(1), pp. 67–72.
- [3] Kaminer, I., Pascoal, A., Hallberg, E., and Silvestre, C., 'Trajectory tracking for autonomous vehicles: An integrated approach to guidance and control,' *Journal of Guidance, Control, and Dynamics*, 1998, **21**(1), pp. 29–38.
- [4] Boyle, D. P. and Chamitoff, G. E., 'Autonomous maneuver tracking for self-piloted vehicles,' *Journal of Guidance, Control, and Dynamics*, 1999, **22**(1), pp. 58–67.
- [5] Ochi, S., Takano, H., and Baba, Y., 'Flight trajectory tracking system applied to inverse control for aerobatic maneuvers,' in 'Inverse Problems in Engineering Mechanics III,' pp. 337–344, Elsevier, 2002.
- [6] Rysdyk, R., 'Unmanned aerial vehicle path following for target observation in wind,' *Journal of guidance, control, and dynamics*, 2006, **29**(5), pp. 1092–1100.
- [7] Chen, K., Fu, B., Ding, Y., and Yan, J., 'Integrated guidance and control method for the interception of maneuvering hypersonic vehicle based on high order sliding mode approach,' *Mathematical Problems in Engineering*, 2015, **2015**.
- [8] Palumbo, N. F., Reardon, B. E., and Blauwkamp, R. A., 'Integrated guidance and control for homing missiles,' *Johns Hopkins APL Technical Digest*, 2004, **25**(2), pp. 121–139.
- [9] Wang, X. and Wang, J., 'Partial integrated guidance and control for missiles with three-dimensional impact angle constraints,' *Journal of Guidance, Control, and Dynamics*, 2014, **37**(2), pp. 644–657.
- [10] Viswanathan, S. P., Sanyal, A. K., and Samiei, E., 'Integrated guidance and feedback control of underactuated robotics system in se (3),' *Journal of Intelligent & Robotic Systems*, 2018, **89**(1-2), pp. 251–263.
- [11] Silvestre, C., Pascoal, A., Kaminer, I., and Hallberg, E., 'Trajectory tracking controllers for auvs: An integrated approach to guidance and control system design,' *IFAC Proceedings Volumes*, 1996, **29**(1), pp. 8041–8046.
- [12] Shen, C., Shi, Y., and Buckham, B., 'Integrated path planning and tracking control of an auv: A unified receding horizon optimization approach,' *IEEE/ASME Transactions on Mechatronics*, 2017, **22**(3), pp. 1163–1173.

- [13] Levy, M., Shima, T., and Gutman, S., 'Linear quadratic integrated versus separated autopilot-guidance design,' *Journal of Guidance, Control, and Dynamics*, 2013, **36**(6), pp. 1722–1730.
- [14] Yang, S., Guo, J., and Zhou, J., 'New integrated guidance and control of homing missiles with an impact angle against a ground target,' *International Journal of Aerospace Engineering*, 2018, **2018**.
- [15] Tarn, T.-J., Xi, N., and Bejczy, A. K., 'Path-based approach to integrated planning and control for robotic systems: A path-based approach provides an analytical integration of robot planning and control. as a result, the task level control can be achieved, and the system is capable of coping with unexpected or uncertain events,' *Automatica*, 1996, **32**(12), pp. 1675–1687.
- [16] Sadeghi, M., Abaspour, A., and Sadati, S. H., 'A novel integrated guidance and control system design in formation flight,' *Journal of Aerospace Technology and Management*, 2015, **7**(4), pp. 432–442.
- [17] Huo, R., Liu, X., Zeng, X., and Lei, Z., 'Integrated guidance and control based on high-order sliding mode method,' in 'Control Conference (CCC), 2017 36th Chinese,' IEEE, 2017 pp. 6073–6078.
- [18] Kim, B. M., Kim, J. T., Kim, B. S., and Ha, C., 'Adaptive integrated guidance and control design for automatic landing of a fixed wing unmanned aerial vehicle,' *Journal of Aerospace Engineering*, 2011, **25**(4), pp. 490–500.
- [19] Liu, W., Wei, Y., Duan, G., and Hou, M., 'Integrated guidance and control with input saturation and disturbance observer,' *Journal of Control and Decision*, 2018, **5**(3), pp. 277–299.
- [20] Bechlioulis, C. P. and Rovithakis, G. A., 'Robust adaptive control of feedback linearizable mimo nonlinear systems with prescribed performance,' *IEEE Transactions on Automatic Control*, 2008, **53**(9), pp. 2090–2099.
- [21] Bechlioulis, C. P. and Rovithakis, G. A., 'Adaptive control with guaranteed transient and steady state tracking error bounds for strict feedback systems,' *Automatica*, 2009, **45**(2), pp. 532–538.
- [22] Bechlioulis, C. P. and Rovithakis, G. A., 'Prescribed performance adaptive control for multi-input multi-output affine in the control nonlinear systems,' *IEEE Transactions on Automatic Control*, 2010, **55**(5), pp. 1220–1226.
- [23] Yucelen, T. and Shamma, J. S., 'Adaptive architectures for distributed control of modular systems,' in '2014 American Control Conference,' IEEE, 2014 pp. 1328–1333.
- [24] Ngo, K. B., Mahony, R., and Jiang, Z.-P., 'Integrator backstepping using barrier functions for systems with multiple state constraints,' in 'Proceedings of the 44th IEEE Conference on Decision and Control,' IEEE, 2005 pp. 8306–8312.

- [25] Tee, K. P., Ge, S. S., and Tay, E. H., 'Barrier lyapunov functions for the control of output-constrained nonlinear systems,' *Automatica*, 2009, **45**(4), pp. 918–927.
- [26] Tee, K. P., Ge, S. S., and Tay, F. E. H., 'Adaptive control of electrostatic microactuators with bidirectional drive,' *IEEE transactions on control systems technology*, 2008, **17**(2), pp. 340–352.
- [27] Ren, B., Ge, S. S., Tee, K. P., and Lee, T. H., 'Adaptive neural control for output feedback nonlinear systems using a barrier lyapunov function,' *IEEE Transactions on Neural Networks*, 2010, **21**(8), pp. 1339–1345.
- [28] Kostarigka, A. K. and Rovithakis, G. A., 'Adaptive dynamic output feedback neural network control of uncertain mimo nonlinear systems with prescribed performance,' *IEEE transactions on neural networks and learning systems*, 2011, **23**(1), pp. 138–149.
- [29] Muse, J., 'A method for enforcing state constraints in adaptive control,' in 'AIAA Guidance, Navigation, and Control Conference,' 2011 p. 6205.
- [30] Arabi, E., Gruenwald, B. C., Yucelen, T., and Nguyen, N. T., 'A set-theoretic model reference adaptive control architecture for disturbance rejection and uncertainty suppression with strict performance guarantees,' *International Journal of Control*, 2018, **91**(5), pp. 1195–1208.
- [31] Arabi, E. and Yucelen, T., 'Set-theoretic model reference adaptive control with time-varying performance bounds,' *International Journal of Control*, 2019, **92**(11), pp. 2509–2520.
- [32] Arabi, E. and Yucelen, T., 'Experimental results with the set-theoretic model reference adaptive control architecture on an aerospace testbed,' in 'AIAA Scitech 2019 Forum,' 2019 p. 0930.
- [33] Deniz, M., Devi, P., and Balakrishnan, S., 'Inverse optimal control with set-theoretic barrier lyapunov function for handling state constraints,' in '2020 American Control Conference (ACC),' IEEE, 2020 pp. 981–986.
- [34] Devi, P., Balakrishnan, S., Deniz, M., and Fernandes, A., 'Barrier function-based sdre control for nonlinear systems with state constraints,' in '2021 American Control Conference (ACC),' IEEE, 2021 pp. 1070–1075.
- [35] Bemporad, A., 'Reference governor for constrained nonlinear systems,' *IEEE Transactions on Automatic Control*, 1998, **43**(3), pp. 415–419.
- [36] Mayne, D. Q., Rawlings, J. B., Rao, C. V., and Scokaert, P. O., 'Constrained model predictive control: Stability and optimality,' *Automatica*, 2000, **36**(6), pp. 789–814.
- [37] Scarritt, S., 'Nonlinear model reference adaptive control for satellite attitude tracking,' in 'AIAA Guidance, Navigation and Control Conference and Exhibit,' 2008 p. 7165.

- [38] Peter, F., Leitão, M., and Holzapfel, F., 'Adaptive augmentation of a new baseline control architecture for tail-controlled missiles using a nonlinear reference model,' in 'AIAA Guidance, Navigation, and Control Conference,' 2012 p. 5037.
- [39] Yucelen, T., Gruenwald, B., Muse, J. A., and De La Torre, G., 'Adaptive control with nonlinear reference systems,' in '2015 American Control Conference (ACC),' IEEE, 2015 pp. 3986–3991.
- [40] Wang, X. and Hovakimyan, N., 'L1 adaptive controller for nonlinear time-varying reference systems,' *Systems & Control Letters*, 2012, **61**(4), pp. 455–463.
- [41] Kawaguchi, Y., Eguchi, H., Fukao, T., and Osuka, K., 'Passivity-based adaptive nonlinear control for active steering,' in '2007 IEEE International Conference on Control Applications,' IEEE, 2007 pp. 214–219.
- [42] Gruenwald, B. C., Yucelen, T., De La Torre, G., and Muse, J. A., 'Adaptive control for uncertain dynamical systems with nonlinear reference systems,' *International Journal of Systems Science*, 2020, **51**(4), pp. 687–703.
- [43] Na, J., Herrmann, G., and Vamvoudakis, K. G., 'Adaptive optimal observer design via approximate dynamic programming,' in '2017 American Control Conference (ACC),' IEEE, 2017 pp. 3288–3293.
- [44] Rohrweck, H., Schwarzgruber, T., and del Re, L., 'Approximate optimal control by inverse clf approach,' *IFAC-PapersOnLine*, 2015, **48**(11), pp. 286–291.
- [45] Walters, P., Kamalapurkar, R., and Dixon, W. E., 'Approximate optimal online continuous-time path-planner with static obstacle avoidance,' in '2015 54th IEEE Conference on Decision and Control (CDC),' IEEE, 2015 pp. 650–655.
- [46] Kamalapurkar, R., Andrews, L., Walters, P., and Dixon, W. E., 'Model-based reinforcement learning for infinite-horizon approximate optimal tracking,' *IEEE transactions on neural networks and learning systems*, 2016, **28**(3), pp. 753–758.
- [47] Walters, P., Kamalapurkar, R., Andrews, L., and Dixon, W. E., 'Online approximate optimal path-following for a mobile robot,' in '53rd IEEE Conference on Decision and Control,' IEEE, 2014 pp. 4536–4541.
- [48] Dierks, T. and Jagannathan, S., 'Optimal control of affine nonlinear continuous-time systems,' in 'Proceedings of the 2010 American Control Conference,' IEEE, 2010 pp. 1568–1573.
- [49] Ballesteros, M., Chairez, I., and Poznyak, A., 'Robust optimal feedback control design for uncertain systems based on artificial neural network approximation of the bellman's value function,' *Neurocomputing*, 2020, **413**, pp. 134–144.
- [50] Garrard, W., McClamroch, N., and Clark, L., 'An approach to sub-optimal feedback control of non-linear systems,' *International Journal of Control*, 1967, **5**(5), pp. 425–435.

- [51] Na, J. and Herrmann, G., ‘Online adaptive approximate optimal tracking control with simplified dual approximation structure for continuous-time unknown nonlinear systems,’ *IEEE/CAA Journal of Automatica Sinica*, 2014, **1**(4), pp. 412–422.
- [52] Abu-Khalaf, M. and Lewis, F. L., ‘Nearly optimal control laws for nonlinear systems with saturating actuators using a neural network hjb approach,’ *Automatica*, 2005, **41**(5), pp. 779–791.
- [53] Bhasin, S., Kamalapurkar, R., Johnson, M., Vamvoudakis, K. G., Lewis, F. L., and Dixon, W. E., ‘A novel actor–critic–identifier architecture for approximate optimal control of uncertain nonlinear systems,’ *Automatica*, 2013, **49**(1), pp. 82–92.
- [54] Vamvoudakis, K. G. and Lewis, F. L., ‘Online actor–critic algorithm to solve the continuous-time infinite horizon optimal control problem,’ *Automatica*, 2010, **46**(5), pp. 878–888.
- [55] Balakrishnan, S. and Biega, V., ‘Adaptive-critic-based neural networks for aircraft optimal control,’ *Journal of Guidance, Control, and Dynamics*, 1996, **19**(4), pp. 893–898.
- [56] Vrabie, D., Abu-Khalaf, M., Lewis, F. L., and Wang, Y., ‘Continuous-time adp for linear systems with partially unknown dynamics,’ in ‘2007 IEEE International Symposium on Approximate Dynamic Programming and Reinforcement Learning,’ IEEE, 2007 pp. 247–253.
- [57] Lv, Y., Na, J., Yang, Q., Wu, X., and Guo, Y., ‘Online adaptive optimal control for continuous-time nonlinear systems with completely unknown dynamics,’ *International Journal of Control*, 2016, **89**(1), pp. 99–112.
- [58] Padhi, R., Unnikrishnan, N., Wang, X., and Balakrishnan, S., ‘A single network adaptive critic (snac) architecture for optimal control synthesis for a class of nonlinear systems,’ *Neural Networks*, 2006, **19**(10), pp. 1648–1660.
- [59] Chowdhary, G. and Johnson, E., ‘Concurrent learning for convergence in adaptive control without persistency of excitation,’ in ‘49th IEEE Conference on Decision and Control (CDC),’ IEEE, 2010 pp. 3674–3679.
- [60] Kamalapurkar, R., Walters, P., and Dixon, W., ‘Concurrent learning-based approximate optimal regulation,’ in ‘52nd IEEE Conference on Decision and Control,’ IEEE, 2013 pp. 6256–6261.
- [61] Xu, D., Wang, Q., and Li, Y., ‘Optimal guaranteed cost tracking of uncertain nonlinear systems using adaptive dynamic programming with concurrent learning,’ *International Journal of Control, Automation and Systems*, 2020, **18**(5), pp. 1116–1127.
- [62] Chowdhary, G., Yucelen, T., Mühlegg, M., and Johnson, E. N., ‘Concurrent learning adaptive control of linear systems with exponentially convergent bounds,’ *International Journal of Adaptive Control and Signal Processing*, 2013, **27**(4), pp. 280–301.

- [63] Klotz, J., Kamalapurkar, R., and Dixon, W. E., 'Concurrent learning-based network synchronization,' in '2014 American Control Conference,' IEEE, 2014 pp. 796–801.
- [64] Herty, M. and Kalise, D., 'Suboptimal nonlinear feedback control laws for collective dynamics,' in '2018 IEEE 14th International Conference on Control and Automation (ICCA),' IEEE, 2018 pp. 556–561.
- [65] Sage, A. and Eisenberg, B., 'Suboptimal adaptive control of a nonlinear plant,' IEEE Transactions on Automatic Control, 1966, **11**(3), pp. 621–623.
- [66] Eller, D. and Aggarwal, J., 'Sub-optimal control of non-linear single input systems,' International Journal of Control, 1968, **8**(2), pp. 113–121.
- [67] Garrard, W. L., 'Suboptimal feedback control for nonlinear systems,' Automatica, 1972, **8**(2), pp. 219–221.
- [68] Sannomiya, N., Itakura, H., *et al.*, 'A method for suboptimal design of nonlinear feedback systems,' Automatica, 1971, **7**(6), pp. 703–712.
- [69] Pearson, J., 'Approximation methods in optimal control i. sub-optimal control,' International Journal of Electronics, 1962, **13**(5), pp. 453–469.
- [70] Rosen, G. and Wismer, D., 'A sub-optimal feedback controller for on-line computer applications,' International Journal of Control, 1972, **15**(1), pp. 115–128.
- [71] Weber, A. and Lapidus, L., 'Suboptimal control of nonlinear systems: I. unconstrained,' AIChE Journal, 1971, **17**(3), pp. 641–648.
- [72] Weber, A. and Lapidus, L., 'Suboptimal control of nonlinear systems: II. constrained,' AIChE Journal, 1971, **17**(3), pp. 649–658.
- [73] Wernli, A. and Cook, G., 'Suboptimal control for the nonlinear quadratic regulator problem,' Automatica, 1975, **11**(1), pp. 75–84.
- [74] Wang, F.-Y. and Saridis, G., 'Suboptimal control for nonlinear stochastic systems,' in '[1992] Proceedings of the 31st IEEE Conference on Decision and Control,' IEEE, 1992 pp. 1856–1861.
- [75] Burghart, J., 'A technique for suboptimal feedback control of nonlinear systems,' IEEE Transactions on Automatic Control, 1969, **14**(5), pp. 530–533.
- [76] Pan, Z., Ezal, K., Krener, A. J., and Kokotovic, P. V., 'Backstepping design with local optimality matching,' IEEE Transactions on Automatic Control, 2001, **46**(7), pp. 1014–1027.
- [77] Krikelis, N. and Kiriakidis, K., 'Optimal feedback control of non-linear systems,' International Journal of Systems Science, 1992, **23**(12), pp. 2141–2153.

- [78] Zhao, J. and Gan, M., 'Finite-horizon optimal control for continuous-time uncertain nonlinear systems using reinforcement learning,' *International Journal of Systems Science*, 2020, **51**(13), pp. 2429–2440.
- [79] Zhao, J., 'Neural network-based optimal tracking control of continuous-time uncertain nonlinear system via reinforcement learning,' *Neural Processing Letters*, 2020, **51**(3), pp. 2513–2530.
- [80] Modares, H. and Lewis, F. L., 'Linear quadratic tracking control of partially-unknown continuous-time systems using reinforcement learning,' *IEEE Transactions on Automatic control*, 2014, **59**(11), pp. 3051–3056.
- [81] Curtis, J. W. and Beard, R. W., 'Successive collocation: An approximation to optimal nonlinear control,' in 'Proceedings of the 2001 American Control Conference.(Cat. No. 01CH37148),' volume 5, IEEE, 2001 pp. 3481–3485.
- [82] Beard, R. W., Saridis, G. N., and Wen, J. T., 'Galerkin approximations of the generalized hamilton-jacobi-bellman equation,' *Automatica*, 1997, **33**(12), pp. 2159–2177.
- [83] Xin, M. and Balakrishnan, S., 'A new method for suboptimal control of a class of nonlinear systems,' in 'Proceedings of the 41st IEEE Conference on Decision and Control, 2002.', volume 3, IEEE, 2002 pp. 2756–2761.
- [84] Li, Q. and Zhou, D., 'Nonlinear autopilot design for interceptors with tail fins and pulse thrusters via θ -d approach,' *Journal of Systems Engineering and Electronics*, 2014, **25**(2), pp. 273–280.
- [85] Xin, M. and Balakrishnan, S., 'A new method for suboptimal control of a class of non-linear systems,' *Optimal Control Applications and Methods*, 2005, **26**(2), pp. 55–83.
- [86] Becerra, H. M., Vázquez, C. R., Arechavaleta, G., and Delfin, J., 'Predefined-time convergence control for high-order integrator systems using time base generators,' *IEEE Transactions on Control Systems Technology*, 2017, **26**(5), pp. 1866–1873.
- [87] Sánchez-Torres, J. D., Sanchez, E. N., and Loukianov, A. G., 'Predefined-time stability of dynamical systems with sliding modes,' in '2015 American control conference (ACC),' IEEE, 2015 pp. 5842–5846.
- [88] Jiménez-Rodríguez, E., Sánchez-Torres, J. D., Gómez-Gutiérrez, D., and Loukianov, A. G., 'Predefined-time tracking of a class of mechanical systems,' in '2016 13th International Conference on Electrical Engineering, Computing Science and Automatic Control (CCE),' IEEE, 2016 pp. 1–5.
- [89] Wang, Y., Song, Y., Hill, D. J., and Krstic, M., 'Prescribed-time consensus and containment control of networked multiagent systems,' *IEEE transactions on cybernetics*, 2018, **49**(4), pp. 1138–1147.

- [90] Jiménez-Rodríguez, E., Sánchez-Torres, J. D., and Loukianov, A. G., ‘On optimal predefined-time stabilization,’ *International Journal of Robust and Nonlinear Control*, 2017, **27**(17), pp. 3620–3642.
- [91] Harl, N. and Balakrishnan, S., ‘Impact time and angle guidance with sliding mode control,’ *IEEE Transactions on Control Systems Technology*, 2011, **20**(6), pp. 1436–1449.
- [92] Meng, Z., Ren, W., and You, Z., ‘Distributed finite-time attitude containment control for multiple rigid bodies,’ *Automatica*, 2010, **46**(12), pp. 2092–2099.
- [93] Polyakov, A., ‘Nonlinear feedback design for fixed-time stabilization of linear control systems,’ *IEEE Transactions on Automatic Control*, 2011, **57**(8), pp. 2106–2110.
- [94] Jin, X., ‘Adaptive decentralized finite-time output tracking control for mimo interconnected nonlinear systems with output constraints and actuator faults,’ *International Journal of Robust and Nonlinear Control*, 2018, **28**(5), pp. 1808–1829.
- [95] Shang, Y., ‘Finite-time consensus for multi-agent systems with fixed topologies,’ *International Journal of Systems Science*, 2012, **43**(3), pp. 499–506.
- [96] Lu, W., Liu, X., and Chen, T., ‘A note on finite-time and fixed-time stability,’ *Neural Networks*, 2016, **81**, pp. 11–15.
- [97] Bhat, S. P. and Bernstein, D. S., ‘Finite-time stability of continuous autonomous systems,’ *SIAM Journal on Control and Optimization*, 2000, **38**(3), pp. 751–766.
- [98] Wang, L. and Xiao, F., ‘Finite-time consensus problems for networks of dynamic agents,’ *IEEE Transactions on Automatic Control*, 2010, **55**(4), pp. 950–955.
- [99] Yong, C., Guangming, X., and Huiyang, L., ‘Reaching consensus at a preset time: Single-integrator dynamics case,’ in ‘Proceedings of the 31st Chinese Control Conference,’ IEEE, 2012 pp. 6220–6225.
- [100] Bhat, S. P. and Bernstein, D. S., ‘Continuous finite-time stabilization of the translational and rotational double integrators,’ *IEEE Transactions on automatic control*, 1998, **43**(5), pp. 678–682.
- [101] Yucelen, T., Kan, Z., and Pasiliao, E., ‘Finite-time cooperative engagement,’ *IEEE Transactions on Automatic Control*, 2018, **64**(8), pp. 3521–3526.
- [102] Kan, Z., Yucelen, T., Doucette, E., and Pasiliao, E., ‘A finite-time consensus framework over time-varying graph topologies with temporal constraints,’ *Journal of Dynamic Systems, Measurement, and Control*, 2017, **139**(7), p. 071012.
- [103] Arabi, E., Yucelen, T., and Singler, J. R., ‘Robustness of finite-time distributed control algorithm with time transformation,’ in ‘2019 American Control Conference (ACC),’ IEEE, 2019 pp. 108–113.

- [104] Cortés, J., ‘Finite-time convergent gradient flows with applications to motion coordination,’ *Automatica*, 2005.
- [105] Cortés, J., ‘Finite-time convergent gradient flows with applications to network consensus,’ *Automatica*, 2006, **42**(11), pp. 1993–2000.
- [106] Ríos, H. and Teel, A. R., ‘A hybrid observer for fixed-time state estimation of linear systems,’ in ‘2016 IEEE 55th Conference on Decision and Control (CDC),’ IEEE, 2016 pp. 5408–5413.
- [107] Basin, M., Shtessel, Y., and Aldukali, F., ‘Continuous finite-and fixed-time high-order regulators,’ *Journal of the Franklin Institute*, 2016, **353**(18), pp. 5001–5012.
- [108] Cloutier, J. R., ‘State-dependent riccati equation techniques: an overview,’ in ‘American Control Conference,’ volume 2, 1997 pp. 932–936.
- [109] Heydari, A. and Balakrishnan, S., ‘Path planning using a novel finite horizon sub-optimal controller,’ *Journal of guidance, control, and dynamics*, 2013, **36**(4), pp. 1210–1214.
- [110] Heydari, A. and Balakrishnan, S., ‘Optimal online path planning for approach and landing guidance,’ in ‘Proc. AIAA Atmospheric Flight Mechanics Conference, Portland, OR,’ 2011 .
- [111] Roskam, J., *Airplane flight dynamics and automatic flight controls*, number pt. 1 in *Airplane Flight Dynamics and Automatic Flight Controls*, DARcorporation, 1995, ISBN 9781884885174.
- [112] Moylan, P. and Anderson, B., ‘Nonlinear regulator theory and an inverse optimal control problem,’ *IEEE Transactions on Automatic Control*, 1973, **18**(5), pp. 460–465.
- [113] Wan, C.-J. and Bernstein, D. S., ‘Nonlinear feedback control with global stabilization,’ *Dynamics and Control*, 1995, **5**(4), pp. 321–346.
- [114] Krstic, M. and Tsiotras, P., ‘Inverse optimal stabilization of a rigid spacecraft,’ *IEEE Transactions on Automatic Control*, 1999, **44**(5), pp. 1042–1049.
- [115] Luo, W., Chu, Y.-C., and Ling, K.-V., ‘Inverse optimal adaptive control for attitude tracking of spacecraft,’ *IEEE Transactions on Automatic Control*, 2005, **50**(11), pp. 1639–1654.
- [116] Bryson, A. E., Denham, W. F., and Dreyfus, S. E., ‘Optimal programming problems with inequality constraints,’ *AIAA journal*, 1963, **1**(11), pp. 2544–2550.
- [117] McIntyre, J. and Paiwonsky, B., ‘On optimal control with bounded state variables,’ in ‘Advances in Control Systems,’ volume 5, pp. 389–419, Elsevier, 1967.

- [118] Kreindler, E., 'Additional necessary conditions for optimal control with state-variable inequality constraints,' *Journal of Optimization theory and applications*, 1982, **38**(2), pp. 241–250.
- [119] Jacobson, D. H., Lele, M. M., and Speyer, J. L., 'New necessary conditions of optimality for control problems with state-variable inequality constraints,' *Journal of mathematical analysis and applications*, 1971, **35**(2), pp. 255–284.
- [120] Han, D. and Balakrishnan, S., 'State-constrained agile missile control with adaptive-critic-based neural networks,' *IEEE Transactions on Control Systems Technology*, 2002, **10**(4), pp. 481–489.
- [121] Haddad, W. M. and Chellaboina, V., *Nonlinear dynamical systems and control: a Lyapunov-based approach*, Princeton university press, 2011.
- [122] Çimen, T., 'State-dependent riccati equation (sdre) control: A survey,' *IFAC Proceedings Volumes*, 2008, **41**(2), pp. 3761–3775.
- [123] Lewis, F., Jagannathan, S., and Yesildirak, A., *Neural network control of robot manipulators and non-linear systems*, CRC Press, 1998.
- [124] Cloutier, J. R., D'Souza, C. N., and Mracek, C. P., 'Nonlinear regulation and nonlinear h_{∞} control via the state-dependent riccati equation technique: Part2, examples,' ” *Inrerna. Conf: On Nonlinear Problems in Aviation and Aerospace*, 1996.
- [125] Lavretsky, E. and Gadiant, R., 'Robust adaptive design for aerial vehicles with state-limiting constraints,' *Journal of guidance, control, and dynamics*, 2010, **33**(6), pp. 1743–1752.
- [126] Lavretsky, E. and Wise, K. A., 'Robust adaptive control,' in 'Robust and adaptive control,' pp. 317–353, Springer, 2013.
- [127] Xiao, F., Wang, L., Chen, J., and Gao, Y., 'Finite-time formation control for multi-agent systems,' *Automatica*, 2009, **45**(11), pp. 2605–2611.

VITA

Meryem Deniz was born in Malatya, Turkey. She received her Bachelor's degree in Electrical & Electronics Engineering at Cumhuriyet University, Sivas, in 2012; and her Master's degree in Electrical & Electronics Engineering at Izmir Institute of Technology, Izmir, in 2015. She graduated first ranked among all Faculty of Engineering at Cumhuriyet University in 2012. Her Ph.D. was sponsored by the Ministry of National Education, the Republic of Turkey. As a doctoral student, she received the Council of Graduate Scholarship Award and Outstanding and Engaged Graduate Student Award from the Council of Graduate students of the Missouri University of Science and Technology in May 2021. During her Ph.D., she served as the Teaching Assistant for a couple of undergraduate-level courses. She was a Treasurer, Vice President, and President of Turkish Student Associations, and she was an Ambassadors of Miner United at Missouri University of Science and Technology. She received a Doctor of Philosophy in the Mechanical Engineering Department at Missouri University of Science and Technology in May 2022.